Iris Recognition Using Support Vector Machines

Kaushik Roy

A Thesis

in

The Department

of

Computer Science & Software Engineering

Presented in Partial Fulfillment of the Requirements
for the Degree of Master of Computer Science at
Concordia University
Montreal, Quebec, Canada

August 2006

Your file Votre référence
ISBN: 978-0-494-20782-6
Our file Notre référence
ISBN: 978-0-494-20782-6

Abstract

Iris Recognition Using Support Vector Machines

Kaushik Roy

In this thesis, an iris recognition system is presented as a biometrically based technology for person identification using support vector machines (SVM). We propose two approaches for iris recognition, namely: The approach I, which is based on the whole information of iris region and the approach II, where only the zigzag collarette region is used for recognition. In approach I, Canny edge detection and Hough transform are used to find the iris/pupil boundary from eye's digital image. The rubber sheet model is applied to normalize the segmented iris image, Gabor wavelet technique is deployed to extract the deterministic features and the traditional SVM is used for iris patterns classification. In approach II, an iris recognition method is proposed using a novel iris segmentation scheme based on chain code and zigzag collarette area. The Multi-Objectives Genetic Algorithm (MOGA) is employed to select features extracted from the normalized collarette region by log-Gabor filters to increase the overall recognition accuracy. The traditional SVM is modified to asymmetrical SVM to treat False Accept and False Reject differently. Our experimental results indicate that the performance of SVM as a classifier is better than the performance of classifiers based on feed-forward neural network using backpropagation and Levenberg-Marquardt rule, K-nearest neighbor, and Hamming distance.

Acknowledgements

Several people helped me to make this research a success. First of all, I owe a great debt of gratitude to my supervisor Professor Dr. Prabir Bhattacharya. I consider myself fortunate working under his guidance and receiving affluent knowledge towards this research and discovery. I really feel privileged for his attention to complete a successful research.

I am also grateful to my graduate colleagues at Concordia Research Laboratory in particular, Abu Sayeed Md. Sohail, Emad Attari, Lilybert Machacha, Mahdi Yektaii, M.M. Rahman, and Sujoy Ray. They influenced me a lot in this research.

I would like to express my deepest gratitude to my parents, brother, and parents-in-law, for their affection and continuous inspiration throughout this research work. Without their help, it would not have been possible to complete this research work.

I would also like to thank my wife, Tithi, for her love and support in every moment.

Kaushik Roy
August 15, 2006

Dedicated

To My Parents

Contents

List of Figures ..... **X**

List of Tables ..... **XIV**

Chapter 1 Introduction **1**

1.1 Motivation 1

1.2 Proposed Approaches: The Main Steps 3

1.3 Objectives of the Thesis 6

1.4 Main Contributions 7

1.5 Organization of the Thesis 8

Chapter 2 Background Study **9**

2.1 Biometric: An Overview 9

2.1.1 Biometric System 11

2.1.2 Biometric Techniques 12

2.1.2.1 Behavioral characteristics 12

2.1.2.2 Physiological characteristics 13

2.2 Iris Recognition: An Overview 14

2.2.1 A Typical Iris Recognition System 17

2.2.2 Approaches of Iris Recognition 18

2.2.3 Iris Recognition System Errors 19

2.2.4 Strengths and weaknesses of Iris as Biometric for Recognition 20

2.2.4.1 Strengths of Iris for Recognition 21

2.2.4.2 Weaknesses of Iris for Recognition 21

2.2.5 Challenges in Iris Recognition 22

2.2.6 Applications of Iris Recognition 23

2.2.7 Issues in Iris Recognition 24

2.3 Related Work 24

Chapter 3 Iris Image Pre-Processing 37

3.1 Introduction 37

3.2 Localization 38

3.2.1 Approach I for Localization using Whole Iris Information 38

3.2.1.1 Iris/Pupil Detection 38

3.2.2 Approach II for Localization based on Zigzag Collarette Region 42

3.2.2.1 Iris Localization 42

3.2.2.2 Pupillary Localization 42

3.2.2.3 Isolation of Zigzag Collarette Area 43

3.2.3 Eyelids and Eyelashes Detection 45

3.3 Unwrapping or Normalization 46

Chapter 4 Feature Extraction and Selection 50

4.1 Introduction 50

4.2 Feature Extraction and Encoding 51

4.2.1 Gabor Wavelets 51

4.2.2 Log-Gabor Filters 52

4.2.3 Feature Extraction and Encoding Scheme for Approaches I & II 54

4.3 Feature Selection 56

4.3.1 Principal Component Analysis (PCA) 57

4.3.2 Bhattacharyya Distance 58

4.3.3 Multi-Objectives Genetic Algorithm (MOGA) 64

4.3.3.1 Proposed Feature Selection Technique Using MOGA 67

Chapter 5 Iris Patterns Classification 70

5.1 Introduction 70

5.2 Hamming Distance 71

5.3 Mahalanobis Distance 72

5.4 k-Nearest Neighbor Classifier 72

5.5 Feed-Forward Neural Network using Backpropagation 74

5.5.1 Feed-Forward Neural Network Model for Iris Recognition using Backpropagation 77

5.5.2 Feed-Forward Neural network using Levenberg-

Marquardt rule 78

5.6 Support Vector Machines as Iris Patterns Classifier 82

5.6.1 Asymmetrical Support Vector Machines 91

Chapter 6 Experimental Results & Discussions 93

6.1 Introduction 93

6.2 Performance Evaluation of the Proposed Approaches I & II 94

6.3 Comparison with Existing Methods 105

6.4 Discussions 109

Chapter 7 Conclusions 111

7.1 Summary of Thesis Work 111

7.2 Findings of Thesis Work 112

7.3 Suggestions for Future Development 114

References 116

Appendix 129

A Training and Testing Procedures of the Proposed Approach I & Approach II 129

B Functional Overview of Approach I & Approach II 133

C List of Abbreviated Terms 136

List of Figures

1 Flow diagram of the proposed approach I 4

2 Flow diagram of the proposed approach II 5

3 Architecture of a typical biometric authentication system 11

4 Samples of iris images 15

5 Structure of a human eye 16

6 Different parts of an eye image 16

7 Diagram of a typical iris recognition system 17

8 (a) Original eye image (b) edge map of the corresponding eye image (c) edge map with horizontal gradients (d) edge map with vertical gradients 40

9 Localization process for approach I (a), (b), (c) are sample iris image, (d), (e), (f) are corresponding images with the localized iris/ pupil boundary, and (g), (h), (i) show the corresponding images after eyelids and eyelashes detection 41

10 Chain code directions for 8-connected boundaries 43

11 (a) Original eye image (b) thresholded image (c) image after applying chain code algorithm (d) small region elimination (e) detected center and radius

of pupil (f) localized pupil 44

12 (a) Circle around the pupil indicates the zigzag collarette region (b) zigzag collarette area is occluded by eyelashes and upper eyelids 44

13 (a), (b) and (c) show zigzag collarette area localization from CASIA iris database..... 45

14 (a), (b), (c) are CASIA iris images with the detected zigzag area and (d), (e) and (f) are the corresponding images after detection of eyelids and eyelashes 46

15 Rubber sheet model to unwrap the localized region 47

16 (a) Unwrapping an iris image (b) noise areas are marked for the corresponding unwrapped iris image 48

17 Histogram equalization (a) before enhancement (b) after enhancement 49

18 Unwrapping the zigzag collarette region 49

19 (a), (b), (c) show the unwrapped collarette region before enhancement and (d), (e), (f) reveal the collarette region after enhancement 49

20 A quadrature pair of 2D Gabor filters (a) real component or even symmetric filter characterized by a cosine modulated by a Gaussian (b) imaginary component or odd symmetric filter characterized by a sine modulated by a Gaussian 53

21 Feature extraction and encoding process (a) feature extraction, (b) phase quantization and (c) generated iris pattern 55

22 Plot of BCD versus nf 63

23 A simple GA cycle 65

24 Basic process of GA 65

25 Three basic operations of GA with simple examples (a) selection, (b) crossover, and (c) mutation 66

26 A binary feature vector for l-dimension 68

27 Feature selection process 69

28 A feed-forward neural network with three input dimensions and one output 75

29 The proposed feed-forward neural network using backpropagation 77

30 A feed-forward neural network 79

31 Illustration of a two class classification process using SVM 84

32 The two-layer architecture of SVM 90

33 Comparison of classification accuracy among traditional SVM, FFBP, FFLM and k-NN for 600-bit feature sequence in Approach I 95

34 Comparison of recognition accuracy of traditional SVM with FFBP, FFLM, k-NN and HD for different feature dimension in Approach I 95

35 Comparison of classification accuracy among SVM, FFBP, FFLM and k-NN for 600-bit feature sequence in Approach II 98

36 Comparison of classification accuracy of SVM with FFBP, FFLM, k-NN and MDC for 5-bit feature sequence in Approach II 98

37 Comparison of recognition accuracy of SVM with FFBP, FFLM, k-NN and HD for different feature dimension in Approach II 99

38 (a), (b), and (c) demonstrate that *nf* does not show any sign of saturation and it requires more samples per iris pattern class to obtain a saturated situation

after a certain number of features reduction 100

39 Variation of recognition rates with generation for approach II 102

40 Variation of fitness values with generation for approach II 102

41 Comparison of recognition accuracy between approaches I & II 104

42 ROC curve shows the comparison between GAR and FAR for proposed approaches I & II 104

43 Comparison of recognition error between proposed approaches II with the approach I for different values of asymmetrical parameter, g 105

44 Training procedure of the proposed approach I 129

45 Testing procedure of the proposed approach I 130

46 Training procedure of the proposed approach II 131

47 Testing procedure of the proposed approach II 132

48 Overview of subsystems and MatLab functions for Approach I 133

49 Overview of subsystems and MatLab functions of Approach II (a) localization, unwrapping, and feature extraction and encoding (b) feature selection using MOGA, (c) feature selection with BD and PCA, and (d) training and prediction 134

List of Tables

1 Efficiency of various kernel functions 97

2 Comparison of recognition rates and equal error rates 107

3 Comparison of average time consumption of different parts of iris recognition system 107

4 Comparison of the computational complexity 109

Chapter 1

Introduction

1.1. Motivation

The increasing demand for enhanced security in the daily life has directed the improvement of the reliable and intelligent personal identification system based on biometrics and it is currently an active topic in the literature of pattern recognition. Biometric deploys the physiological and behavioral characteristics to identify the person accurately. Commonly used biometric features include face, fingerprints, voice, facial thermograms, iris, retina, gait, palm-prints, hand geometry, etc. Biometrically based identification systems using the fingerprint, iris, face, and palm print, etc., have many advantages over the traditional authentication techniques based on what you know or what you possess ([6], [39], [70]). In the biometric community, iris recognition is treated as one of the most accurate manners of personal identification ([40], [55], [56], [98]). Therefore, nowadays, many automatic security systems based on iris recognition have been deployed worldwide for border control, secured access to bank accounts, ticketless traveling, rapid processing of passengers, restricted access of privileged information, and so on. The iris of the human eye is an annular part between the black pupil and the white sclera and usually, iris contains extraordinary structure and provides interlacing minute

characteristics, such as freckles, coronas, stripes, furrows, crypts, and zigzag collarette region. These visible characteristics, denoted as the texture of the iris, are regarded as unique to each individual and the uniqueness of the iris structure assists to differentiate between individuals. In research work, it is found that the iris remains stable throughout a person's life time and furthermore, the iris based identification system is non invasive to the users since iris is an integral organ of the body as well as externally visible. All these advantageous attributes make iris recognition an attractive solution for increasing security requirements.

In recent years, several research work has been conducted in iris recognition area. Most of the current researches on iris recognition mainly focus on iris segmentation scheme which are usually based on the complete information of iris region. In this thesis, we emphasize on the iris segmentation approach based on zigzag collarette area, the most complex part of the iris structure with the sufficient distinguishing features. The traditional approach of iris segmentation based on the whole iris information is also utilized. A very few research work has been accomplished on feature selection in the area of iris recognition and there are lots of research yet to be done. In this thesis, we propose a feature selection strategy using multi-objectives genetic algorithm (MOGA) for dimensionality reduction as well as to minimize the recognition error. Furthermore, most of the existing iris recognition schemes utilize the Hamming distance for matching purpose. In this research work, we apply support vector machines (SVM) as iris pattern classifiers and provide a comparative analysis of SVM with other classical methods of classification such as Artificial Neural Network (ANN) with backpropagation and

Levenberg-Marquardt rule, k-nearest neighbor (k-NN) classifier, and Hamming and Mahalanobis distances.

1.2. Proposed Approaches: The Main Steps

We illustrate our proposed iris recognition method into two approaches: First, Approach I, where recognition is based on the whole information of iris region. In this approach iris patterns are classified using traditional SVM [72]. Second, Approach II [74], where the idea of using the zigzag collarette region for recognition is exploited instead of utilizing the complete information of iris and an asymmetrical approach of SVM is applied for iris patterns classification.

In approach I, we propose an iris recognition method with a segmentation scheme based on the Canny edge detection and the Hough transform techniques. The traditional SVM is used for iris pattern classification. Figure1 illustrates the main steps of the approach I. In the image pre-processing stage, iris and pupil boundaries are detected using circular Hough transform and Canny edge detection techniques. The linear Hough transform is applied for isolating the upper and lower eyelids. Eyelashes and other non-iris regions are eliminated using 1D Gabor wavelets and thresholding methods. In order to avoid the size inconsistencies of the localized region, the annular iris part is normalized into a rectangular block. Gabor wavelet technique is applied to extract the discriminating iris features from this normalized region and a conventional approach of SVM is then deployed for iris patterns classification.

In approach II, we propose a novel iris segmentation method based on chain code and zigzag collarette region for matching purpose. Figure 2 illustrates the main steps of our proposed approach II. First, the image preprocessing step performs the localization of

iris, detects the pupil with linear thresholding and chain code from the localized iris, and isolates the zigzag collarette region which is regarded as one of the most important area of the iris complex pattern along with the similar techniques of eyelids, eyelashes and noise detection used in the approach I. Zigzag collarette region is insensitive to the pupil dilation and usually not affected by the eyelids and eyelashes. In order to achieve the invariance to translation and scale, the isolated zigzag collarette region is transformed to a rectangular block of fixed dimension by Daugman's rubber sheet model and the normalized image is enhanced using Histogram equalization technique.

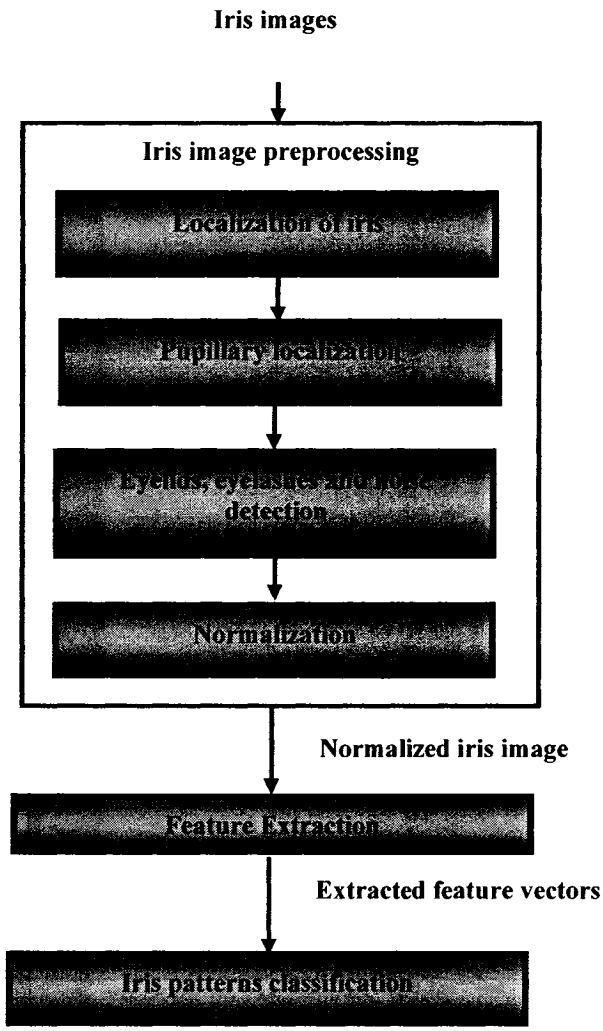

Figure 1: Flow diagram of the proposed approach I.

The deterministic iris features are extracted from the unwrapped image with the help of Gabor wavelets technique and the optimum features sequence is selected using MOGA to increase the recognition accuracy and reduce redundant features.

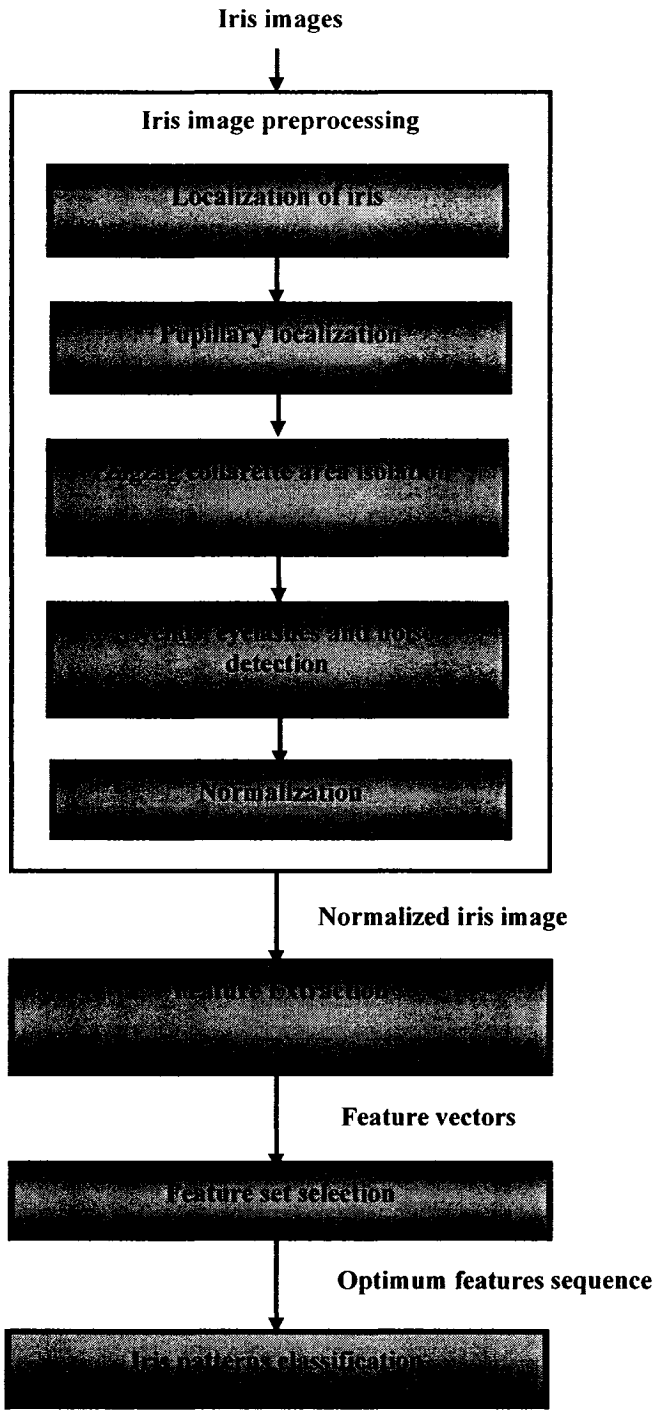

Figure 2: Flow diagram of the proposed approach II.

We also propose another feature selection strategy with Bhattacharyya distance (BD) and principal Component Analysis (PCA). Finally, the selected features are used for classification using SVM. Furthermore, the parameters of SVM are tuned to improve the overall generalization performance. The traditional SVM is modified to an asymmetrical SVM to treat the cases of False Accept or False Reject differently and also to solve the problem of unbalanced data of a class with respect to other classes. The classification accuracy of the proposed SVM is also compared with feed-forward neural network by backpropagation (FFBP), feed-forward neural network by Levenberg-Marquardt rule (FFLM), k-nearest neighbor (k-NN), and Hamming and Mahalanobis distances. In this research work, both of the approaches are described in details and a comparison between approaches I & II is provided. In this thesis, we emphasize on the approach II due to its encouraging performance over the approach I.

1.3. Objectives of the Thesis

The objectives of this research work are listed as follows:

- Study and investigation of the existing iris recognition systems.
- Localization of the iris, pupil and zigzag collarette area.
- Eyelids, eyelashes and noise detection to increase the recognition accuracy in subsequent processing.
- Unwrapping or normalizing the localized or segmented iris region to avoid the size inconsistencies.
- Extraction and selection of distinctive iris features from the unwrapped or normalized iris region.

- Performance evaluation of SVM as iris pattern classifiers and comparison of SVM with other classical techniques of classification.
- Application of the asymmetrical SVM to separate the False Accept Rate (FAR) and False Reject Rate (FRR) for satisfying several security demands and solving the issue of the unbalanced data of a specific class with respect to other classes.
- Introducing, designing and building a novel and effective iris recognition system.
- Accelerating the iris recognition process.
- System performance evaluation and comparison with the other existing iris recognition schemes.

1.4. Main Contributions

In approach I, the main contribution is enlisted as follows:

- An iris recognition method using SVM for iris pattern classification is proposed. Here a conventional approach of SVM is applied.

In approach II, the contributions are depicted as follows:

- A novel iris segmentation approach based on chain code [25] and zigzag collarette area along with the isolation techniques of eyelids, eyelashes and other non-iris regions are presented.
- Multi-objectives genetic algorithm (MOGA) [29] is used to select the optimum features from the extracted feature sequence and to increase the recognition accuracy. Another feature selection technique with BD and PCA is also proposed [22].
- The concept of asymmetrical SVM ([19], [93]) is used as iris classifiers and in order to improve the classification accuracy, the parameters of SVM are tuned.

- Most of the current iris recognition methods are based on iris segmentation and feature extraction techniques. In this thesis, we also focus on the optimum feature selection strategy and iris patterns classification.

A series of experiments to evaluate the performance of the proposed approach is conducted. In order to exhibit the efficiency of the proposed approaches, extensive quantitative comparisons with some existing methods are carried out and the discussions on the experimental results are presented.

1.5. Organization of the Thesis

The rest of this research work is organized as follows. Chapter 2 provides a brief overview of biometrics and iris recognition techniques, and a description of the related work is also depicted in this chapter. Chapter 3 deals with the iris image preprocessing which consists of iris localization using circular Hough transform and Canny edge detection, pupil detection by chain code method and circular Hough transform, eyelids, eyelashes and noise detection, and unwrapping the segmented iris or zigzag collarette region using rubber sheet model. In chapter 4, feature extraction technique using Gabor wavelet is depicted and feature selection strategies by Principal Component Analysis (PCA), Bhattacharyya Distance (BD), Multi-objectives Genetic Algorithms (MOGA) techniques are described. Different iris pattern classification techniques such as SVM, FFBP, FFLM, k-NN, and distance measures like Mahalanobis and Hamming distances are described in Chapter 5. Experimental results, comparisons with other existing methods and discussions are reported in Chapter 6. Chapter 7 provides the conclusion.

Chapter 2

Background Study

2.1. Biometric: An Overview

Nowadays, a rapid improvement of the biometrically-based personal identification system has been accomplished with the recent progresses of the information technology and the increasing requirements of security ([55], [56]). The physiological or behavioral characteristics of biometrics ([97], [98]) are deployed to accurately identify each subject. Commonly used biometric features include face, fingerprints, voice, facial thermograms, iris, retina, gait, palm-prints, hand geometry, etc. Trustworthy and automatic recognition of persons have long been an attractive goal. Reliable authentication and authorization are becoming necessary for many everyday applications, namely: Boarding an aircraft, performing a financial transaction, and even picking up a child from daycare. Personal identification and verification are regarded as the elemental activities of our society and culture especially for those organizations where the identity and authenticity of people is a prerequisite [6]. Biometric identification, also termed as biometrics, refers to identify an individual by using his or her distinguishing characteristics. More specifically, biometrics based identification or verification technology employs the physiological or behavioral characteristics to recognize a person ([6], [97], [98]).

According to [6], we can use the term 'a biometric' to refer a specific mode for recognizing people or examples of the specific characteristics being recognized. Because, identification cards may be lost, forged, or misplaced and passwords may be forgotten or compromised, the conventional methods of identification, based on unique ID cards, ID numbers or exclusive knowledge are not sufficient. It is important that any reliable positive person identification should entail biometric identification. It is already being accepted by the government and industry alike that the automated biometric authentication will become a necessary fact of life [6].

However, in a practical biometric system, there is a number of issues that should be considered, including ([6], [39]):

- Performance, which indicates the achievable recognition accuracy and speed, the resources required to achieve the desired recognition accuracy and speed as well as the operational and environmental factors that effect the accuracy and speed;
- Acceptability, which indicates the extent to which people are willing to accept the use of a particular biometric identifier in their daily lives;
- Circumvention, which reflects how easily the system can be fooled using fraudulent methods.

A specific biometric system should meet the specified recognition accuracy, speed, and resource requirements. Furthermore, it should be safe to the users, accepted by the intended population and adequately robust to various fraudulent methods and attacks to the system. Biometrics may provide protection to applications in a number of ways [6]:

- Physical access controls, e. g., in an airport. Here the airport infrastructure or travel infrastructure in general is regarded as the application.

- Logical access control, e. g., in a bank account; i.e., the application is the access to and the handling of money.
- Uniqueness of individuals. Here the focus is typically on preventing double enrollment in some applications, e. g., a social benefits program.

2.1.1 Biometric System

Any biometric authentication system is regarded as a pattern recognition system as shown in Figure 3 [6]. This type of system consists of:

- Biometrics readers or sensors,
- Feature extractors to compute salient attributes from input signals,
- Feature matchers for comparing two sets of biometric features.

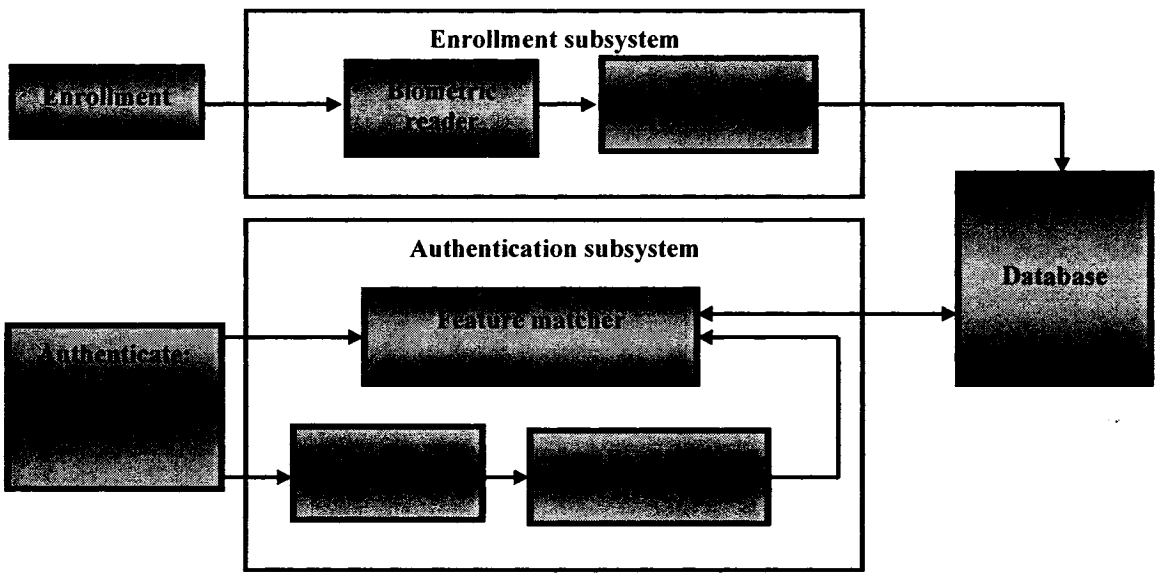

Figure 3: Architecture of a typical biometric authentication system.

An authentication system consists of two subsystems: First one is for enrollment and the second, for authentication. During the enrollment, biometric measurements are captured from a subject, the feature extractor gleans information from raw measurements, and this

information is stored in the database. The task of the authentication module of Figure 3 is to recognize a subject at a later stage. For identification, the system acquires the biometric sample from the subject, extracts features from raw measurements, and searches the entire database for matches using the extracted biometrics features. For verification, a subject presents some form of identifier and a biometric. The system senses the biometric measurements, extracts features, and compares the input features to the features enrolled in the system database under the subject's ID. The system then determines to accept or reject the subject.

2.1.2 Biometric Techniques

Currently, there are many different techniques available to identify/verify a person based on biometrics [70]. These techniques can be divided into behavioral characteristics and physiological characteristics. Physiological biometrics is usually measured at a specific point of time while the behavioral biometrics consists of the way some action is carried out and extended overtime. Physiological biometrics provides richness so that one-time sample may be sufficient for comparing biometrics identifiers, on the contrary, any given sample of behavioral biometrics may not contain any information about person's identity. All techniques have in common that the acquired data is compared with templates enrolled earlier.

2.1.2.1 Behavioral characteristics

The following are examples of biometric techniques based on behavioral characteristics ([6], [70]):

Voice recognition: Voice recognition systems use characteristics of the voice, such as pitch, tone, and frequency.

Signature recognition: Signature recognition systems measure pressure of the pen and frequency of writing to identify a person via a signature.

Keystrokes dynamics: Keystrokes dynamics systems use statistics, e.g. time between keystrokes, word choices, word combinations, general speed of typing, etc.

2.1.2.2 Physiological characteristics

The following are examples of biometric techniques based on physiological characteristics ([6], [70]):

Fingerprint recognition: Fingerprint recognition systems scan the fingerprint pattern for recognition.

Recognition of hand or finger: Hand or finger recognition systems scan the entire hand or larger parts of the finger and make a comparison of patterns in the skin. The difference between a fingerprint recognition system and a hand/finger recognition system lies mostly in the size of the scanner and the resolution of the scanning array.

Face recognition: Face recognition systems detect patterns, shapes, and shadows in the face.

Face geometry: Face geometry systems work similar to face recognition systems, but focus more on shapes and forms instead of patterns.

Vein pattern recognition: Vein pattern recognition systems detect veins in the surface of the hand. These patterns are considered to be as unique as fingerprints, but have the advantage of not being as easily copied or stolen as fingerprints are.

Retina recognition: Retina recognition systems scan the surface of the retina and compare nerve patterns, blood vessels and such features.

Iris recognition: Iris recognition systems scan the surface of the iris to compare patterns. From the extensive literature survey, we found that among all the human characteristics, the usage of iris pattern can be considered as the most reliable and robust biometric technique for the purposes of person identification and verification of individuals ([6], [57], [97], [98]).

In this research work, we explore the idea of iris recognition for person identification, introduce iris recognition approaches and emphasize on constructing a robust iris recognition system for person authentication.

2.2. Iris Recognition: An Overview

With the recent technological advances in audio and visual microelectronic systems [40] and the increasing emphasis on security requirements of the current commercial society, a significant development of intelligent personal identification systems based on biometrics has been achieved. Iris recognition has been regarded as one of the most reliable biometrics technologies in recent years ([98], [40]). The human iris, an annular part between the pupil and the white sclera, see Figure 4, has an extraordinary structure and provides many interlacing minute characteristics such as freckles, coronas, stripes, and zigzag collarette area, which are unique to each subject [55]. The iris is an internal organ of the body that is readily visible from outside and it controls the amount of light that enters the eye through the pupil, by using the dilator and sphincter muscles to control the pupil size [57]. An elastic fibrous tissue makes up iris structure that gives it a very complex and unique texture pattern. This texture pattern is independent of the genetic structure of an individual and is generated by chaotic processes. The human iris begins to form in the third month of gestation and the structure is completed by the eight month,

even though the color and pigmentation continue to build through the first year of birth [57].

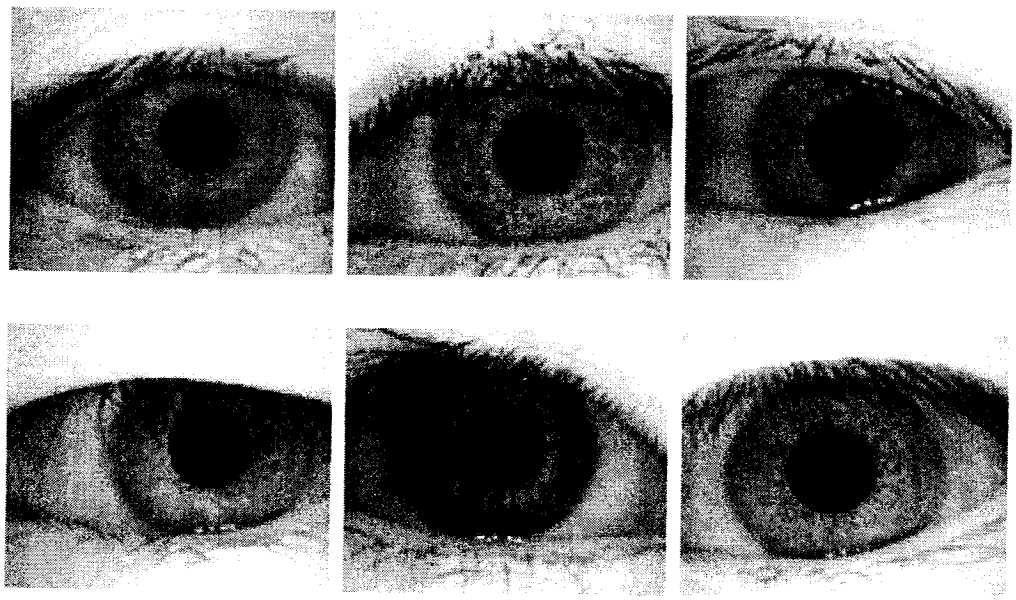

Figure 4: Samples of iris images.

After that, the structure of the iris remains stable throughout a person's life, except for direct physical damage or changes caused by eye surgery. This makes the usage of iris pattern as unique as the fingerprint, however, further advantage is that it is an internal organ and less susceptible to damages over a person's lifetime. The general structure of a typical human eye and the position of the iris in the eye are shown in Figure 5, and different parts of a typical iris are depicted in Figure 6. Iris based recognition system thus is noninvasive to the users, which is of great importance for real-time applications [59]. All these desirable properties make iris recognition a particularly promising solution for surveillance. Based on the technology developed by Daugman ([15], [18]), iris scans are nowadays being used in several international airports for the rapid processing of

passengers through the immigration who have pre-registered their iris images. Iris technology is also being widely used in several countries for various security purposes (and also by the United Nations High Commission for refugees). A new technology development project for iris recognition namely, the Iris Challenge Evaluation (ICE) is being conducted by the National Institute of Standards and Technology (NIST) [104]. The ICE is a technology development project for iris recognition and it is regarded as the first large-scale, open, and independent technology evaluation for iris recognition.

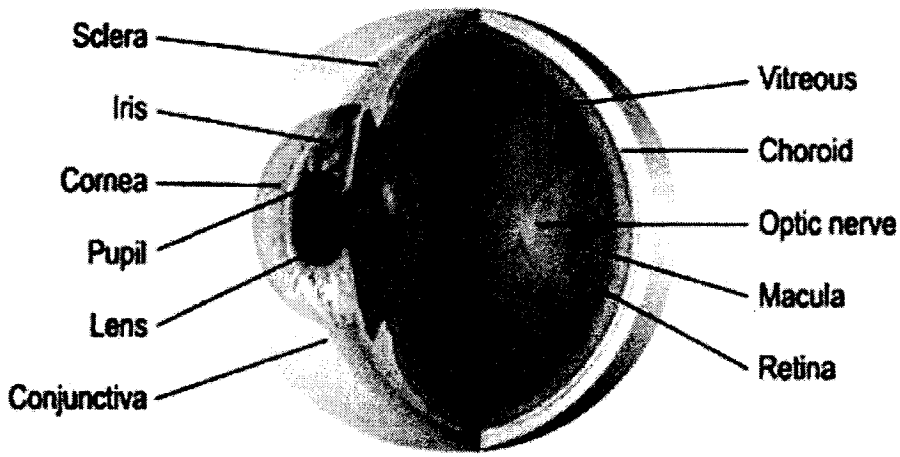

Figure 5: Structure of a human eye [57].

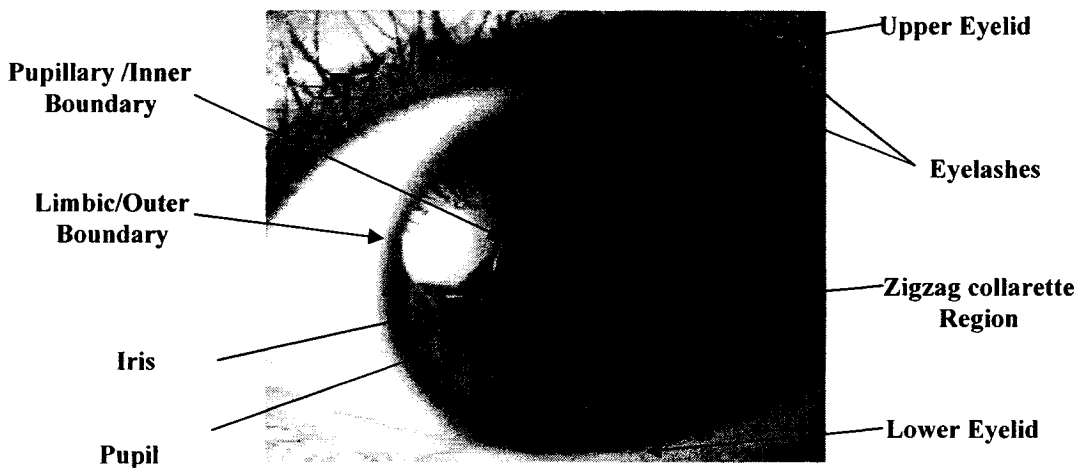

Figure 6: Different parts of an eye image.

The prime objectives of the ICE projects are to promote the development and advancement of iris recognition technology and assess its state-of-the-art capability. The ICE projects encourage the biometric researchers to participate from academia, industry and research institutes.

2.2.1 A Typical Iris Recognition System

A typical iris recognition system is shown in Figure 7. It consists of three major building blocks ([55], [56]):

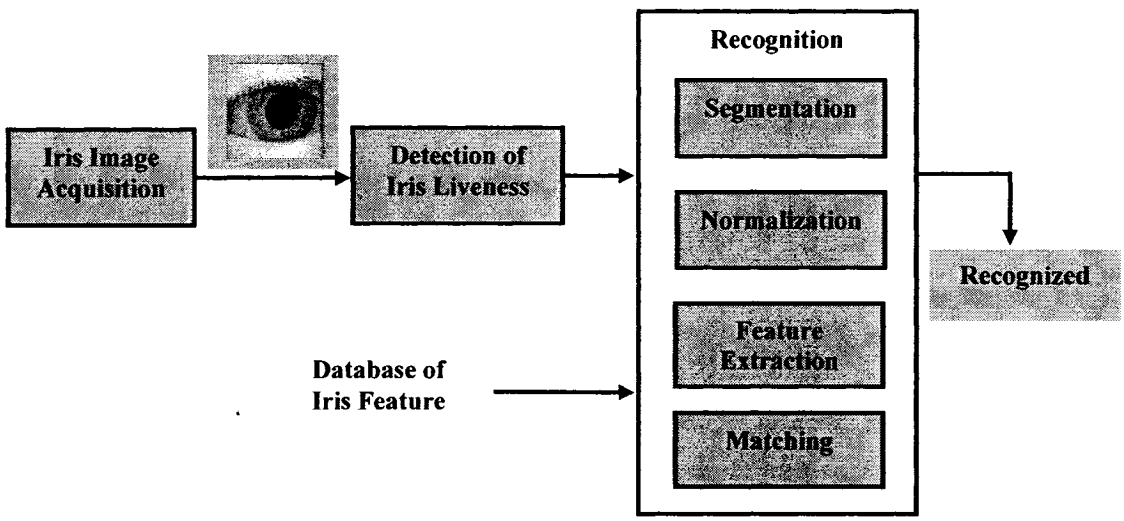

Figure 7: Diagram of a typical iris recognition system.

- Iris Image Acquisition: Image acquisition is considered as the most critical step for building the iris recognition system since all subsequent stages depend highly on the image quality. Another challenge of capturing the iris images is due to the smaller size of the iris and exhibition of more abundant texture features of iris under infrared lighting. A specifically designed sensor is used to capture the sequence of iris images. An iris image capturing device considers the following

three key factors [55]: 1) the lighting of the system, 2) the position of the system, and 3) the physical capture system.

- Detection of Iris Liveness: In order to avoid the forgery and the illegal usage of iris biometric features, the detection of iris liveness ensures that the captured input image sequence comes from a live subject instead of an iris picture, a video sequence, a glass eye, and other artifacts. No such major researches have been conducted for iris liveness detection except for [17] and [98]. The utilization of the optical and physiological characteristics of the live eye is considered as the most important aspects for the assurance of the liveness of the input iris image sequence.
- Recognition: The accuracy of the iris recognition system depends on this module. This module can be further subdivided into four main stages: Segmentation, Normalization or Unwrapping, Feature extraction, and Matching. In the first stage, the iris region is localized from the eye image, the segmented iris region is normalized in order to avoid the size inconsistencies in the second stage, then the most discriminating features are extracted from the normalized image and finally, the extracted features are used for matching with the known pattern in the feature database.

2.2.2 Approaches of Iris Recognition

From the extensive literature review, we divide the iris recognition approaches roughly into four major categories based on feature extraction strategy: Phase-based approaches ([15], [16], [17]), zero-crossing representation approaches ([5], [76]), texture-analysis based approaches ([1], [52], [53], [55] [66], [98], [102]) and intensity variation analysis approaches ([54], [56]).

- Phase-based approach: In this method, the iris structure is encoded by demodulating it with Gabor wavelets. Each phasor is quantized in the complex plane to the quadrant in which it lies for each local element of the iris structure, and this operation is repeated all across the iris, at different scales of analysis [16].
- Zero-crossing representation approach: The zero-crossing representation of the 1D wavelet transform at different resolution levels of a concentric circle on an iris image is used to characterize the texture of the iris [5].
- Texture-analysis based approach: The iris pattern provides abundant texture information and it is desirable to explore the representation scheme to acquire the local information in an iris. According to the iris recognition approach based on texture analysis, the discriminating frequency information of the local spatial pattern in an iris is captured which reflect the significant local structure of the iris [55].
- Intensity variation analysis approach: In this scheme, the local sharp variation is used to represent the distinctive structure of the iris. The most discriminative variations of an iris image are characterized by constructing a set of 1-D signals by adopting wavelet transform to represent these signals [56].

In this research work, we adopt the phase-based approach for feature extraction.

2.2.3 Iris Recognition System Errors

The following terminologies are vastly used to estimate the errors of an iris recognition system:

- False Accept (FA): Accepting an imposter as an authorized subject. The probability at which the false accept errors are occurred is called False Accept Rate (FAR).
- False Reject (FR): Rejecting an authorized subject incorrectly. The probability at which the false reject occurs is denoted as False Reject Rate (FRR).
- Equal Error (EE): When the FA and FR are equal, the error is referred as equal error (ER) and the probability at which FAR=FRR, is called Equal Error Rate (EER).

Generally, the verification performance of an iris recognition system is demonstrated using the Receiver Operator Characteristics (ROC) curve. If the functions FAR (t) and FRR (t) provide the error rates when the recognition decision is made at a threshold t, the ROC curve is used to plot the error rates against each other:

$$ROC(t) = (FAR\ (t), FRR\ (t)) \tag{2.1}$$

The FAR and FRR are mapped as a function of t:

$$ROC(t) = (FAR(t), FRR(t)) \rightarrow \begin{cases} (1,0) & when\ \ t \rightarrow -\infty \\ (0,1) & when\ \ t \rightarrow \infty \end{cases} \tag{2.2}$$

which implies that if the t is high, the FRR is high and FAR is low and conversely when t is low, the FAR is high and FRR is low.

2.2.4 Strengths and weaknesses of Iris as Biometric for Recognition

Though the usage of iris as biometric has been considered as the most robust and accurate biometric, it has some inherent pitfalls that cannot be overlooked. The major strengths and weaknesses of the iris for recognition are pinpointed as follows:

2.2.4.1 Strengths of Iris for Recognition

- Iris is well protected and an internal organ of the eye. It contains high degree of randomness [105].
- Iris is externally visible and iris image acquisition is possible from a distance [105].
- Iris pattern does not change throughout the lifetime of a person and it is assumed that each individual has a unique iris pattern [57].
- It is possible to encode the iris pattern and decidability is tractable.
- No evidence of genetic pentrance has been found in the structure of the iris. Therefore, the iris structure of both eyes of the same person and those of the identical twins are different [57].
- Iris recognition itself incurs extremely low maintenance costs and offers seamless interoperability between different hardware vendors, and this technology also has the ability to work well with other applications.

2.2.4.2 Weaknesses of Iris for Recognition

- It is difficult to capture the iris image since the size of the iris is very small (approximate diameter is 1 cm). A specialized camera is needed to acquire the iris images with an extensive apparatus setup.
- The iris could be partially occluded by lower and upper eyelids, and obscured by eyelashes, reflections, and lenses ([57], [105]).
- Non-elastic deformation as the size of the pupil changes is another source of pitfall to use the iris as biometric.
- Iris image enrollment procedure takes more time since the iris image acquisition is a difficult task.

2.2.5 Challenges in Iris Recognition

Even though iris recognition system performs reasonably well with 0% false accept and false reject rate ([15], [16], [17], [55]), there are still few issues that should be resolved. The challenges that should be overcome are listed below:

- Acquisition of iris images of high quality is one of the major challenges for practical applications as the iris is fairly small and reveals more abundant texture features under infrared lighting [55].
- Though iris liveness detection is highly desirable, the efforts on iris liveness detection are still limited. Since biometric features can be forged and used illegally, the iris liveness detection is an important issue in this area ([55], [56]). It aims to ensure that an input image sequence is from a live subject instead of an iris photograph, a video playback, a glass eye, or other artifacts.
- Most of the existing iris recognition techniques that are currently available have never been tested on a large scale database. Since iris recognition technology requires reasonably controlled and cooperative user interaction, creation of a large database has been a great problem [57].
- The development of a standard iris image quality assessment technique is still a challenging issue in iris recognition area. No such standard methods for acquiring the iris images have been introduced yet. The lack of a proper standard for iris images makes it difficult to compare various techniques on a common platform ([55], [56], [57]).
- Recall that most of the current researches on iris recognition system can be divided into four categories based on feature extraction, namely: The phase-based methods,

the zero-crossing representation, texture analysis, and intensity variation analysis. However, the question of which approach is most suitable for extracting iris features has still remained unanswered.

- None of the iris recognition approaches to date describe the actual process of defining the iris pattern even though several systems for iris recognition are available. A user specific matching algorithm could be used for recognition if the iris pattern is analyzed and characterized correctly ([57], [105]).

2.2.6 Applications of Iris Recognition

We enlist the application areas of iris recognition as follows ([15], [16], [17], [105]):

- The iris can be used as a living passport in national border control system.
- Instead of memorizing a password for computer login, the iris can be applied as a living password.
- The iris is used for mobile and wireless-device-based authentication.
- The iris may be used for secured access to bank accounts at cash machines and financial transaction.
- The iris may be used in traveling which leads to a ticketless traveling.
- It can be applied in driving licenses and for credit card authentication.
- The iris may replace the existing identification technologies such as keys, cards, PINS, or passwords.
- It may be applied for rapid processing of passengers through the immigration procedure who have pre-registered their iris images.
- An important usage of iris recognition is in internet security where controlled access to the privileged information is necessary.

- Forensics and birth certificates are some other areas of application of iris recognition.
- Iris recognition technology can be deployed in automobile ignition, unlocking and anti-theft devices.

2.2.7 Issues in Iris Recognition

The following important issues could be raised to implement an iris-based solution:

- Iris recognition technology requires reasonably controlled and cooperative user interaction; the enrollee must hold still in a certain spot, even if only momentarily. Many users struggle to interact with the system until they become accustomed to its operations [57].
- In applications whose user interaction is frequent (e.g. employee physical access), the technology grows easier to use, however, applications in which user interaction is infrequent (e.g. national ID) may encounter ease-of-use issues. Over time, with improved acquisition devices, this issue should grow less problematic ([70], [57]).
- Since iris technology is designed to be an identification technology, fallback procedures may not be as fully developed as in a verification deployment (users accustomed to identification may not carry necessary ID, for example) [6].

2.3. Related Work

The concept of automated iris recognition was first proposed by Flom and Safir in 1987 [24]. Since then, many researchers worked on iris segmentation, feature extraction, recognition process and have achieved a great progress in this area. In ([15], [16], [17]), the multiscale Gabor filters were applied to demodulate the texture phase structure information of the iris. A 1024 complex-valued phasor which denotes the phase structure

of the iris at different scales was produced by filtering an iris image with a family of filters. Each phasor was then quantized to one of the four quadrants in the complex plane. The resulting 2048-component iriscode was used to represent an iris and the matching between a pair of iriscodes was measured by their Hamming distance. In [5], zero-crossing of the wavelet transform at various resolution levels was calculated over the concentric circles on the iris, and the resulting 1-D signals were compared with model features using different dissimilarity functions. The iris representation method of [5] was further developed in [76] where different distance measures for matching, such as: Euclidean distance and Hamming distance were used. The iris recognition algorithm depicted in [76] exploited the integro-differential operators to detect the inner and outer boundaries of iris, and the Gabor filters to extract unique binary vectors constituting iriscode. In [96], the Hough transform was applied for iris localization, a Laplacian pyramid was used to represent distinctive spatial characteristics of the human iris and the modified normalized correlation was applied for matching process. An iris image was decomposed in [49] into four levels using 2D Haar wavelet transform, the fourth-level high-frequency information was quantized to form an 87-bit code and a modified competitive learning neural network (LVQ) was adopted for classification. In [92], authors introduced an iris detection strategy based on the combination of integro-differential operators with a Hough transform. It consists of first, an edge calculation method, to approximate the position of the eye in the global image and second, integro-differential operators, to search for pupil boundary, iris center and iris boundary. The iris characteristics were analyzed using the analytic image constructed by the original image and its Hilbert transform. Emergent frequency functions were used to extract the local iris

features. The extracted features were encoded to produce the iriscode by thresholding both the modules of emergent frequency, and the real and the imaginary parts of the instantaneous phase. The Hamming distance was used to measure the fraction of disagreeing bits between a pair of iriscodes by a bit by bit comparison.

In [66], the band-pass filtering was applied on the input iris image to reduce the effect of high frequency noise and DC energy difference. The image was then decomposed into eight directional subband outputs using a directional filter bank and the normalized directional energy was extracted as features. Iris matching was performed by measuring the Euclidean distance between the input and enrolled feature vector. The correlation filters were introduced to measure the consistency of the iris images from the same eye in [46] and the two dimensional (2-D) Fourier transform was used to design the correlation filter of each class of training images. The input image was recognized as an authorized subject if the outcome of the correlation filter i.e., the inverse Fourier transform of the product of the Fourier transform of the input image and correlation filter reveals a sharp peak. Otherwise that subject was treated as an imposter. In [1], independent component analysis (ICA) was deployed to generate the optimal basis vectors for the problem of extracting the discriminant feature vectors which was represented as the iris signals. The basis vectors learned by ICA were used to isolate both in the space and frequency domain and the coefficients of the ICA expansion were used as feature vectors. Then, each iris feature vector was encoded as iriscode. The Gabor filters were used to extract the global texture features of iris at different scales and orientations in [52]. In [53], a bank of circular symmetric filters were applied to capture local iris characteristics to form a fixed length feature vector and the nearest feature line (NFL) approach was used for

recognition purpose. A Gaussian-Hermite moments-based method was developed in [54] where the local intensity variations of the iris features were used. In [55], the quality of each image of an input sequence was assessed and a clear image was selected from such a sequence for further recognition. The local characteristics of the iris were captured to produce the discriminating texture features using a bank of spatial filters whose kernels are suitable for iris recognition. Fisher linear discriminant was used to reduce the dimensionality of the feature vector. Then, the nearest center classifier was adopted for classification.

In [56], an iris recognition approach based on characterizing key local intensity variations was proposed. The basic idea was to use the local sharp variation points to represent the characteristics of iris. Feature extraction was performed by constructing a set of 1-D intensity signals to isolate the most important information of the original 2-D image. A position sequence of local sharp variations points in such signals were captured as features using a particular class of wavelets. A matching scheme based on excusive OR operation was then adopted to measure the similarity between a pair of position sequences. In [62], authors presented an algorithm for iris recognition using phase-based image matching. The phase components in 2-D discrete Fourier transform of iris images were used for iris recognition with a simple matching scheme. An iris recognition method based on the histogram of local binary pattern for global iris texture representation and a graph matching scheme for structural classification was proposed in [83]. In [9], a wavelet-based quality measure for iris images was introduced. This approach intended to provide good spatial adaptivity and detect local quality measures for different regions of an iris image. The approach proposed in [11] introduced a private biometrics formulation

based on the concealment of random kernel and the iris images to synthesize minimum average correlation energy for iris authentication. The product of the training images with user-specific random kernel in frequency domain was measured prior to the creation of biometric filter. In [48], a method was proposed to determine the fake iris attack based on Purkinje image to solve the problems found by the previous researchers on fake iris detection. The theoretical positions and distance between the Purkinje images, based on the human eye model, were measured and the efficiency of the fake detection algorithm seemed to be enhanced by using such information. A box counting technique was deployed in [100] to estimate the fractal dimension of the iris for the automatic coarse classification of the iris images. The iris image was isolated into sixteen blocks where eight blocks belonged to the upper group and the remaining blocks to a lower group. The fractal dimension value of these image blocks was calculated and the average value of the fractal dimension was measured. The global iris texture information was used for ethnic classification in [71]. In this scheme, a bank of multichannel 2-D Gabor filters was adopted to capture the iris texture information and AdaBoost was used to learn a discriminant classification principle from the sequence of candidate feature set. Finally, the iris images were categorized into Asian and non-Asian. In [103], a model based/anatomy based method was described to synthesize iris images and to measure the performance of the synthetic irises by adopting a traditional Gabor filter. The local independent components extracted from synthetic iris images were compared with the real iris images. In [41], iris recognition technology was applied in mobile phones and an approach of extracting the accurate iris code based on adaptive Gabor filter was proposed. An improvement of the iris localization algorithm was described in [85]. A

binary threshold was calculated, the center of the chords was averaged to coarsely estimate the center and radius of the pupil. Then a circle detection algorithm was used in the binary graphic to precisely locate the pupil. A statistical method was exploited to exclude eyelashes and eyelids. The method of wavelet packets decomposition (WPD) was applied for iris recognition in [28]. Singular Value decomposition (SVD) was employed for further feature extraction and compression. The weighted Euclidean distance (WED) was used for the recognition purpose. In order to improve the quality of the captured iris images, an iris quality assessment technique was proposed in [28]. The algorithm considered three distinctive features to distinguish three kinds of poor quality images, namely: Defocus, motion blur and occlusion.

In [34], an iris segmentation method for Hand-held capture device was presented. The pupil was binarized using the intensity threshold, and then the morphological operations were deployed to denoise the eyelids and eyelashes noise. The Hough transform and Canny edge detection technique were applied to localize the outer boundary. A similar approach for iris recognition was applied in [14]. The Hough transform and Canny edge detection were used to find the iris boundary and Haar wavelet technique was employed to extract the iris features. For matching purpose, the Hamming distance technique was applied. In [43], the authors emphasized on the feature extraction. The disc-shaped iris image was convolved with a low pass filter along the radial direction and then the radially smooth iris image was decomposed in the angular direction using 1-D continuous wavelet transform technique. The decomposed 1-D waveform was approximated by an optimal piecewise linear curve which was used to connect a small set of node points and this set was used as feature vector. The normalized cross-correlation coefficients were

used to measure the similarity between two iris images. In [64], the variation of the directional properties of the image intensity was used to describe the iris features. The derivative of grey level was investigated to determine the continuous increase (concave-down) or decrease (concave-up). Only the direction of concavity, not the magnitude, was considered and the Hamming distance was utilized for matching purpose. The wavelet packets were used in [44] for feature extraction and color information of the iris images were considered in wavelet packets to improve the discriminating power of the identification. An appearance-based algorithm for iris detection was proposed in [13]. This method detected the existence of pupil in the image using the SVM. Then twelve sample vectors are selected along the radial direction from the center of the pupil. These vectors determine the iris-like structure outside the pupil using the Linear Discriminant Analysis (LDA). Finally, a decision was made by combining the above two results. In [50], a modification to the Hough transform was made to improve the iris segmentation and an eyelid detection technique was used where each eyelid was modeled as two straight lines. In [51], a Daugman-like iris matching method was implemented and its performance was evaluated on an image dataset of over 12,000 images from over 300 persons, with iris images of different qualities. A system was proposed in [63] that may analyze the eye region images in terms of the position of the iris, degree of eyelid opening, and the shape, complexity and texture of the eyelids. A generative eye region model was used by this system to parameterize the structure and motion of an eye. The individuality of the eye was represented by the structure parameters, while the motion parameters represent the movement of eye. The eye model was registered in a specific frame and individualized by adjusting the structure parameters. The motion of the eye

was tracked by calculating motion parameters by estimating the entire image sequence. A biometric system was introduced in [98] based on the processing of the human iris by the dyadic wavelet transform and iris signature of 256 bits was used for recognition. In [77], the main emphasis was applied in order to obtain low template size of 256 bits and fast verification algorithms. The effort was intended to enable a human authentication in small embedded systems, e. g., an Integrated Circuit Card. A technique to represent the features of the iris by fine-to-coarse approximations was described in [60] at different resolution levels based on the discrete dyadic wavelet transform zero-crossing representation. The extracted 1-D signals were compared with model features using different distances. Before feature extraction, a pre-processing was accomplished by image processing techniques, isolating the iris and enhancing the area of study. The technique was based on translation, rotation and scale invariant.

An approach of iris pattern extraction by utilizing the least significant bit plane was introduced in [7]. The pupillary boundary of the iris was determined through the application of binary morphology to the bit-plane and the limbic boundary was identified by evaluating the standard deviation of the image intensity along the vertical and horizontal axes. In [102], multi-channel Gabor filtering and wavelet transform were used for feature extraction. In [21], an adaptive thresholding was proposed for iris identification. The iris images were processed in the spatial domain using distinct features of the iris. An adaptive thresholding was used to segment the patterns from the rest of the iris image. A biometric system for the identification of people was proposed in [79], called Eyecerts. Eyecerts achieved offline verification of the certified and cryptographically secure documents. In the proposed Eyecert system, an iris analysis

technique was used to extract and compress the unique features from specific iris image by a discriminating criterion using a limited storage. This iris analysis algorithm was divided into three phases: First, the detection of iris using a model based approach which can compensate for the noise incurred by eyelids and eyelashes, second, the conversion of the detected iris into a standard domain using modified Fourier–Mellin transform, and third, the optimal selection, alignment and compression of the most distinctive transform coefficients. A dual-factor authentication methodology, named as S-Iris Encoding, was introduced in [10] based on the iterated inner-products among the secret pseudo-random number, the iris feature and with the thresholding to produce a unique compact binary code per person. The thresholding approach was devised to exclude the weak inner-product during the encoding process to improve the performance. S-Iris Encoding was developed based on the cancelable biometrics principle to protect against biometrics fabrication. In [81], an iris recognition system was described using an artificial neural network model in the form of multi-lever perception using back propagation algorithm and generalized delta rule. An approach for performance analysis of iris-based identification system at the matching score level was proposed in [78]. The major processing stages of the system was designed to include enhancement and transformation of an input iris image into a pseudo polar representation, encode using Gabor wavelets, and for a component-by-component quantization into two levels based on the sign of the corresponding filtered image entry. In [12], an iris image synthesis method based on Principal Component Analysis (PCA) and super-resolution was proposed. The iris recognition algorithm based on PCA was first introduced and then, iris image synthesis method was presented. The synthesis method constructed the coarse iris images with the

given coefficients and then, the synthesized iris images were enhanced using super-resolution. An algorithm was proposed in [37] for the resolution enhancement of iris images captured by the low resolution camera in less cooperative situations. The artificial color filtering was used in [26] which can provide an orthogonal discriminant to the spatial iris pattern. In [87], eye blink states were determined by tracking iris and eyelids. In [89], 1-D log polar Gabor wavelet was deployed to extract the textural features and Euler numbers were used for topological feature extraction. A new iris image acquisition method to capture the focused eye images at very fast speed was introduced in [89] based on corneal specular reflection. In [84], an elastic iris blob matching algorithm was introduced to overcome the limitations of local feature based classifiers (LFC). The idea was intended to recognize various iris images efficiently and a novel cascading scheme was proposed to combine the LFC and an iris blob matcher. In [101], a robust algorithm was presented to extract eye features, including pupil center and radius, eye corners and eyelid contours, from frontal face images. In [68], a new filterbank-based iris recognition method was proposed that could effectively extract the spatial and directional features of iris patterns on multiple scales. The proposed method first localized the iris area from an input iris image and established a region of interest for feature extraction. Second, the iris features were extracted on multiple scales from that region and a feature vector was generated using a band pass filter and directional filter bank (DFB), which decomposed the image into several directional subband outputs. Finally, iris pattern matching was performed based on finding the Hamming distance between the corresponding feature vectors.

A few research work has been conducted on MOGA and SVM in iris recognition area. In [30], the steerable pyramid was used for feature extraction while the multi-objectives genetic algorithms were applied for optimum feature selection, and SVM were utilized for classification. The intra-class and inter-class distance measures were utilized by MOGA to exclude the redundant features. In [69], the basis of genetic algorithms was applied to develop a technique for the improvement in the performance of an iris recognition system. The iris region normalization technique described in [69], was developed using the method proposed by Daugman in ([15], [16], [17]). Daugman used a rectangular representation of the iris that was generated from a uniform selection of points along the whole extension of the iris. The work proposed in [69] introduced the idea that if the points are selected non-uniformly over the iris region, it is possible to find a distribution of points to make the system more reliable. The genetic algorithms were used to find a distribution of points for a better accuracy of the system. In [82], the direct linear discriminant analysis (DLDA), as a discriminative learning method, and the multi-resolution wavelet transform for feature extraction were exploited. The similarity measure was estimated using SVM. A methodology was proposed in [99] to establish the discriminative power of iris biometric data. The multi-class problem was transferred into dichotomy by using a distance measure between two samples of the same class and those of two different classes to establish the inherent distinctness of the classes. For feature extraction simple binary and multi-level 2D wavelet features were compared and for distance measures; scalar distances, feature vector distances, and histogram distances were calculated. Finally, the classifiers such as Bayes decision rule, nearest neighbor, artificial neural network, and SVM were used and compared. Based on the performance

of the eleven different combinations, multi-level 2D wavelet feature extraction technique, the histogram distance measure, and a SVM classifier were selected. From the background study, we found that no such works on collarette region have been conducted except for ([33], [86]). An iris segmentation method for recognition was described in [33] where the segmentation approach was based on crossed chord theorem and zigzag collarette area along with the eyelashes detection technique and the claimed recognition accuracy was 100%. In [86], an approach for localizing the iris area between the inner boundary and the collarette boundary was described and the removal of unnecessary areas to increase the recognition rate was proposed. For finding the collarette boundary, histogram equalization and a high pass filter, after using a one-dimensional DFT, were applied to the iris image. The collarette boundary was found using statistical information from the image, which removes low-frequencies. Finally, the iris was localized between the inner boundary and the collarette boundary.

Based on an extensive literature survey, we understood that in most of the state-of-art iris recognition schemes, the main emphasis is given on iris segmentation and feature extraction strategies. No such major researches have been conducted on iris pattern classification and optimum feature selection. None of the iris recognition methods to date have demonstrated the performance of different classification techniques and comparison among them. The optimum feature selection method is another uncovered area in iris recognition except ([30], [55]). In this thesis, we focus on the feature selection and iris patterns classification along with iris segmentation and feature extraction strategies. Furthermore, we emphasize on exploiting the zigzag collarette region since this area provides sufficient discriminative information to characterize the iris. Our earlier

attempts on iris recognition were based on iris segmentation, iris pattern classification techniques and utilization of zigzag collarette area ([72], [73], [74], [75]). We proposed an iris recognition method based on backpropagation neural network in [73] for person identification. In [72], we developed an iris recognition method based on SVM, where we used the information of the whole iris region for recognition purpose and a traditional SVM was used as iris classifiers. In [75], we proposed a novel pupil detection approach based on chain code [25] and the unique pattern of zigzag collarette region was used instead of using the whole iris information for recognition. The pupil detection approach was considered to speed up the iris segmentation process and the usage of zigzag collarette pattern allowed to uniquely identifying a person. The traditional SVM used in ([72], [75]) was further modified in [74] to an asymmetrical SVM [19] and in order to reduce the computational cost, the parameters of SVM were tuned [20]. In this research, we also propose a multi-objectives genetic (MOGA) algorithm to reduce the feature and minimize the recognition error of the matching accuracy along with the mentioned techniques of segmentation, feature extraction and matching strategy proposed in ([72], [73], [74], [75]). We also introduce an approach based on Bhattacharyya distance (BD) and principal component analysis (PCA) for optimum feature selection.

Chapter 3

Iris Image Pre-Processing

3.1. Introduction

The iris is surrounded by various non-relevant iris regions such as the pupil, the sclera, the eyelids, and also noise that include the eyelashes, the eyebrows, the reflections and the surrounding skin [56]. The variation in camera-to-eye position results the inconsistency in the size of the same eye. Furthermore, the intensity level of iris image is not uniformly distributed due to the effect of nonuniform illumination [55]. Therefore, the original iris image needs to be preprocessed to select the pertinent region of the iris as well as to reduce the effect of non-relevant regions and noise before the feature extraction. Generally, preprocessing phase involves three major steps:

- First, iris and pupil are localized,
- Second, the eyelids, eyelashes and other irrelevant parts of iris are removed, and
- Third, localized iris region is unwrapped to a rectangular block of a fixed dimension to reduce the size inconsistencies caused by variations of the pupil and the effect of approximate scale invariance.

In the following sections, we illustrate the proposed steps of preprocessing of the approaches I & II.

3.2. Localization

The iris is an annular part between the pupil (inner boundary) and the sclera (outer boundary). Both the inner boundary and the outer boundary of a typical iris can be approximately considered as circles, however, two circles are not concentric ([55], [56]). In the proposed approach I, we introduce an idea to detect the iris/pupil boundary using the edge detection and Hough transform techniques and then, we remove the eyelids, eyelashes and other irrelevant parts from the iris for subsequent processing. In the proposed approach II, we propose a novel pupil detection method using linear thresholding and chain code [25], and utilize the idea of using the zigzag collarette region instead of whole iris information. We adopt the similar approach applied in the approach I to isolate the irrelevant regions and noise from the zigzag collarette region.

3.2.1 Approach I for Localization using Whole Iris Information

In this approach, we deploy the Hough transform and Canny edge detection techniques to calculate the exact parameters of the iris and pupil.

3.2.1.1 Iris/Pupil Detection

A standard computer vision algorithm called Hough transform is used to determine the exact parameters of iris and pupil. The Hough transform technique is used to detect the shape of a given curve in an image. In classical Hough transform, it is required to specify the curves in some parametric form and hence, this technique is generally used to isolate the regular curves, such as lines, circles, ellipses etc. However, besides the classical approach, the Hough transform can be generalized to detect the arbitrary curved shapes within an image. The main strength of this technique is that it accepts the gaps in the actual object boundaries or curves and it is relatively unaffected by noise. There are also

a number of pitfalls with the Hough transform method. First of all, threshold values are required to be selected for edge detection. This may result in critical edge points being removed, which in turn may fail to detect circles/arcs. Secondly, the Hough transform is computationally intensive due to its 'brute-force' approach, and thus is not suitable for real time applications.

An automatic localization algorithm based on the circular Hough transform is employed for inner and outer boundaries detection ([56], [92], [98]). Firstly, an edge map is generated by calculating the first derivatives of intensity values in an image and a threshold is applied on the result. From the edge map, votes are cast in the Hough space to estimate the parameters of circles passing through each edge point ([61], [106]). These parameters are the centre coordinates x_c and y_c, and the radius r, which define circle according to the equation

$$x^2{}_c + y^2{}_c - r^2 = 0 \tag{3.1}$$

A maximum point in the Hough space represents the radius and edge points denote the centre coordinates of the circle. In this phase of the thesis, a parabolic Hough transform is employed to detect the eyelids, approximating the upper and lower eyelids with parabolic arcs, which are represented as

$$\left(-\left(x-h_j\right)\sin\theta_j+\left(y-k_j\right)\cos\theta_j\right)^2 = a_j\left(\left(x-h_j\right)\right)\cos\theta_j+\left(\left(y-k_j\right)\sin\theta_j\right) \tag{3.2}$$

where a_j controls the curvature, (h_j, k_j) is the peak of the parabola, and θ_j is the angle of rotation relative to X-axis. The edge detection technique is deployed by taking the derivatives in horizontal direction to detect the eyelids since the eyelids are considered to be horizontally aligned, furthermore, the eyelid edge map corrupts the circular iris boundary edge map, if all gradient data are considered. The derivatives are taken in the

vertical direction to detect the iris boundary as illustrated in Figure 8. The effect of the eyelids can be removed if vertical gradients for locating the iris boundary can be used while performing the circular Hough transform, and moreover, not all of the edge pixels defining the circle are required for successful localization. In this thesis, an edge map is generated by first employing canny edge detection. Gradients are biased in the vertical direction for the outer iris/sclera boundary, as suggested by [98].

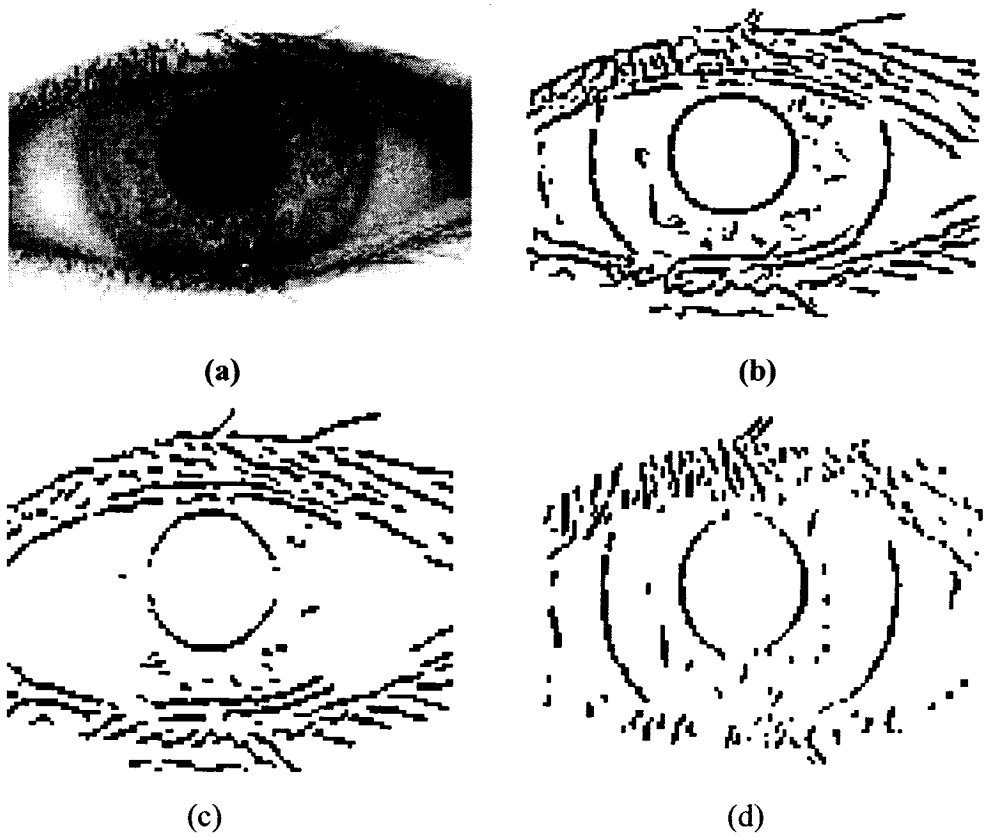

Figure 8: (a) Original eye image (b) edge map of the corresponding eye image (c) edge map with horizontal gradients (d) edge map with vertical gradients.

Vertical and horizontal gradients were weighted equally for the inner iris/pupil boundary. In order to make the circle detection process more efficient and accurate, the Hough

transform for the iris/sclera boundary is performed first, then the Hough transform for the iris/pupil boundary is applied within the iris region instead of the whole eye region since the pupil is always within the iris region. Figure 9 illustrates the iris/pupil localization process.

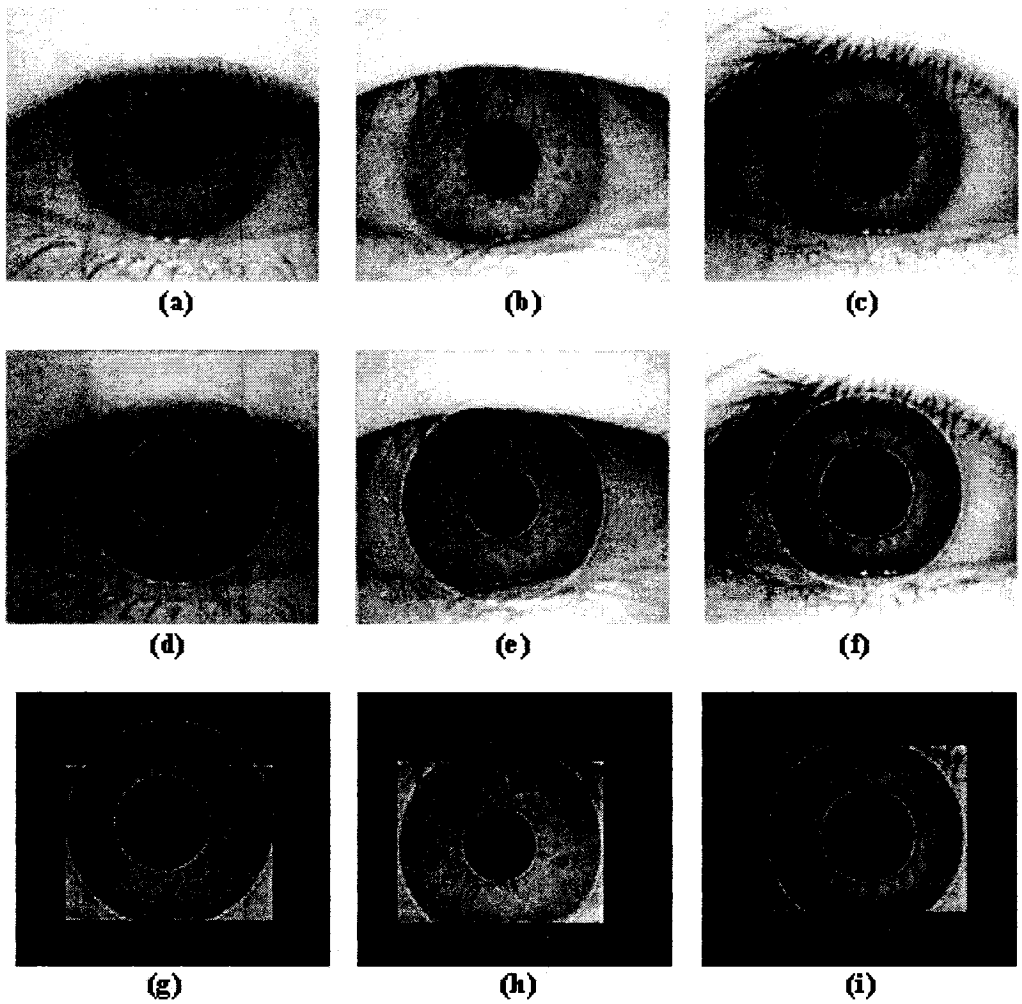

Figure 9: Localization process for approach I (a), (b), (c) are sample iris images, (d), (e), (f) are corresponding images with the localized iris/ pupil boundary, and (g), (h), (i) show the corresponding images after eyelids and eyelashes detection.

3.2.2 Approach II for Localization based on Zigzag Collarette Region

In the proposed approach II for localization, iris is localized from the original eye image using the previous knowledge of the iris, and then the pupil is detected using thresholding and chain code. The zigzag collarette region is isolated using the parameters obtained from the localized pupil.

3.2.2.1 Iris Localization

From an empirical study [33], it is found that an imaging system should resolve a minimum of 70 pixels in iris radius to capture the rich details of iris patterns. In most implementations of these algorithms to date, a resolved iris radius of 100 to 130 pixels has been more typical. Therefore, we can use this prior information to approximately locate the iris from the original eye image. In this proposed approach for localization, the Canny edge detection and Hough transforms are used to compute the center values and radius of the iris. This iris localization process results in reducing the search space since the pupil detection process is performed only within the previously obtained iris region. Therefore, this step eliminates some irrelevant regions from the whole eye image for subsequent processing, which in turn results a lower computational cost.

3.2.2.2 Pupillary Localization

To localize the pupil within the predetermined iris region, a linear threshold and chain code ([25], [94]) for 8-connected boundaries, see Figure 10, are applied. The detailed steps are as follows:

1) To find the pupil boundary, a linear threshold is applied:

$$g(x) = \begin{cases} 1 & if \quad f(x) > 65 \\ 0 & if \quad f(x) \leq 65 \end{cases} \tag{3.3}$$

Here f denotes the original image and g is the thresholded image. In this thesis, intensity value of the pixels greater than 65 is assigned as 1 (as white) in 0-256 gray-scale images and the intensity level of pixels less than or equal to 65 are converted to 0 (as black).

2) Chain code [25] is then used to find the 8-connected regions of pixels that are assigned with value equal to 1. Eyelashes may satisfy the applied thresholding condition, however, the eyelash area is much smaller than pupil area. Using this previous knowledge, we traverse all the regions of the localized iris image and a '0' value is assigned to all pixels of the region where the area of a region is less than 2500 pixels.

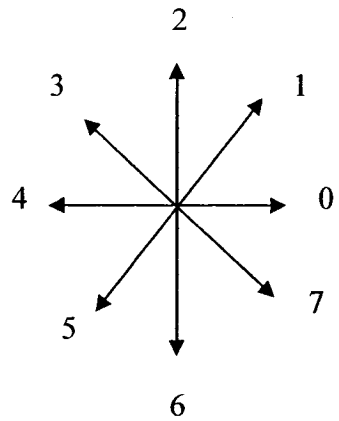

Figure 10: Chain code directions for 8-connected boundaries.

3) Chain code is applied again to retrieve the pupil region. From this region, the central moments are estimated and the edges of the pupil are obtained with the creation of two imaginary orthogonal lines passing through the centroid of the region. The boundaries of the binarized pupil are defined by the first pixel with intensity zero, from the center to the extremities. Figure 11 illustrates overall pupillary localization process.

3.2.2.3 Isolation of Zigzag Collarette Area

Iris complex pattern provides many distinguishing characteristics such as arching

ligaments, furrows, ridges, crypts, rings, freckles, coronas, stripes, and zigzag collarette area ([55], [56]). Zigzag collarette area is one of the most important part of the iris complex pattern, see Figure 12.

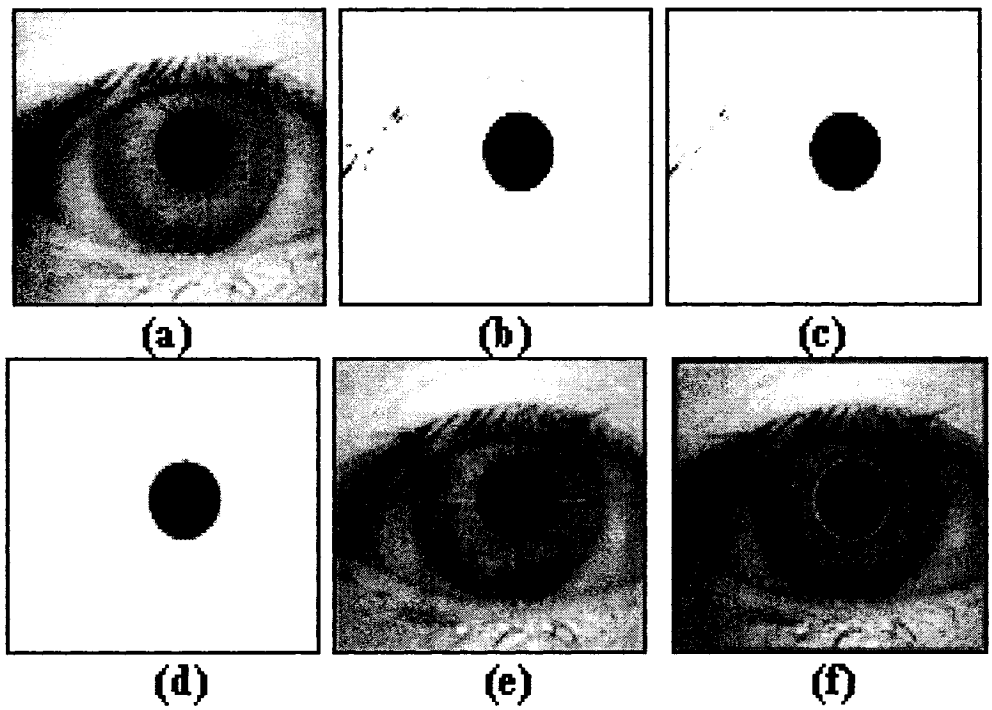

Figure 11: (a) Original eye image (b) thresholded image (c) image after applying chain code algorithm (d) small region elimination (e) detected center and radius of pupil (f) localized pupil.

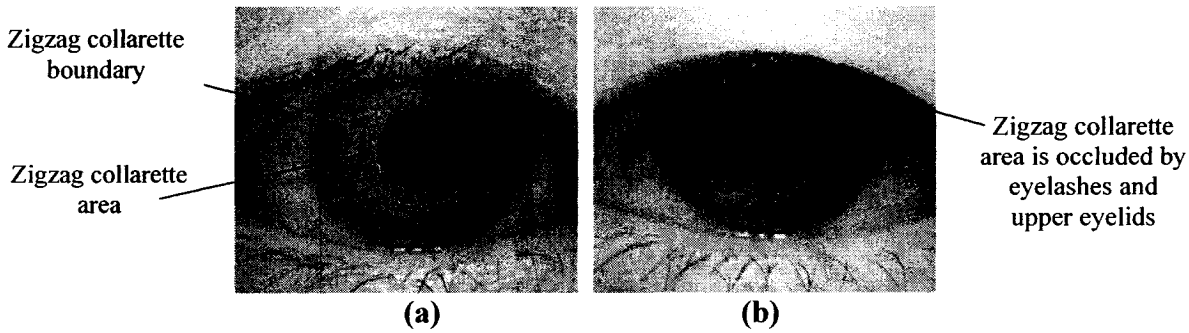

Figure 12: (a) Circle around the pupil indicates the zigzag collarette region (b) zigzag collarette area is occluded by eyelashes and upper eyelids.

This collarette region is usually insensitive to the pupil dilation and not affected by eyelids and eyelashes unless the iris is partly occluded since it is closed with the pupil. From the empirical study it is found that zigzag collarette region is generally concentric with the pupil and the radius of this area is restricted in a certain range. The zigzag collarette area is detected using the previously obtained center values and radius of the pupil, see Figure 13.

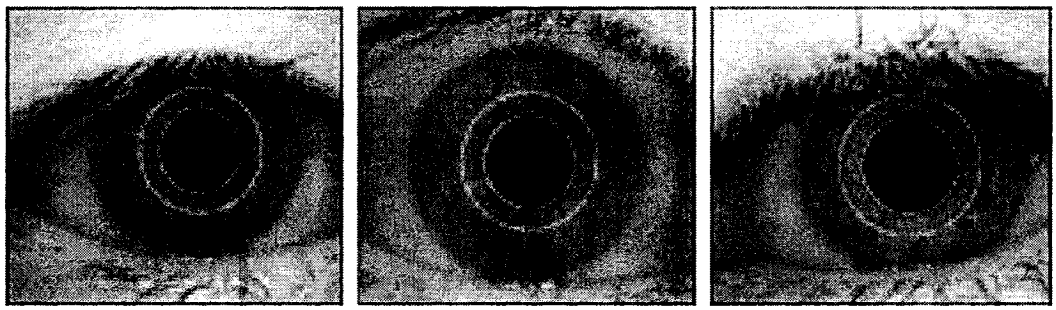

Figure 13: (a), (b) and (c) show zigzag collarette area localization from CASIA iris database.

3.2.3 Eyelids and Eyelashes Detection

We need to remove the noise area from the iris image to improve the iris recognition accuracy. An iris image consists of irrelevant parts such as eyelids, eyelashes, reflections etc. In this thesis, Eyelids are isolated by first fitting a line to the upper and lower eyelids using the linear Hough transform [106]. A second horizontal line is then drawn, which intersects with the first line at the outer edge (iris or zigzag collarette region) that is closest to the pupil. Eyelashes are treated as belonging into two types, namely: The separable eyelashes and the multiple eyelashes [45]. Separable eyelashes are isolated in the image, and multiple eyelashes are bunched together and overlapped in the eye image. Separable eyelashes are detected using 1D Gabor filters, since a low output value is

produced by convolution of a separable eyelash with the Gaussian smoothing function ([45], [61]). Thus, if a resultant point is smaller than a threshold, it is noted that this point belongs to an eyelash. Multiple eyelashes are detected using the variance of intensity and if the values in a small window are lower than a threshold, the centre of the window is considered as a point in an eyelash. Figure 9 (g, h, i) shows the segmented iris images after the eyelids and eyelashes separation in the approach I and the isolated zigzag collarette region is depicted in Figure 14 after applying the similar technique for eyelids and eyelashes detection in proposed approach II.

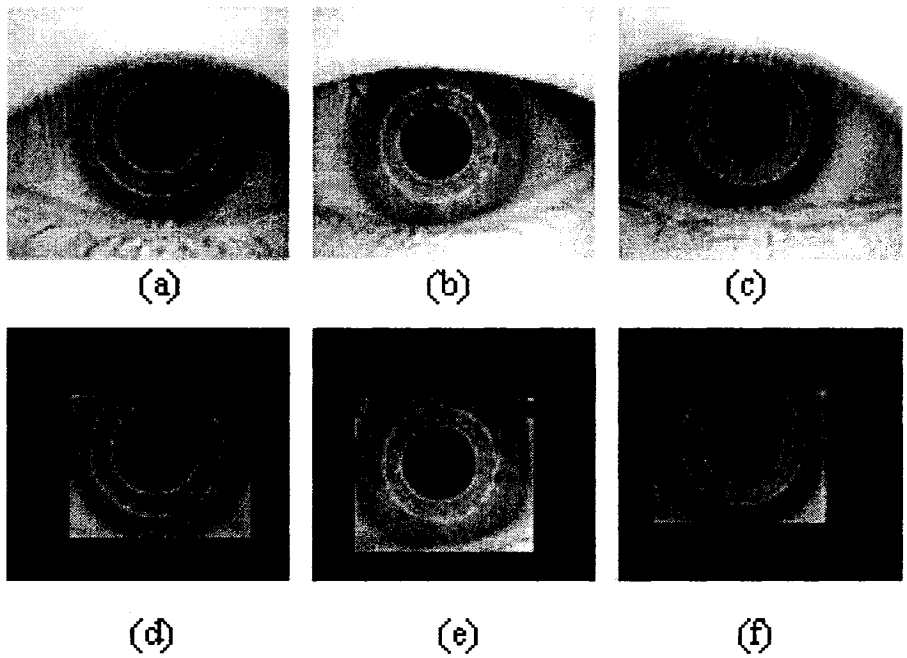

Figure 14: (a), (b), (c) are CASIA iris images with the detected zigzag area and (d), (e) and (f) are the corresponding images after detection of eyelids and eyelashes.

3.3. Unwrapping or Normalization

Once the iris region or zigzag collarette area is successfully localized, the next step is to unwrap or normalize the localized region into a fixed dimension for further comparison.

The captured iris images from different persons may differ in sizes and even for irises from the same eye, the size may change mainly due to stretching of the iris caused by pupil dilation from variations of illumination. The other sources of dimensional inconsistencies include changes of the camera-to-eye distance, rotation of the camera, head tilt, and the rotation of the eye within the eye socket ([55], [56]). These elastic deformations in the iris texture affect the recognition accuracy. In order to achieve more accurate matching results, it is necessary to compensate for such deformation.

We apply the homogenous rubber sheet model proposed by Daugman ([15], [16], [17]) to unwrap the localized region. Each point within the localized region is mapped to a pair of polar coordinates (r, θ) where r is on the interval [0, 1] and θ is angle $[0, 2\pi]$, see Figure 15.

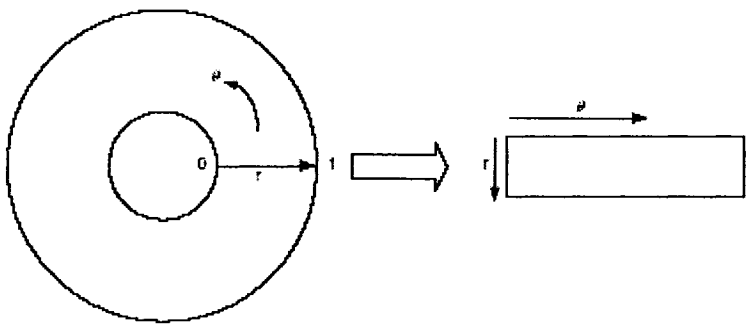

Figure 15: Rubber sheet model to unwrap the localized region.

The localized region is mapped from Cartesian coordinates to normalized non-concentric polar representation of fixed size using the following procedure

$$I(x(r,\theta), y(r,\theta)) \rightarrow I(r,\theta) \tag{3.4}$$

where $x(r,\theta) = (1-r)x_p(\theta) + rx_i(\theta)$ and

$$y(r,\theta) = (1-r)y_p(\theta) + ry_i(\theta)$$

Here, *I(x,y)* is the localized (iris or zigzag collarette) image, *(x,y)* are the original Cartesian coordinates, *(r ,θ)* are the corresponding normalized polar coordinates. The rubber sheet model considers several pupil dilation and size inconsistencies to produce a normalized representation of localized image with constant dimension. In this way the localized region is modeled as a flexible rubber sheet anchored at the iris or collarette boundary with the pupil centre as the reference point. The centre of the pupil is considered as the reference point, and radial vector is passed through the iris region. Figure 16 shows the unwrapped iris image for the approach I where the whole isolated iris region is normalized. Since the unwrapped iris image has relatively low contrast and may have nonuniform intensity values due to the position of the light sources, simple histogram equalization technique is applied to enhance the quality of normalized iris image which increases the recognition accuracy as illustrated in Figure 17.

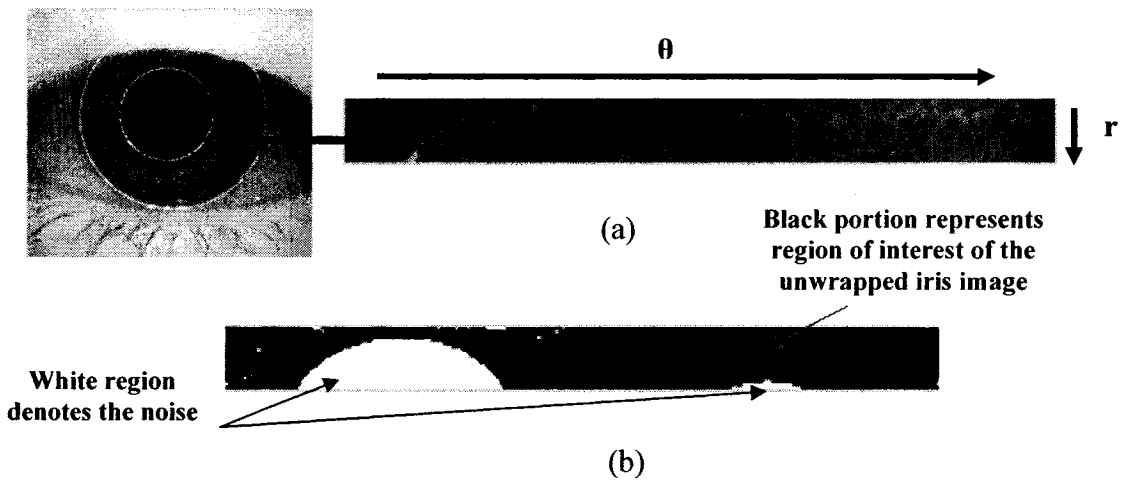

Figure 16: (a) Unwrapping an iris image (b) noise areas are marked for the corresponding unwrapped iris image.

In the approach-II, the isolated zigzag collarette region is also unwrapped to a fixed dimension for subsequent comparisons. The successful normalization process produces a

zigzag collarette region with a constant dimension so that the iris images of the same eye under different conditions will have the iris characteristic features at the same spatial condition.

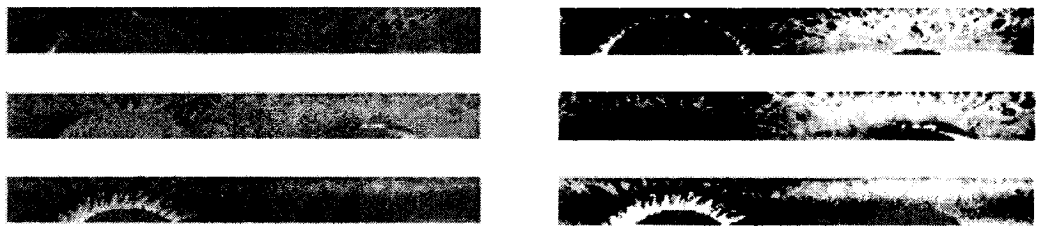

(a) (b)

Figure 17: Histogram equalization (a) before enhancement (b) after enhancement.

The rubber sheet model mentioned before is deployed again to normalize the isolated zigzag collarette area. Figure 18 demonstrate the unwrapped collarette region using the rubber sheet model. Figure 19 (a, b, c) shows the normalized images after the isolation of the zigzag collarette area. Figure 19 (d, e, f) also shows the effect of enhancement on the normalized iris images.

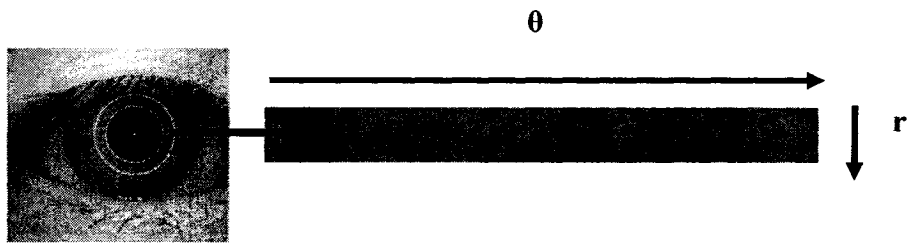

Figure 18: Unwrapping the zigzag collarette region.

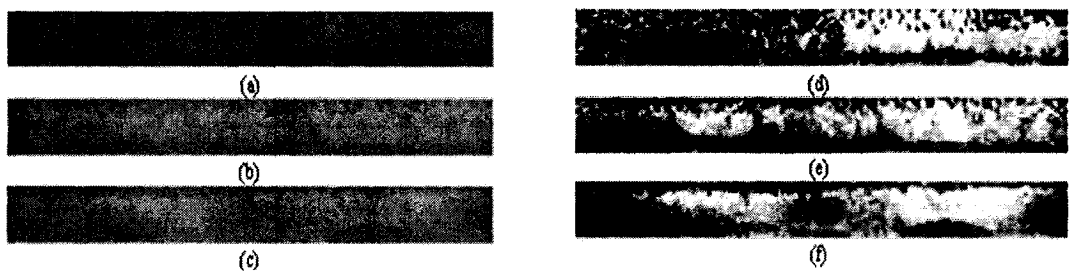

Figure 19: (a), (b), (c) show the unwrapped collarette region before enhancement and (d), (e), (f) reveal the collarette region after enhancement.

Chapter 4

Feature Extraction and Selection

4.1. Introduction

The most distinctive features are required to be extracted from the localized iris region for accurate identification of persons. The most significant features are needed to be encoded to construct the iris patterns to compare between several iris patterns for recognition. Due to the extraordinary structure and rich texture information of iris, it is desirable to explore representation methods which can capture local underlying information in an iris [55]. Features involved in an image are categorized as follows:

- Spectral features: special color or tone, gradient, spectral parameter etc.
- Geometric features: edge, lineament, shape, size, etc.
- Textural features: pattern, spatial frequency, homogeneity, etc.

In this thesis, we focus on textural features since the human iris provides many interconnected minute characteristics namely freckles, coronas, stripes, furrows, crypts and collarette region which are referred as the texture of the iris and these visible characteristics are unique to each subject [56].

In many real world problems, dimensionality reduction of features is an essential step before any analysis of data can be performed. The general criterion for reducing the

dimension is to preserve the most of the relevant information of the original data according to some optimality criteria. Actually, feature selection procedure maps the original feature spaces to a lower dimensional feature space. In some applications, it might be required to pick a subset of the original features rather then find a mapping that uses all of the original features. The benefits of finding this subset of features could be in cost of computations of unnecessary features, and cost of sensors. In this thesis, three approaches for feature selection are deployed and best one is chosen for optimum feature selection.

4.2. Feature Extraction and Encoding

In proposed approaches I & II, the Gabor wavelet technique is utilized to extract the most discriminative features from the unwrapped iris region. First, we provide a basic theory of Gabor wavelets, and then we introduce the feature extraction approach using the Gabor wavelet technique.

4.2.1 Gabor Wavelets

Wavelets are used to decompose the data in the iris region into components that appear at different resolutions. A number of wavelet filters, also called a bank of wavelets, is applied to the 2D iris region, one for each resolution with each wavelet as a scaled version of some basis functions ([15], [16], [17], [61]). The output is then encoded in order to provide a compact and discriminating representation of the iris pattern. A Gabor filter is constructed by modulating a sine/cosine wave with a Gaussian. This allows providing the optimum conjoint localization both in space and frequency, since a sine wave is perfectly localized in frequency, but not localized in space. The decomposition of a signal is accomplished by using a quadrature pair of Gabor filters, with a real part

specified by a cosine modulated by a Gaussian, and an imaginary part specified by a sine modulated by a Gaussian. The real and imaginary filters are also known as the even symmetric and odd symmetric components respectively. The centre frequency is specified by the frequency of the sine/cosine wave, and the bandwidth of the filter is specified by the width of the Gaussian. In [16], Daugman used a 2D version of Gabor filters in order to encode iris pattern data. A 2D Gabor filter over an image domain (x, y) is represented as

$$G(x, y) = e^{-\pi\left[(x-x_0)^2/\alpha^2+(y-y_0)^2/\beta^2\right]} \quad e^{-2\pi i[u_0(x-x_0)+v_0(y-y_0)]} \tag{4.1}$$

where (x_0, y_0) specifies position in the image, (α, β) denotes the effective width and length, and (u_0, v_0) indicates modulation, which has spatial frequency $\omega_0 = \left(u^2{}_0 + v^2{}_0\right)^{1/2}$. The odd symmetric and even symmetric 2D Gabor filters are shown in Figure 20. Daugman [15] used polar coordinates for normalization and in polar form the filters are given as

$$H(r, \theta) = e^{-i\omega(\theta-\theta_0)} e^{-(r-r_0)^2/\alpha^2} e^{-i(\theta-\theta_0)^2/\beta^2} \tag{4.2}$$

where (α, β) are the same as in (4.1) and (r_0, θ_0) specify the centre frequency of the filter. The demodulation and phase quantization process can be represented as

$$h_{\{R_e, I_m\}} = \mathrm{sgn}_{\{R_e, I_m\}} \int_{\rho} \int_{\phi} I(\rho, \phi) \quad e^{-i\omega(\theta_0-\phi)} e^{-(r_0-\rho)^2/\alpha^2} e^{-(\theta_0-\phi)/\beta^2} \tag{4.3}$$

where h{Re, Im} can be regarded as a complex-valued bit whose real and imaginary components are dependent on the sign of the 2D integral, and $I(\rho, \varphi)$ is the raw iris image in a dimensionless polar coordinate system.

4.2.2 Log-Gabor Filters

Gabor filters based methods have been widely used as feature extractor in computer vision, especially for texture analysis [33]. However, one weakness of the Gabor filter is

that the even symmetric filter will have a DC component whenever the bandwidth is larger than one octave. To overcome this disadvantage, a type of Gabor filter known as log-Gabor filter, which is Gaussian on a logarithmic scale, can be used to produce zero DC components for any bandwidth. The log-Gabor function more closely reflects the frequency response for the task of analyzing natural images and is consistent with measurement of the mammalian visual system [10].

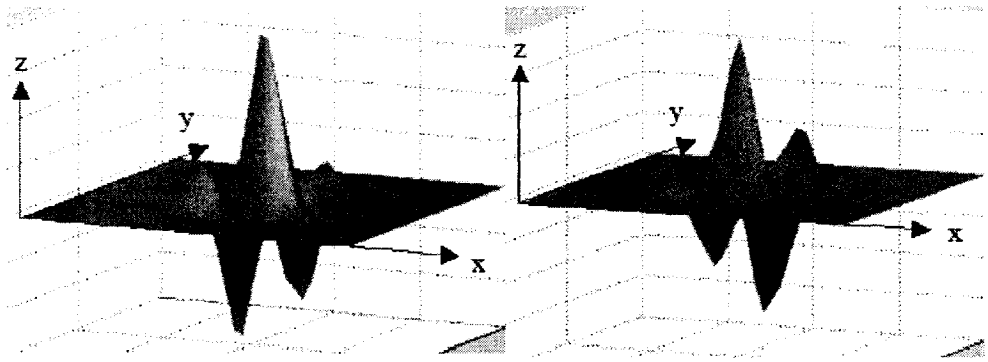

(a) (b)

Figure 20: A quadrature pair of 2D Gabor filters a) real component or even symmetric filter characterized by a cosine modulated by a Gaussian b) imaginary component or odd symmetric filter characterized by a sine modulated by a Gaussian [61].

The log-Gabor filters are obtained by multiplying the radial and angular components together where each even and odd symmetric pair of log-Gabor filters comprises a complex log-Gabor filter at one scale [10]. The frequency response of log-Gabor filters is given as

$$G(f) = \exp\left(\frac{-(\log(f/f_0))^2}{2(\log(\sigma/f_0))^2}\right) \tag{4.4}$$

where f_0 is the centre frequency, and σ provides the bandwidth of the filter.

4.2.3 Feature Extraction and Encoding Scheme for Approaches I & II

In order to extract the discriminating features from the normalized iris or zigzag collarette region, the normalized pattern is convolved with 1-D log-Gabor filter. First, the 2-D normalized pattern is isolated into a number of 1-D signals, and then these 1-D signals are convolved with 1-D Gabor filter [61]. We consider the rows of the 2-D normalized pattern as the 1-D signals and each row denotes a circular ring of the zigzag collarette or iris region. We use angular direction which corresponds to the columns of the normalized pattern instead of choosing the radial one since the maximum independence occurs in the angular direction. We prefer to set the intensity values of the known noise areas in the normalized pattern to the average intensity level of the neighboring pixels. Thus, we can prevent the influence of noise in the output of the filtering. The phase-quantization approach proposed in [15] is applied to four levels on the outcome of filtering with each filter producing two bits of data for each phasor. The desirable feature of the phase code is selected to be a grey code where only a single bit is changed while rotating from one phase quadrant to another, unlike a binary code. This minimizes the number of bits disagreeing when two intra-class patterns are slightly misaligned and provides more accurate recognition. The encoding process produces a bitwise iris pattern or template containing a number of bits of information, and a corresponding noise mask which corresponds to corrupt areas within the zigzag collarette pattern or iris pattern, and marks bits in the iris pattern as corrupt. Since the phase information will be meaningless at regions where the amplitude is zero, we mark these regions in the noise mask. The total number of bits in the template will be the double of

the product of the angular resolution, the radial resolution, and the number of filters used. The feature extraction process is shown in Figure 21.

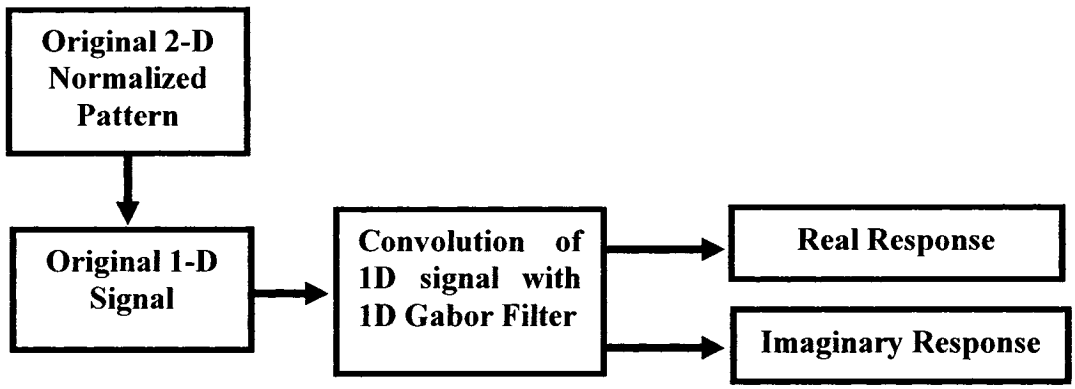

(a)

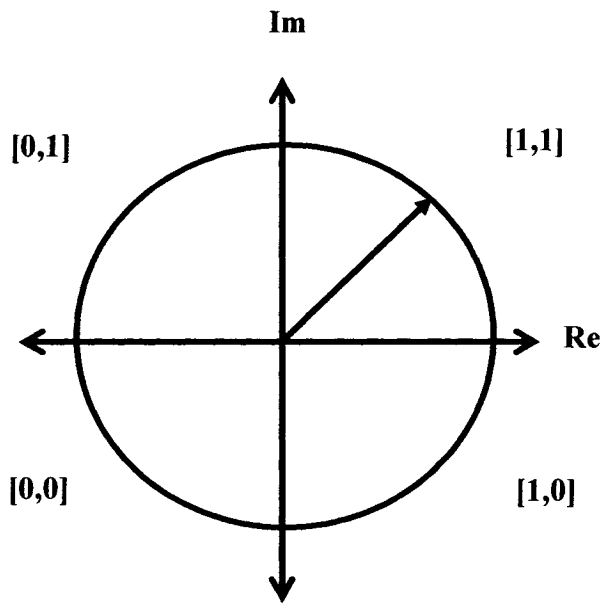

(b)

1 0 0 1 1 1 1 1 0 0 0 0 1 1 0 1 0 0 1 0 1 0 1 0 1 0 0 0 0 0 1 1 1 1 1 0 0 0
0 0 1 0 1 1 0 1 0 1 0 0 0 1 0 0 0 0 1 1 1 1 1 1 0 0 0 1 1 1 1 0 0 1 0 1 0 0

(c)

Figure 21: Feature extraction and encoding process (a) feature extraction, (b) phase quantization and (c) generated iris pattern.

4.3. Feature Selection

In order to improve computational efficiency and classification accuracy, several feature selection schemes are employed here. We apply principal component analysis (PCA), Bhattacharyya distance (BD) and multi-objectives genetic algorithms (MOGA) to select the most significant features from the extracted feature vectors.

Dimensionality reduction is regarded as one of the most important factor in pattern classification systems since the redundant numbers of features often create a lot of problems. PCA has been extensively used in feature reduction [22]. However, the users can apply an ad-hoc approach to define the number of features after reduction. The new number of features is the inherent dimensionality of the main problem and the rest of dimensions are attributed to noise [42]. For applications involving image data, this inherent number of dimensions would not be very clear. Sometimes the number of training data points is less than the number of original features. Therefore, the statistical measures of the training points are not well-behaved. In these cases, the new dimensionality is upper-bounded by the number of data points. In order to find the directions in the original data space that consists of greatest variations along them, several components analysis techniques are exploited. This demonstrates the fact that these techniques are based on manipulation of covariance matrices of the data and covariance matrices consist of major information about data variations. If it is assumed that the data are distributed normally with each class having a specific parameter set (mean and covariance), there are number of ways to measure the distances among these distributions and this is an important factor since higher distances lead to the better classification results. Bhattacharyya distance is one of the measures to determine the

distance between two normal distributions [27]. Both the Bhattacharyya and Mahalanobis distances could be used for any distribution because they only need imperial mean and covariance [22]. Bhattacharyya distance is vastly used as a tool in distance computation in many applications such as speech, automatic target recognition and signal selection. However, no such research work using Bhattacharyya distance has been conducted in iris recognition area. In this thesis, a technique is proposed for finding the number of features in PCA based on the distances between different iris pattern classes' distributions.

In this thesis, we also adopt another feature selection strategy by applying the genetic algorithms (GA), which has been currently receiving considerable attention regarding their potential as an optimization technique for complex problems. GA is regarded as the stochastic search process based on the mechanism of natural selection and genetics. Optimum feature selection in the context of practical applications such as iris recognition presents a multicriterion optimization function. GA may offer a particularly attractive approach for this kind of problem since they are generally quite effective for rapid global search of large, non-linear and poorly understood spaces. Moreover, genetic algorithms are very effective in solving large-scale problems [3].

4.3.1 Principal Component Analysis (PCA)

One of the most popular methods in feature reduction is principal component analysis (PCA). The basic idea of PCA is to select those directions in feature space so that the maximum variation of data can be obtained along them. Those directions could also be interpreted as maximum-energy directions when the data points are zero mean. Covariance matrix is the key part in PCA. Let us assume that $\mathbf{S}$ is the covariance matrix of the training data points

$$\mathbf{S} = \sum_{i=1}^{M} (\mathbf{x}_i - \boldsymbol{\mu})^T (\mathbf{x}_i - \boldsymbol{\mu}), \mathbf{x}_i \in R^N, \mathbf{S} \in R^{N \times N} \tag{4.5}$$

where $\mathbf{x}_i$ is the i^{th} data point and $\boldsymbol{\mu}$ is the mean of those data points. M is the number of data points. It is crucial to have enough data points in computation of $\mathbf{S}$ to make it statistically meaningful and representative of data vectors to be classified. Dimension of data points is N and should be reduced to $L(< N)$. The eigenvectors corresponding to largest L eigenvalues of $\mathbf{S}$ are then used to compose a transformation matrix

$$\boldsymbol{\Phi} = \begin{bmatrix} \mathbf{V}_1^T \\ \mathbf{V}_2^T \\ \vdots \\ \mathbf{V}_L^T \end{bmatrix}, \boldsymbol{\Phi} \in R^{L \times N} \tag{4.6}$$

This transformation is a linear one and reduces data by transferring them to R^L.

4.3.2 Bhattacharyya Distance

Bhattacharyya distance (BD) is a well-known approach to measure the distance between two distributions ([3], [22])

$$bd(i,j) = \frac{1}{8}(\boldsymbol{\mu}_i - \boldsymbol{\mu}_j)^T \left(\frac{\mathbf{S}_i + \mathbf{S}_j}{2} \right)^{-1} (\boldsymbol{\mu}_i - \boldsymbol{\mu}_j) + \frac{1}{2} \ln \frac{\left| \frac{\mathbf{S}_i + \mathbf{S}_j}{2} \right|}{\sqrt{|\mathbf{S}_i||\mathbf{S}_j|}} \tag{4.7}$$

In this equation $bd(i,j)$ is the Bhattacharyya distance between two normal (multi-dimensional) distributions represented by sufficient statistics: mean vectors (μ_i, μ_j) and covariance matrices (S_i, S_j).

The other distance measure is the Mahalanobis distance. Mahalanobis distance is simply the first part of Bhattacharyya distance defined above [3]

$$md(i,j) = (\boldsymbol{\mu}_i - \boldsymbol{\mu}_j)^T \left(\frac{\mathbf{S}_i + \mathbf{S}_j}{2} \right)^{-1} (\boldsymbol{\mu}_i - \boldsymbol{\mu}_j) \tag{4.8}$$

In its other form, Mahalanobis distance could also be used as a means for computing the distance of a vector from a distribution. When there are c classes of data with each class based on a distribution, it is natural to define another criterion that brings into account all the pairs of classes [3]

$$BCD = \sum_{i=2}^{c} \sum_{j=1}^{i-1} bd(i,j) \text{ and } MCD = \sum_{i=2}^{c} \sum_{j=1}^{i-1} md(i,j) \tag{4.9}$$

BCD or *Bhattacharyya Cumulative Distance* defined in this way is a good measure of the difference between all classes of distributions. It is noted that the limits of the summations in (4.8) and (4.9) are based on the Bhattacharyya and Mahalanobis distance properties. These measures are symmetric, meaning that there is no distance between a distribution and itself, that is

$$\begin{aligned} &bd(i,j) = bd(j,i), md(i,j) = md(j,i) \\ &md(i,i) = 0, bd(i,i) = 0 \end{aligned} \tag{4.10}$$

The BCD defined in (4.10) provides useful information about the distances between several classes. Now if there are two feature selection algorithms, it is possible to compute BCD for each case and compare them. The algorithm corresponding to higher BCD is superior in the sense that it produces more separable classes than the other algorithm. The last point to be emphasized again is that the distribution underlying the data in each class is assumed to be normal. PCA and its various derivatives are powerful techniques to reduce the dimensionality of the original data points. The number of original features is reduced to nf, the *new features*. nf can be any integer from one up to f, the original number of features where $nf \in [1, f]$. For every nf, it is possible to

compute the BCD measure. A plot of BCD versus *nf* provides meaningful information regarding the optimum feature selection strategy. The following lemma says that it has an increasing behavior.

Lemma: under PCA, BCD and MCD are increasing functions of L–the number of reduced features.

Proof: If it is proved that the Bhattacharyya distance is an increasing function of *nf* or simply L, then according to (4.9) as its definition, BCD will also be an increasing function of L. According to (4.7), the BD could be separated as two parts (each part in one brackets pair)

$$bd(L)=\left[\left(\boldsymbol{\mu}_{1,L}-\boldsymbol{\mu}_{2,L}\right)^{T}\left(\frac{\mathbf{S}_{1,L}+\mathbf{S}_{2,L}}{2}\right)^{-1}\left(\boldsymbol{\mu}_{1,L}-\boldsymbol{\mu}_{2,L}\right)\right]+\left[\ln\frac{\left|\frac{\mathbf{S}_{1,nf}+\mathbf{S}_{2,L}}{2}\right|}{\sqrt{\left|\mathbf{S}_{1,L}\right|\left|\mathbf{S}_{2,L}\right|}}\right] \tag{4.11}$$

The first part is nothing but the Mahalanobis distance between the two distributions. Also, it is noted that some coefficients are also deleted, since they do not introduce any errors in this analysis. Now, we can prove that both parts are increasing functions in L. The Mahalanobis distance part mainly consists of two constituents: the new mean vector $\boldsymbol{\mu}_L$ and new covariance matrix $\mathbf{S}_L$. These two parts could be expanded as

$$\boldsymbol{\mu}_{1,L}=\frac{1}{N}\sum_{i=1}^{N}\boldsymbol{\Phi}_1(L)\mathbf{x}_{1i}=\boldsymbol{\Phi}_1(L)\frac{1}{N}\sum_{i=1}^{N}\mathbf{x}_{1i}=\boldsymbol{\Phi}_1(L)\boldsymbol{\mu}_1 \tag{4.12}$$

$$\begin{aligned}\mathbf{S}_{1,L}&=\frac{1}{N}\sum_{i=1}^{N}\left(\boldsymbol{\Phi}_1(L)\mathbf{x}_{1i}-\boldsymbol{\mu}_{1,L}\right)\left(\boldsymbol{\Phi}_1(L)\mathbf{x}_{1i}-\boldsymbol{\mu}_{1,L}\right)^{T}\\&=\frac{1}{N}\sum_{i=1}^{N}\boldsymbol{\Phi}_1(L)\left(\mathbf{x}_{1i}-\boldsymbol{\mu}_1\right)\left(\mathbf{x}_{1i}-\boldsymbol{\mu}_1\right)^{T}\boldsymbol{\Phi}_1^{T}(L)=\boldsymbol{\Phi}_1(L)\mathbf{S}_1\boldsymbol{\Phi}_1^{T}(L)\end{aligned} \tag{4.13}$$

Now considering the definition of the transformation matrix $\mathbf{\Phi}$ which is composed of eigenvectors of covariance matrix $\mathbf{S}$, (4.13) could further be simplified as

$$\mathbf{S}_{1,L}=\begin{bmatrix}\mathbf{V}_{11}^T\\ \mathbf{V}_{12}^T\\ \vdots\\ \mathbf{V}_{1L}^T\end{bmatrix}\mathbf{S}_1\begin{bmatrix}\mathbf{V}_{11} & \mathbf{V}_{12} & \cdots & \mathbf{V}_{1L}\end{bmatrix}=\begin{bmatrix}\mathbf{V}_{11}^T\\ \mathbf{V}_{12}^T\\ \vdots\\ \mathbf{V}_{1L}^T\end{bmatrix}\begin{bmatrix}\lambda_{11}\mathbf{V}_{11} & \lambda_{12}\mathbf{V}_{12} & \cdots & \lambda_{1L}\mathbf{V}_{1L}\end{bmatrix}=\begin{bmatrix}\lambda_{11} & 0 & \cdots & 0\\ 0 & \lambda_{12} & \cdots & 0\\ \vdots & \vdots & \ddots & 0\\ 0 & 0 & 0 & \lambda_{1L}\end{bmatrix} \quad (4.14)$$

It is noticeable that $\mathbf{V}_1,\mathbf{V}_2,\cdots,\mathbf{V}_L$ belong to an orthonormal set because they are eigenvectors of a real symmetric matrix $\mathbf{S}$. The middle matrix in the Mahalanobis distance definition then simplifies to [22]

$$\left(\frac{\mathbf{S}_{1,L}+\mathbf{S}_{2,L}}{2}\right)^{-1}=2\begin{bmatrix}1/(\lambda_{11}+\lambda_{21}) & 0 & \cdots & 0\\ 0 & 1/(\lambda_{12}+\lambda_{22}) & \cdots & 0\\ \vdots & \vdots & \ddots & 0\\ 0 & 0 & 0 & 1/(\lambda_{1L}+\lambda_{2L})\end{bmatrix}\in R^{L\times L} \quad (4.15)$$

On the other hand the term $\boldsymbol{\mu}_{1,L}-\boldsymbol{\mu}_{2,L}$ in Mahalanobis distance definition is a vector in R^L

$$\boldsymbol{\mu}_{1,L}-\boldsymbol{\mu}_{2,L}=\mathbf{\Phi}_1(L)\boldsymbol{\mu}_1-\mathbf{\Phi}_2(L)\boldsymbol{\mu}_2=\begin{bmatrix}\mathbf{V}_{11}^T\boldsymbol{\mu}_1-\mathbf{V}_{21}^T\boldsymbol{\mu}_2\\ \mathbf{V}_{12}^T\boldsymbol{\mu}_1-\mathbf{V}_{22}^T\boldsymbol{\mu}_2\\ \vdots\\ \mathbf{V}_{1L}^T\boldsymbol{\mu}_1-\mathbf{V}_{2L}^T\boldsymbol{\mu}_2\end{bmatrix}\in R^L \quad (4.16)$$

The Mahalanobis distance of first bracket in (4.11), then reduces to

$$\sum_{i=1}^{L}\frac{2}{\lambda_{1i}+\lambda_{2i}}(\mathbf{V}_{1i}^T\boldsymbol{\mu}_1-\mathbf{V}_{2i}^T\boldsymbol{\mu}_2)^2 \quad (4.17)$$

This simply means that if L is increased, Mahalanobis distance will also increase. This result is based on properties of PCA and symmetric real covariance matrix that has positive real eigenvalues as well. We now pay attention to the second term in Bhattacharyya distance in (4.7). Due to the fact $|\alpha A|=\alpha^L, A\in R^{L\times L}, \alpha\in R$ and (4.14), this second term could be written as

$$\ln\frac{\left|\mathbf{S}_{1,nf}+\mathbf{S}_{2,L}\right|}{2^{L}\sqrt{\left|\mathbf{S}_{1,L}\right|\left|\mathbf{S}_{2,L}\right|}}=\ln\frac{\prod_{i=1}^{L}(\lambda_{1i}+\lambda_{2i})}{\prod_{i=1}^{L}2\sqrt{\lambda_{1i}\lambda_{2i}}}=\ln\left(\prod_{i=1}^{L}\frac{\lambda_{1i}+\lambda_{2i}}{2\sqrt{\lambda_{1i}\lambda_{2i}}}\right)=\sum_{i=1}^{L}\ln\left(\frac{\lambda_{1i}+\lambda_{2i}}{2\sqrt{\lambda_{1i}\lambda_{2i}}}\right) \tag{4.18}$$

Now it is sufficient to show that each *ln* term inside the summation is positive or equivalently every term inside the *ln* is greater than one

$$\left(\sqrt{\lambda_{1i}}-\sqrt{\lambda_{2i}}\right)^{2}\geq 0\Rightarrow\lambda_{1i}+\lambda_{2i}\geq 2\sqrt{\lambda_{1i}\lambda_{2i}}\Rightarrow\frac{\lambda_{1i}+\lambda_{2i}}{2\sqrt{\lambda_{1i}\lambda_{2i}}}\geq 1 \tag{4.19}$$

This means that the second term in (4.14) is a non-decreasing function if it is expressed as a function of L. The first term in (4.14) is proved to be increasing then the total Bhattacharyya distance is an increasing function in L.

A good result out of this proof process is that using (4.17) and (4.18), the Bhattacharyya distance between classes could be computed very fast by having only the eigenvalues of covariance matrices. Regarding the above lemma, two cases could be considered for BCD, if plotted as a function of L (the number of reduced dimensions using PCA), see Figure 22. For curve 1 in Figure 22, the BCD tends to saturate and if the number of features is increased, there is no more increase in BCD. This behavior could be interpreted as follows: after some specific *nf* it is just a waste of resources to increase the number of new features *nf*. For curve 2, it could be seen that increasing *nf* does not show any sign of saturation and then it is necessary to keep on increasing the new features or simply the feature reduction has no significant benefit.

Based on the two curves characteristics discussed above, it could be said that when the slope of the BCD curve falls bellow a certain level, then the corresponding *nf* is a sub-

optimum number of features. It is noted that it could not be expected for the curve slope to become zero or negative because there is always some noise in the original data.

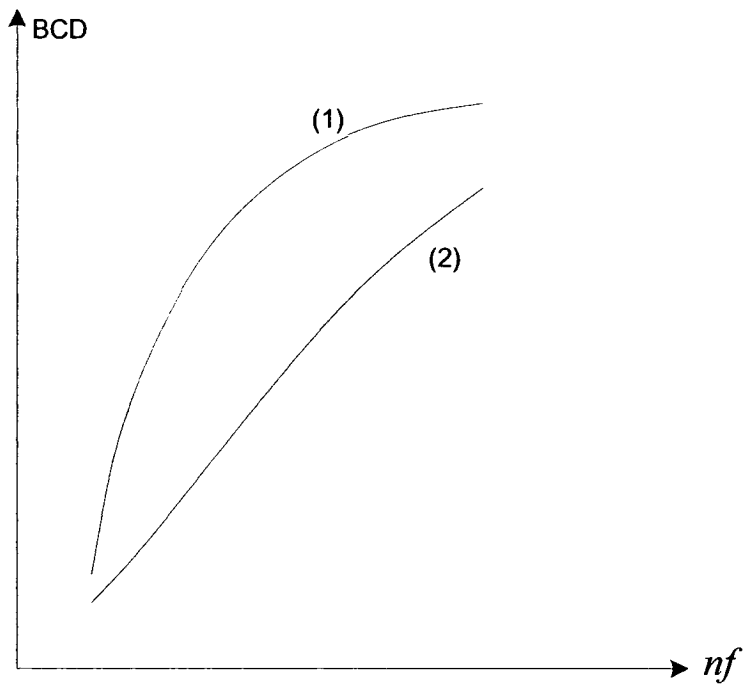

Figure 22: Plot of BCD versus nf.

This noise comes from data acquisition hardware, quantization and round off computations, and most importantly from the changes of patterns with different conditions. The other reason behind positiveness of slope is that increasing number of features always introduces new bits of information. An increase of the information simply translates to more distinguishing ability or distance in distributions. Based on the above discussion the following algorithm could be devised:

1. Set $nf = 1$

2. Calculation of BCD among all the classes of the problem using (4.9)

3. Increase nf by one and if it is still less than a maximum number, go to step (5)

4. Plot the BCD values versus nf

5. If the plot has a saturating characteristic use one criterion for selecting the optimal *nf* by studying the plot otherwise the feature reduction technique has not been successful and still the number of features should be increased.

4.3.3 Multi-Objectives Genetic Algorithm (MOGA)

Genetic Algorithms (GA) are a class of optimization procedures inspired by the mechanisms of evolution in nature [29]. GA operates on a population of structures, each of which represents a candidate solution to the optimization problem, encoded as a string of symbols ("chromosome"). GA starts its search from the randomly generated initial population. In GA, the individuals are typically represented by n-bit binary vectors and the resulting search space corresponds to an n-dimensional boolean space. The quality of each candidate solution is evaluated by a fitness function. The fitness-dependent probabilistic selection of individuals is used by GA from the current population to produce the new individuals [65]. The three of the most commonly used parameters of GA that represent individuals as binary strings are selection, mutation and crossover.

- Selection: In this process, individuals are copied based on the objective function values. The strings with a higher value have a higher probability for contributing one or more offsprings in the next generation.
- Mutation: It operates on a single string and changes a bit randomly.
- Crossover: It is the process of merging two chromosomes from current generation to produce two similar offsprings.

GA repeats the process of fitness-dependent selection and applies the genetic operators to generate successive generations of individuals for several times until an optimize solution is obtained. A simple GA is depicted in Figure 23 and the general flow of GA is

outlined in Figure 24. Figure 25 demonstrates the basic operations of GA with simple examples. Feature subset selection algorithms can be classified into two categories namely: The filter and the wrapper approaches, based on whether the feature selection is performed independently of the learning algorithm or not to construct the verifier.

- Filter Approach: In this approach, the feature selection is accomplished independently of learning algorithms.

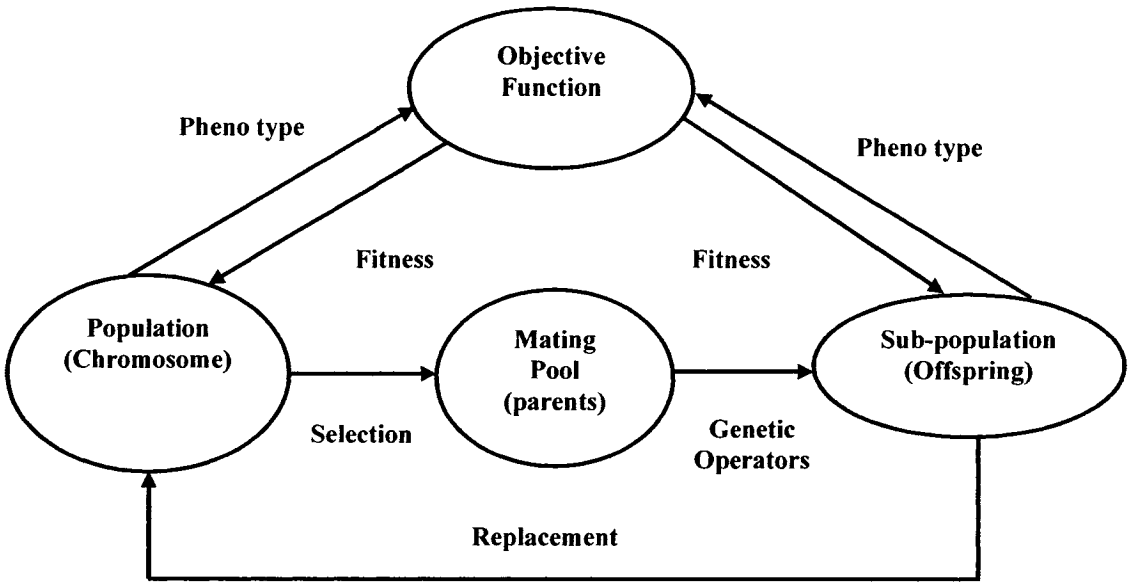

Figure 23: A simple GA cycle [65].

```
Procedure:
begin
t <- 0
initialize P(t)
while (not termination condition)
t <- t + 1
select P(t) from p(t - 1)
crossover P(t)
mutate P(t)
evaluate P(t)
end
end
```

Figure 24: Basic process of GA.

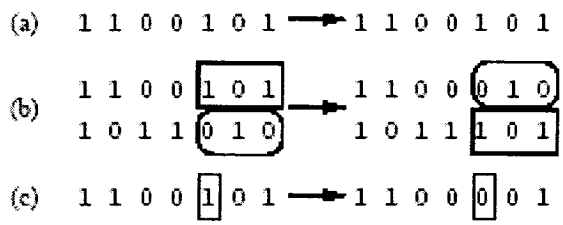

Figure 25: Three basic operations of GA with simple examples
(a) selection, (b) crossover, and (c) mutation [65].

The filter approach is computationally more efficient but its major drawback is that an optimal selection of features may not be independent from the inductive and representational biases of the learning algorithm that is used to build the classifier.

- Wrapper Approach: If the feature selection process depends on learning algorithms, the approach is called a wrapper approach. The wrapper method involves the computational overhead of evaluating a candidate feature subset by executing a selected learning algorithm on the database using each feature subset under consideration.

The performance of the GA depends on various factors such as the choice of genetic representation and operators, the fitness function, fitness dependent selection procedure, and the several user-specified parameters like population size, probability of mutation and crossover, etc.

In this thesis, our problem consists of optimizing two objectives: minimization of the number of features and the error rate of the classifier. Therefore, we are concerned with the multi-objectives genetic algorithms (MOGA). A general multi-objectives

optimization problem contains number of objectives and is associated with a number of inequality and equality constraints [65]. Solutions of a multi-objectives optimization problem can be expressed mathematically in terms of nondominated points, i.e., a solution is dominant over another only if it has superior performance in all criteria. A solution termed as 'Pareto-optimal' is used, if this is not dominated by any other solution in the entire search space. It has been observed that feature selection using MOGA is a very powerful tool to find a set (Pareto-optimal) of good classifiers [30].

4.3.3.1 Proposed Feature Selection Technique Using MOGA

It is necessary to select the most representative feature sequence from a features set with relative high dimension [3]. We propose MOGA to select the optimum set of features. In this thesis, we prefer to use the wrapper approach since an optimal selection of features is dependent on the inductive and representational biases of the learning algorithm which is used to build the classifier. Feature subset selection in the context of practical applications such as iris images classification presents a multicriterion optimization function, e.g. number of features and accuracy of classification. We use them for subset selection in the context of iris image classification problem. Each iris image is represented as a vector of features. The most discriminating feature is selected after feature extraction described in Section 4.2. In the encoding scheme, the chromosome is a bit string whose length is determined by the number of parameters in the image and each parameter is associated with one bit in the string. If the i^{th} bit is 1, then the i^{th} parameter is selected, otherwise, that component is ignored as shown in Figure 26. Each chromosome thus represents a different parameter subset. The goal of

feature subset selection is to use fewer features to achieve the better performance. Therefore, the fitness evaluation contains two terms:

- Accuracy from the validation data and,
- Number of features used.

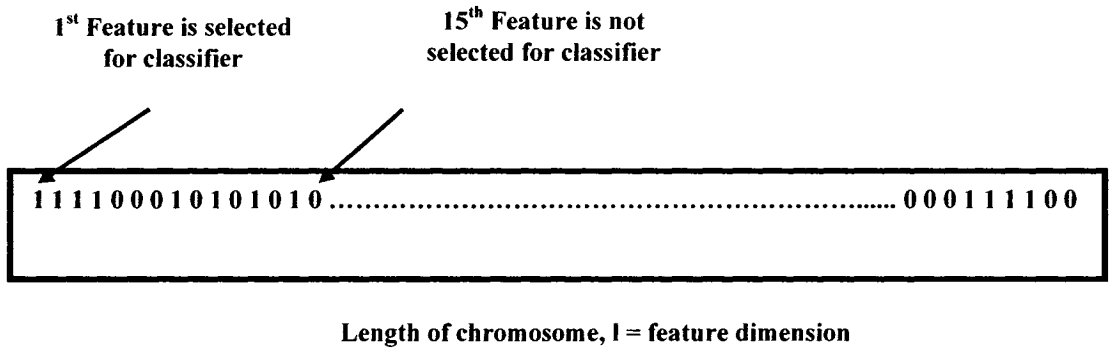

Figure 26: A binary feature vector for l-dimension.

Only the features in the parameter subset encoded by an individual are used in order to train SVM classifier. The performance of the SVM classifier is estimated using a validation data set and used to guide the genetic algorithm as shown in Figure 27. Each feature subset contains a certain number of parameters. Between accuracy and feature subset size, accuracy is our major concern. Combining these two terms, the fitness function is given by

$$\text{Fitness}=(10^4\times\text{Accuracy}+(10^2\times\text{NOZ/NOF}))/10^4 \quad (4.20)$$

where Accuracy denotes the accuracy rate that an individual achieves, NOZ is the number of zeros in the chromosome and NOF represents the number of features used for optimization. The accuracy ranges roughly from 0.7 to 1 (i.e., the first term assumes values in the interval of 7000 to 10000). The NOZ and NOF range from 0 to l where l is

the length of the chromosome code. Therefore, the second term consumes values in the interval of 0 to 60000. Overall, higher the accuracy implies higher fitness. Also, fewer features used imply a greater number of zeros, and as a result, the fitness increases. Notice that individuals with higher accuracy would outweigh individuals with lower accuracy, no matter how many features they contain.

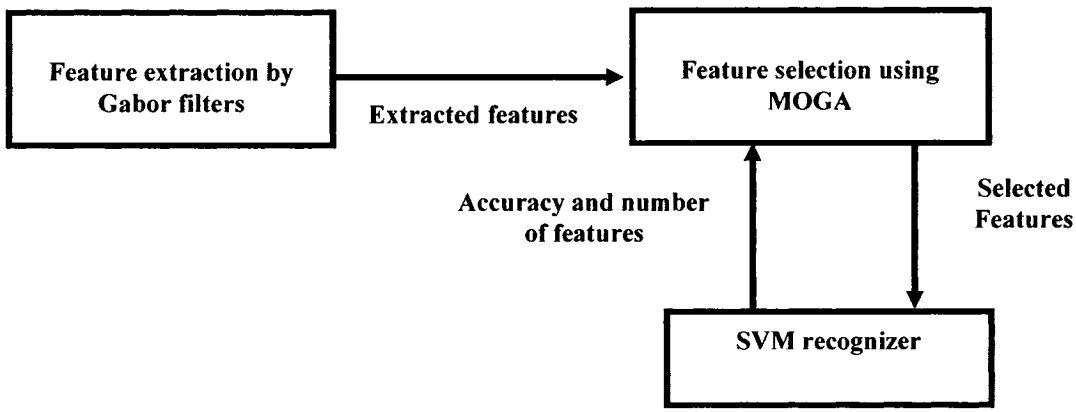

Figure 27: Feature selection process.

Chapter 5

Iris Patterns Classification

5.1. Introduction

Pattern classification is the process of assigning a class label to an object, a physical process or an event. The assignment depends on the measurements that are acquired from the object or physical process or event [35]. In this thesis, we focus on SVM as the main classifier of the iris patterns due to its better generalization capability compared to the other methods of classification [47]. In the proposed approach I, we utilize the traditional approach of SVM for classification. However, the main drawback of the traditional SVM is that it does not differentiate between False Accept and False Reject, which is regarded as a major issue to meet different security requirements. Another problem of the conventional SVM is to manage the unbalanced data of a specific class with respect to other classes. In the proposed approach II, the traditional SVM is modified to an asymmetrical SVM [19] to satisfy several security demands for the specific applications and also, to handle the unbalanced data of specific iris classes. In order to increase the classification accuracy and generalization performance, we also tune the parameters of SVM. The classification accuracy of the proposed modification to SVM is also compared with feed-forward neural network by backpropagation (FFBP), feed-forward

neural network by Levenberg-Marquardt rule (FFLM), k-nearest neighbor (k-NN) classifier, and Hamming and Mahalanobis distances. In the training phase, the iris patterns are used to train the SVM and in the verification stage, the recognition of unknown iris pattern is performed by comparing this pattern to the pattern for which an iris pattern is already built.

5.2. Hamming Distance

The Hamming distance is used to measure the similarity between two bit patterns or templates. This distance metric is deployed to provide a decision whether the two patterns are generated from the different irises or from the same one. If X and Y are two bitwise templates, and N denotes the total number of bits in the template, then the Hamming distance is defined as the sum of exclusive-OR between X and Y ([16],[61])

$$HD = \frac{1}{N}\sum_{i=1}^{N} X_i (XOR) Y_i \tag{5.1}$$

Each iris region produces an iriscode which is independent to that produced by another iris; on the other hand, the two bitwise templates produced from the same iris will be highly correlated due to high degree of freedom in an iris region. If two bit patterns are generated from the same iris, the Hamming distance between them is approximately equal to 0.0, on the contrary, if the two bitwise iris patterns are fully independent such as iris patterns derived form the different irises, the ideal Hamming distance should be 0.5. For recognition purpose, we apply the Hamming Distance metric for comparison between iris patterns. In order to consider only the significant bits in calculating the Hamming distance between two iris patterns, a noise mask is also incorporated in the Hamming distance approach. Therefore, only those bits in the iris pattern that correspond to '0' bits in noise masks of both the iris patterns will be used in the calculation of Hamming

distance. The formula of Hamming distance based on the template derived from the true iris region is given as follows ([16], [61])

$$HD = \frac{1}{N - \sum_{j=1}^{N} Xn_j (OR) Yn_j} \sum_{i=1}^{N} X_i (XOR) Y_i (AND) Xn_i' (AND) Yn_i' \qquad (5.2)$$

where X_i and Y_i are the two bit-wise templates to compare, Xn_i and Yn_i denote the corresponding noise masks for X_i and Y_i, and N is the total number of bits represented by each iris pattern.

5.3. Mahalanobis Distance

We have also used Mahalanobis distance classifier to compare the classification accuracy with the proposed SVM technique. If d_{ij} is the distance from the new sample X_i during recognition to each of the classes C_j, then the Mahalanobis distance is defined as [22]

$$d_{ij} = (C_j - X_i)^T S^{-1} (C_j - X_i) \qquad (5.3)$$

where ^{T} represents a matrix transpose, **S** is the covariance matrix of the independent variables over the entire class, and S^{-1} is its inverse.

5.4. k-Nearest Neighbor Classifier

Nearest neighbor (NN) classifier uses an estimator with high resolution in regions where the training set is dense and low resolution in other regions. The main advantage of this classifier is that a balance between resolution and variance can be adjusted locally [35]. Let $R(z) \subset R^N$ denotes the hyperspace with the volume V and z represents the center of *R (z)*. Now if N_k is the number of samples in the training set T_k, then the

probability of having exactly n samples within $R(z)$ has a binomial distribution with expectation

$$E[n] = N_k \int_{y \in R(z)} p(y \mid w_k) dy \approx N_k V_p (Z \mid W_k) \tag{5.4}$$

Let the radius of the sphere around z is selected so that the sphere contains exactly k samples. Since the radius depends on the position of z in the measurement space, the volume also depends on z. Therefore, an estimate of the density is

$$\hat{p}(z \mid w_k) = \frac{k}{N_k V(z)} \tag{5.5}$$

This expression reveals that in regions where $p(z \mid w_k)$ is large, the volume tends to be small, on the other hand, if $p(z \mid w_k)$ is small, the sphere requires to grow to collect the k samples. The parameter k is used to control the balance between the bias and variance, and a suitable choice of k is to make proportional to $\sqrt{N_k}$. Like the other classifiers, NN estimation technique directly uses the training set without explicitly estimating the probability densities. In order to classify a vector z, the radius of the sphere around z is selected such that this sphere consists of exactly k samples taken from T_s. These samples are denoted as the k-nearest neighbor of z. If k_k is the number of samples in class w_k, an estimate of the conditional density is given below

$$\hat{p}(z \mid w_k) \approx \frac{k_k}{N_k V(z)} \tag{5.6}$$

If we consider that the entire training is set denoted as *Ts* and the total number of samples is N_S. then the estimates of the prior probabilities are defined as follows

$$\hat{p}(w_k) = \frac{N_k}{N_s} \tag{5.7}$$

Therefore, the following suboptimal classification can be deduced from the combination of (5.6) and (5.7) in the Bayes classification with uniform cost function $\hat{w}_{map}(z) = \arg\max \{p(z \mid w)p(w)\}$

$$\hat{w}(z) = w_k \text{ with}$$

$$k = \underset{i=1,\ldots,K}{\arg\max}\{\hat{p}(z \mid w_i)\hat{P}(w_i)\} = \underset{i=1,\ldots,k}{\arg\max}\left\{\frac{k_i}{N_i V(z)} \; \frac{N_i}{N_s}\right\} = \underset{i=1,\ldots,K}{\arg\max}\{k_i\} \tag{5.8}$$

Here, the class assigned to a vector z is the class with the maximum number of votes coming from k samples nearest to z. This classification technique is known as k-nearest neighbor classification (k-NN). In this thesis, we adopt k-NN to compare the classification accuracy with the SVM ([93], [106]).

5.5. Feed-Forward Neural Network using Backpropagation

Neural networks are biologically motivated and statistically based [4] technique. The networks are made up of processing units called neurons (or cells or nodes). The structure of a neuron is the basic building block of the network. The neuron computes the weighted-sum over the outputs of neurons connected to its input. Then activation function is applied to the weighted sum to determine the neuron's output. The sigmoid function is used as an activation function and it is defined as [35]

$$g(y) = f(w^T y) = \frac{1}{1 + \exp(-w^T y)} \tag{5.9}$$

Here, **y** is the vector **z** augmented with a constant value 1, where the vector **z** represents the set of features of a specific sample of an object called the measurement vector. The **w**

is the weight vector, and the specific weight which corresponds to the constant value 1 in **z** is denoted as the bias weight. In a neural network, several layers of different number of neurons are constructed as shown in Figure 28.

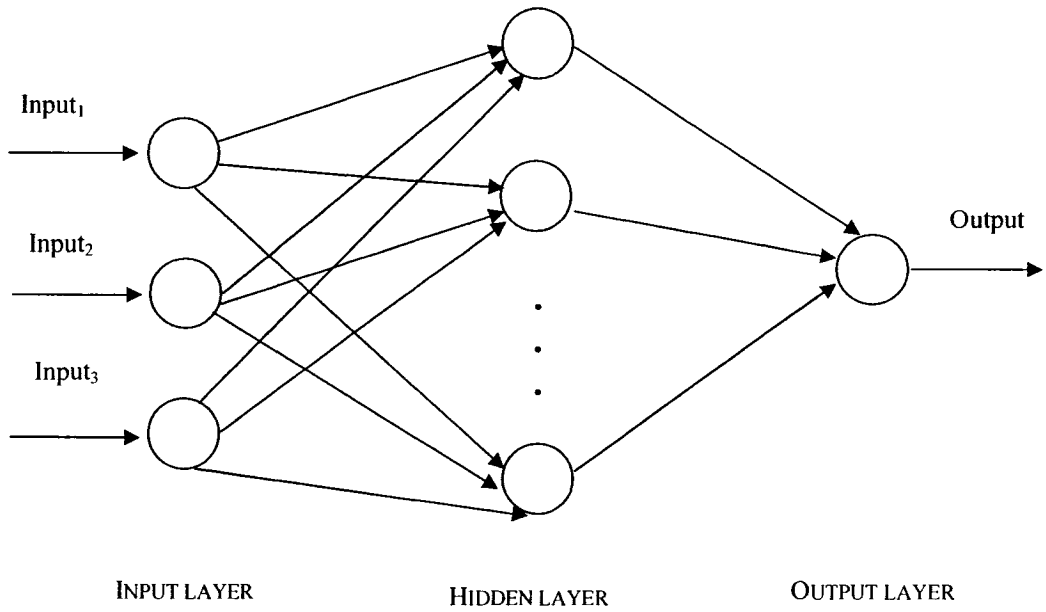

Figure 28: A feed-forward neural network with three input dimensions and one output.

The neurons which are not connected directly to the input or output are regarded as hidden neurons and these are organized in hidden layers. If all the neurons in the network measure their output based on only the output of neurons in the previous layers, the network is called feed-forward neural network and no loops are allowed in such network. If there is only one hidden layer with H hidden neurons, the output of the total neural network is calculated as [35]

$$g_k(y) = f\left(\sum_{h=1}^{H} v_{k,h} f\left(w_h^T y\right) + v_{k,H+1}\right) \tag{5.10}$$

Here, w_h denotes the weight vector of the inputs to hidden neuron h and v_k represents the weight vector of the inputs to output neurons k. The sum of squared errors between the output of the neural network and the target vector is defined as

$$E_{OT} = 0.5 * \sum_{n=1}^{N_s} \sum_{k=1}^{k} \left(g_k(y_n) - t_{n,k}\right)^2 \tag{5.11}$$

Here N_s is the total number of samples. If the class label of sample y_n is ω_k, then $t_{n,k} = 1$, otherwise it is 0. The derivative of the error E_{OT} can be measured with respect to the weights since every neuron has continuous transfer functions and the weights can then be updated using gradient descent. The updates of $v_{k,h}$ are calculated using the chain rule as follows

$$\Delta v_{k,h} = -\eta \frac{\partial E_{OT}}{\partial v_{k,h}} = \sum_{n=1}^{N_S} \left(g_k(y_n) - t_{n,k}\right) f\left(\sum_{h=1}^{H} v_{k,h} f\left(w_h{}^T y\right) + v_{k,H+1}\right) f\left(w_h{}^T y\right) \tag{5.12}$$

and the derivation of the gradient descent with respect to $w_{h,i}$ is estimated as

$$\Delta w_{h,i} = -\eta \frac{\partial E_{OT}}{\partial v_{k,h}} = \sum_{k=1}^{K} \sum_{n=1}^{N_S} \left(g_k(y_n) - t_{n,k}\right) v_{k,h} f\left(w_h{}^T y\right) Y_i f\left(\sum_{h=1}^{H} v_{k,h} f\left(w_h^T y\right) + v_{k,H+1}\right) \tag{5.13}$$

The error between the output and the target value over all weights in the network can be distributed when the updates for $v_{k,h}$ are calculated first, and those for $w_{h,i}$ are computed from that. Therefore, the error is back-propagated and the process is called back-propagation training. The nonlinearity of the decision boundary can be controlled by the number of hidden nodes and hidden layers in a neural network. Since it is very difficult to

predict how many nodes in the hidden layers is suitable for a specific task, we train a number of neural networks of varying complexity and compare their performance on the independent validation set.

5.5.1 Feed-Forward Neural Network Model for Iris Recognition using Backpropagation

In this thesis, we apply a feed forward neural network using backpropagation rule (FFBP) algorithm for iris patterns classification. A feed-forward neural network, having 600 neurons in the input layer assuming that the iris pattern consists of 600 features, 7 neurons in the output layer and hidden layer with variable number of neurons as shown in Figure 29. In this thesis, 108 iris patterns of 108 persons' iris image from CASIA iris database are considered to be input patterns represented by the vectors **A** [NOI] [i], where NOI (Number of input iris pattern) = 0, 1, 2,....107 and i (extracted feature elements) = 0,1,2, ... 599, formed (108 × 600) pattern matrix .

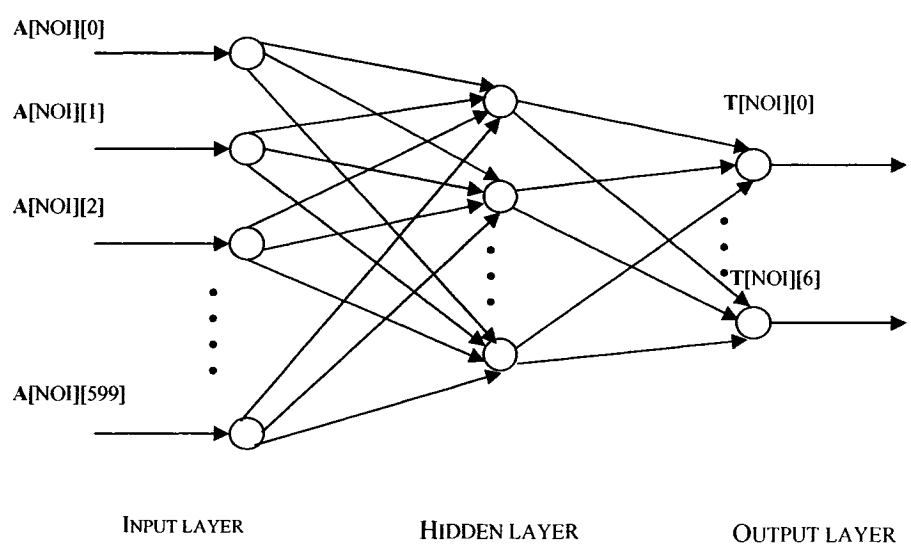

Figure 29: The proposed feed-forward neural network using backpropagation.

Here, NOI=0 for the first iris pattern, NOI=1 for the second pattern, and so on and i = 0 for the first input iris pattern element, i = 1 for the second input pattern element, and so on. Thus **A** [1] [4] represents the 5^{th} input pattern element for iris pattern 2. The output **T**[NOI][i] represents the target output, where NOI = 0, 1, 2,…,107 and i = 0, 1, 2,…..,6.

5.5.2 Feed-Forward Neural Network using Levenberg- Marquardt rule

In this thesis, we also apply the feed-forward neural network using Levenberg-Marquardt rule (FFLM) proposed in [31] for iris patterns classification and compare the classification accuracy with the SVM.

Let us consider the feed forward network, see Figure 30. The network input to unit i in the layer $k+1$ is defined as

$$n^{k+1}(i) = \sum_{j=1}^{Sk} w^{k+1}(i,j)a^{k}(j) + b^{k+1}(i) \tag{5.14}$$

and the output of the unit i is calculated as

$$a^{k+1}(i) = f^{k+1}\left(n^{k+1}(i)\right) \tag{5.15}$$

The system equations for a M layer network can be presented in matrix form as follows

$$\underline{a}^{0} = \underline{p} \tag{5.16}$$

$$\underline{a}^{k+1} = \underline{f}^{k+1}\left(W^{k+1}\underline{a}^{k} + \underline{b}^{k+1}\right), \quad k = 0,1, \ldots\ldots\ldots, M-1. \tag{5.17}$$

The neural network learns the associations between a specified set of input-output pairs represented as [31]

$$\left\{ \left(\underline{p}_1, \underline{t}_1\right), \left(\underline{p}_2, \underline{t}_2\right), \ldots\ldots\ldots\ldots \left(\underline{p}_Q, \underline{t}_Q\right) \right\}$$

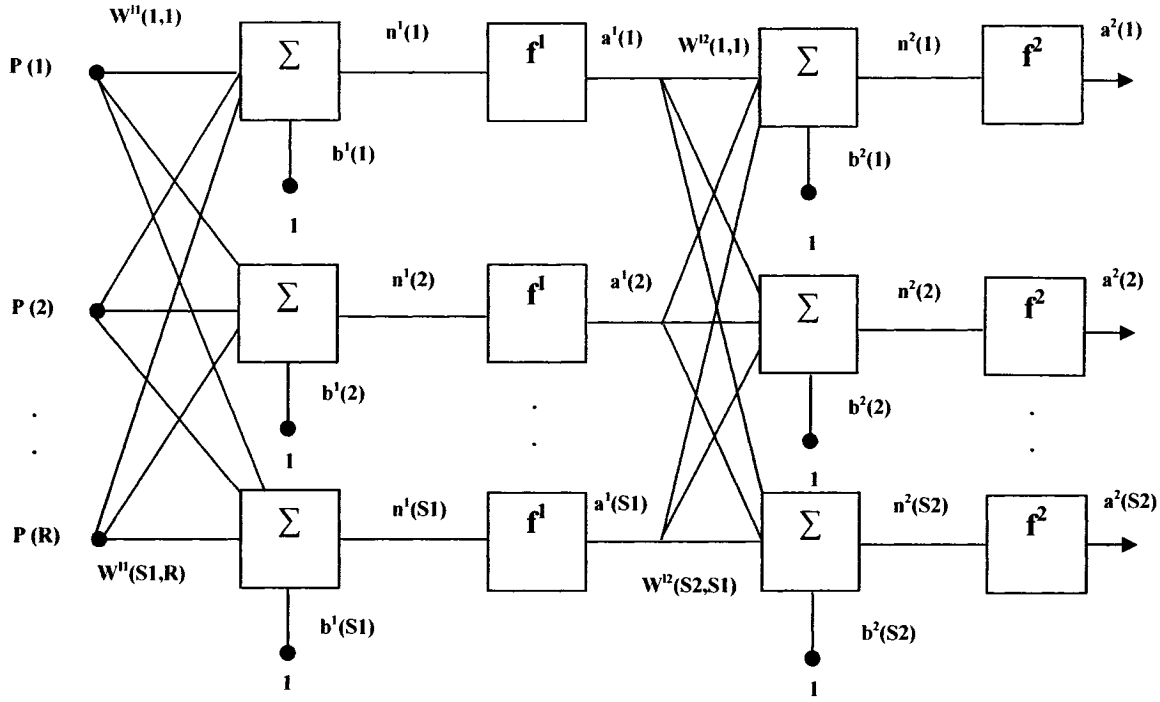

Figure 30: A feed-forward neural network [31].

The performance index of the neural network is measured as

$$V = \frac{1}{2}\sum_{q=1}^{Q}\left(\underline{t}_q - \underline{a}_q^M\right)^T\left(\underline{t}_q - \underline{a}_q^M\right) = \frac{1}{2}\sum_{q=1}^{Q}\underline{e}_q^T\underline{e}_q \qquad (5.18)$$

Here, q th input of the network is p_{-q} and a_{-q}^M denotes the output of the network. Then the error for the q th input is estimated as $e_q = t_{-q} - a_{-q}^M$. The gradient (steepest) decent rule is used for standard backpropagation algorithm [31] mentioned in the section 5.5.

The Levenberg- Marquardt algorithm is an approximation of the Newton's method [31]. Let us consider the function $V(\underline{x})$ which is required to be minimized with respect to the parameter vector $\underline{x}$, and then the Newton's method is defined as

$$\Delta \underline{x} = -\left[\nabla^2(\underline{x})\right]^{-1} \nabla V(\underline{x}) \tag{5.19}$$

where $\nabla^2 V(\underline{x})$ denotes the Hessian matrix and $\nabla V(\underline{x})$ is the gradient. Suppose that $\nabla V(\underline{x})$ is a sum of squares function

$$V(\underline{x}) = \sum_{i=1}^{N} e_i^2(\underline{x}) \tag{5.20}$$

then we can show that $$\nabla V(\underline{x}) = J^T(x) e(\underline{x}) \tag{5.21}$$

$$\text{and } \nabla^2 V(\underline{x}) = J^T(\underline{x}) J(\underline{x}) + S(\underline{x}) \tag{5.22}$$

where $J(\underline{x})$ presents the Jacobian matrix calculated as follows

$$J(\underline{x}) = \begin{bmatrix} \frac{\partial e_1(\underline{x})}{\partial x_1} & \frac{\partial e_1(\underline{x})}{\partial x_2} & \cdots & \frac{\partial e_1(\underline{x})}{\partial x_n} \\ \frac{\partial e_2(\underline{x})}{\partial x_1} & \frac{\partial e_2(\underline{x})}{\partial x_2} & \cdots & \frac{\partial e_2(\underline{x})}{\partial x_n} \\ . & . \quad . & & . \\ . & . & . & . \\ . & . & . & . \\ \frac{\partial e_N(\underline{x})}{\partial x_1} & \frac{\partial e_N(\underline{x})}{\partial x_2} & \cdots & \frac{\partial e_N(\underline{x})}{\partial x_n} \end{bmatrix} \tag{5.23}$$

$$\text{and } \quad S(\underline{X}) = \sum_{i=1}^{N} e_i(\underline{x}) \nabla^2 e_i(\underline{x}) \tag{5.24}$$

We assume that $S(\underline{x}) \approx 0$, for the Gauss-Newton method and then the (5.19) can updated as

$$\Delta \underline{x} = \left[J^T(\underline{x}) J(\underline{x})\right]^{-1} J^T(\underline{x}) e(\underline{x}) \tag{5.25}$$

Now the Gauss-Newton method is modified as follows

$$\Delta \underline{x} = \left[J^T(\underline{x}) J(\underline{x}) + \mu I\right]^{-1} J^T(\underline{x}) e(\underline{x}) \tag{5.26}$$

which is treated as the Levenberg- Marquardt modification. Here the parameter μ plays an important role. The parameter μ is divided by β if the step reduces $V(\underline{x})$ and on the other hand, if step increases $V(\underline{x})$, then μ is multiplied by β . If the value of μ is large then the algorithm becomes gradient (steepest) decent and while for small μ the algorithm becomes Gauss-Newton. The terms of the Jacobian matrix can be calculated by a simple modification of the backpropagation algorithm for the mapping problem of the neural network. It can be observed that the performance index given in (5.18) for the mapping problem is equivalent to (5.20), where $\underline{x} = \left[w^1(1,1)w^1(1,2) \ \ldots\ldots \ w^1(S1,R)b^1(1) \ \ldots\ldots \ b^1(S1)w^2(1,1) \ \ldots\ldots \ b^M(SM)\right]^T$, and $N = Q \times SM$. The terms of the standard backpropagation algorithm is calculated as

$$\frac{\partial \hat{V}}{\partial w^k(i,j)} = \frac{\partial \sum_{m=1}^{SM} e_q^2(m)}{\partial w^k(i,j)} \tag{5.27}$$

The following term is measured for the elements of the Jacobian matrix which are required for the Levenberg- Marquardt algorithm

$$\frac{\partial e_q(m)}{\partial w^k(i,j)} \tag{5.28}$$

These terms are estimated using the backpropagation algorithm where one modification at final layer is accomplished as follows

$$\Delta^M = -\dot{F}^M\left(\underline{n}^M\right) \tag{5.29}$$

Now each column of the matrix in (5.27) is called the sensitivity vector which is back-propagated through the network to produce the one row of the Jacobian. Thus, we can summarize the procedure of the Levenberg- Marquardt algorithm as follows [31]:

1. The output corresponding to all inputs to the network and the errors $e_{-q} = t_{-q} - a_{-q}^{M}$ are computed and the sum of squares of errors over all inputs $V(\underline{x})$ is calculated.
2. The Jacobian matrix $J(\underline{x})$ is estimated.
3. Solve (5.26) in order to calculate $\Delta \underline{x}$.
4. The sum of squares of errors is re-estimated using $\underline{x} + \Delta \underline{x}$. If the newly computed sum of squares is smaller than that calculated in step 1, then μ is decreased by β, and go back to step 1. If the sum of squares is greater than that in step 1, μ is increased by β and go to the step 3.
5. It is assumed that the algorithm is converged if the norm of the gradient (5.21) is less than some predetermined value, or when the sum of squares is decreased to some error goal.

5.6. Support Vector Machines as Iris Patterns Classifier

Support vector machines (SVM) are well-accepted approach for classification due to their attractive features and promising performance [47]. The support vector classifiers devise a computationally efficient way of learning good separating hyperplane in a high dimensional feature space [93]. In this research work, we apply the SVM for iris patterns classification due to their outstanding generalization performance. Unlike the conventional neural networks in which the network weights are determined by minimizing the mean of squared error between the actual and target outputs denoted as empirical risk minimization, SVM optimizes their parameters by minimizing the classification error called the structural risk minimization. Empirical risk minimization

strategy depends on the availability of large amounts of training data. In other words, we can say that the empirical risks will be closed to the true risk when the sample size is large and even a small empirical risk does not guarantee a low level of true risk for the problem of limited amount of training data, In these circumstances, structural risk minimization strategy which maintains a balance between empirical risk and complexity of the mapping function is required. Therefore, due to the special property called structural risk minimization, SVM provides particularly good solution in the cases where the training data is limited or difficult to obtain. In this classification scheme, nonlinear boundaries can also be used without much extra computational cost. In the thesis, SVM is deployed as iris patterns classifiers due to its advantageous features over other classification schemes along with the promising performance as multi-class classifiers.

The Fisher's discriminant analysis aims to maximize the average class distance, projected onto the direction of discrimination, while having the intraclass variance normalized. For certain critical applications, the influence of patterns that are far from the decision boundary is ignored because their influence on the decision accuracy may not be critical. This motivates the consideration of learning models such SVM, which in contrast to Fisher's discriminant, maximize the minimal margin of separation. In SVM, a few important data points called support vectors (SV) are selected on which decision boundary is dependent exclusively. For linearly separable problems, such as the one shown in Figure 31, SV are selected from the training data so that the distance between two hyperplanes represented by dotted lines passing through the SV is at a maximum. For linearly separable cases, the main decision hyperplane represented as solid line in Figure 31, which is midway between two hyperplanes, should minimize classification error [47].

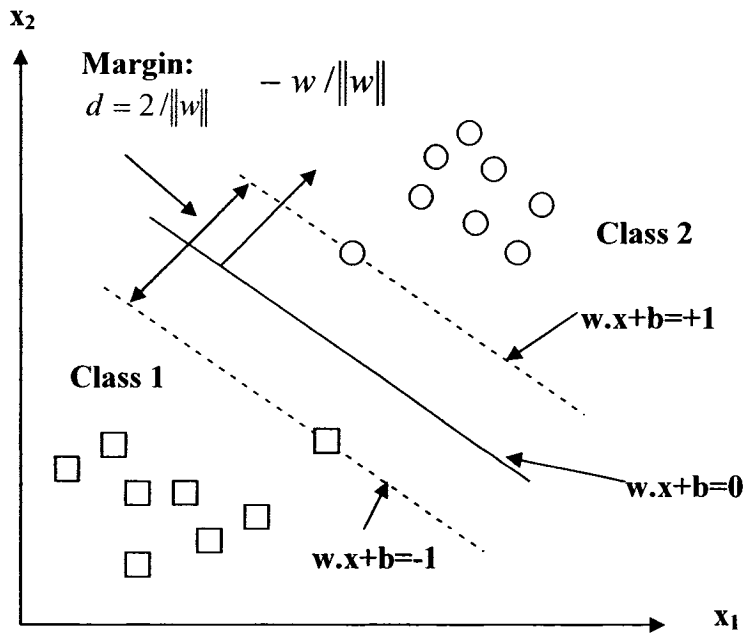

Figure 31: Illustration of a two class classification process using SVM.

Let us consider N sets of labeled input/output pairs $\{x_i, y_i; i = 1,.....,N\} \in X \times \{+1,-1\}$, where X is the set of input data in $\Re^D$ and y_i are the labels. The SVM approach aims to obtain the largest possible margin of separation. The decision hyperplane in Figure 31 can be expressed as

$$x.w + b = 0 \tag{5.30}$$

If all the training data satisfy the constraints, then

$$x_i.w + b \geq +1 \quad for \quad y_i = +1 \quad i = 1,....., N \tag{5.31}$$

$$x_i.w + b \leq -1 \quad for \quad y_i = -1 \quad i = 1,....., N \tag{5.32}$$

If the equality holds for a data point x, then it is said to be right on the marginal hyperplane. Mathematically, the marginal hyperplanes are denoted as

$$x.w + b = \pm 1 \tag{5.33}$$

The two data points x_1 and x_2, that satisfy the followings

$$x_1.w + b = +1 \text{ and} \tag{5.34}$$

$$x_2.w + b = -1 \tag{5.35}$$

will, respectively fall on the two hyperplanes that parallel to the decision plane and orthogonal to w shown in Figure 31. If we subtract (5.35) from (5.34), we get

$$w.(x_1 - x_2) = 2$$

$$\Rightarrow \quad \left(\frac{w}{\|w\|}\right).(x_1 - x_2) = \frac{2}{\|w\|} \tag{5.36}$$

Therefore, the distance between the two hyperplanes are expressed as

$$2d = \frac{2}{\|w\|}, \tag{5.37}$$

Where *2d* is the width of separation, which denotes how separable the two classes of training data are. The distance *d* is considered as the safety margin of the classifier. Now, by combining (5.31) and (5.32) into a single constraint, we get

$$y_i(x_i.w + b) \geq 1 \qquad \forall i = 1,....., N \tag{5.38}$$

In the training phase, the main goal is to find the SV that maximize the margin of separation, *d*. Alternatively, the similar objective can be achieved if we minimize $\|w\|^2$. Thus, the goal is to minimize $\|w\|^2$ subject to the constraint in (5.38). We can solve it by introducing Lagrange multipliers $\alpha_i \geq 0$ and a Lagrangian

$$L(w, b, \alpha) = \frac{1}{2}\|w\|^2 - \sum_{i=1}^{N} \alpha_i (y_i(x_i.w + b) - 1), \tag{5.39}$$

where $L(w, b, \alpha)$ is simultaneously minimized with respect to *w* and *b* and maximized with respect to α_i.

Now setting,

$$\frac{\partial}{\partial b}L(w,b,\alpha)=0 \quad and \quad \frac{\partial}{\partial w}L(w,b,\alpha)=0 \tag{5.40}$$

subject to the constraint $\alpha_i \geq 0$, results in

$$\sum_{i=1}^{N}\alpha_i y_i = 0 \text{ and} \tag{5.41}$$

$$w=\sum_{i=1}^{N}\alpha_i y_i x_i \tag{5.42}$$

We substitute (5.41) and (5.42) into (5.39), which produces

$$\begin{aligned} L(w,b,\alpha) &= \frac{1}{2}(w.w)-\sum_{i=1}^{N}\alpha_i y_i (x_i.w)-\sum_{i=1}^{N}\alpha_i y_i b+\sum_{i=1}^{N}\alpha_i \\ &= \sum_{i=1}^{N}\alpha_i - \frac{1}{2}\sum_{i=1}^{N}\sum_{j=1}^{N}\alpha_i\alpha_j y_i y_j (x_i.x_j) \end{aligned} \tag{5.43}$$

This results in the following Wholfe dual optimization problem

$$\max_{\alpha}\sum_{i=1}^{N}\alpha_i - \frac{1}{2}\sum_{i=1}^{N}\sum_{j=1}^{N}\alpha_i\alpha_j y_i y_j (x_i.x_j) \tag{5.44}$$

subject to

1. $\sum_{i=1}^{N}\alpha_i y_i = 0$ and
2. $\alpha_i \geq 0, \quad i = 1,.....,N$

The solution of the dual optimization problem contains two types of multipliers α_k :

1. One type with $\alpha_k = 0$ and
2. the other with $\alpha_k \neq 0$.

The data points corresponding to the zero multipliers are considered to be irrelevant to the classification problem. The data points denoted as SV for which multipliers, $\alpha_k \neq 0$

are considered to be more critical for the classification problem. According to the Karush-Kuhn-Tucker conditions of optimization theory [47] the following equality must be satisfied at all of the saddle points

$$\alpha_i \{y_i(x_i.w+b)-1\} = 0, \qquad for \quad i = 1,2,\ldots\ldots\ldots, N.$$

Therefore, only those data points for which $y_i(x_i.w+b)-1=0$ can be SV since these points have a non-zero value of multipliers α_i. Thus, SV satisfy the following

$$y_k(x_k.w+b)-1=0 \qquad \forall k \in S, \tag{5.46}$$

where S is the set consisting of the indexes to the SV. The values of α_i can be found from (5.44) and w from (5.42). From (5.46), we calculate the threshold b as follows

$$b = 1 - x_k.w, \qquad \text{where } y_k = 1 \text{ and } x_k \in S.$$

Finally, the decision boundary can be derived as follows

$$f(x) = w.x + b = \sum_{i=1}^{N} y_i \alpha_i (x.x_i) + b = 0 \tag{5.47}$$

Sometimes the training data points are not clearly separable. Therefore, the concept of fuzzy or soft decision region is introduced to cope with the situations of such non separable data points. A fuzzy SVM allows more relaxed separation which in turn provides more robust decision. In the case of fuzzy SVM, we denote the separation of width as fuzzy separation region. Thus, the distance $2d = \frac{2}{\|w\|}$ denotes the width of fuzzy separation. If the data points are not separable by a linear separating hyperplane, a set of slack or relax variables $\{\xi = \xi_1,\ldots\ldots\ldots,\xi_N\}$ is introduced with $\xi_i \geq 0$ such that (5.38) becomes

$$y_i(x_i.w+b) \geq 1-\xi_i \qquad \forall i = 1,\ldots\ldots,N \tag{5.48}$$

The slack variables allow some data points to violate the constraints noted in (5.38), which denotes the minimum safety margin required for training data in the clearly separable case. The slack variables measure the deviation of the data points from the marginal hyperplane. In other words, they measure how severely the safety margin is violated. The new objective function to be minimized becomes

$$\frac{1}{2}\|w\|^2 + C\sum_i \xi_i, \text{ subject to } y_i(x_i.w+b) \geq 1-\xi_i, \tag{5.49}$$

where C is the user defined penalty parameter to penalize any violation of the safety margin for all training data. A smaller C leads to more SV while a larger C leads for fewer SV. It is also noted that a smaller C leads to a wider width of fuzzy separation while a larger C has a narrower fuzzy separation region. Now the new Lagrangian becomes

$$L(w,b,\alpha) = \frac{1}{2}\|w\|^2 + C\sum_i \xi_i - \sum_{i=1}^{N}\alpha_i(y_i(x_i.w+b)-1+\xi_i) - \sum_{i=1}^{N}\beta_i\xi_i, \tag{5.50}$$

where $\alpha_i \geq 0$ and $\beta_i \geq 0$ are, respectively, the Lagrangian multipliers to satisfy that $y_i(x_i.w+b) \geq 1-\xi_i$ and $\xi_i > 0$. Therefore, the Wholfe dual is calculated

$$\max_{\alpha} \sum_{i=1}^{N}\alpha_i - \frac{1}{2}\sum_{i=1}^{N}\sum_{j=1}^{N}\alpha_i\alpha_j y_i y_j (x_i.x_j) \tag{5.51}$$

subject to $0 \leq \alpha_i \leq C, \quad i = 1,\ldots\ldots,N, \qquad \sum_{i=1}^{N}\alpha_i y_i = 0$. The output weight w is calculated as $w = \sum_{i=1}^{N}\alpha_i y_i x_i$ and the bias or threshold term is measured by $b = 1 - x_k.w$, where $y_k = 1$ and x_k is a support vector that lies on the plane $w^T x + b = 1$.

A nonlinear hidden-layer is inserted between input and output layers so that a two-layer network can provide an adequate flexibility in the classification of fuzzily separable data. The original linearly nonseparable data points are mapped to a new feature space, denoted by hidden nodes such that the mapped patterns become linearly separable. In order to obtain a nonlinear decision boundary, we replace the inner product $(x.x_i)$ of (5.47) with a nonlinear kernel $K(x,x_i)$ and get

$$f(x)=\sum_{i=1}^{N} y_i\alpha_i K(x,x_i)+b \tag{5.52}$$

The decision function in (5.51) can be implemented by a two-layer architecture shown in Figure 32 where it is depicted that the original input feature space is converted to a new feature space, manifested by the hidden-layer in the middle of the network.

The basic idea behind the nonlinear SVM is to use a kernel function $K(x,x_i)$ to map the data x from the input space to the new higher dimensional feature space on which the mapped data points become linearly separable. The hidden units on the hidden-layer are represented by the kernel function adopted by the SVM. The three basic kernels used in this thesis are

Polynomial kernel: $K(x,x_i)=\left(1+\frac{x.x_i}{\sigma^2}\right)^p, p>0$

Radial Basis Function (RBF) kernel: $K(x,x_i)=\exp\left\{-\frac{\|x-x_i\|^2}{2\sigma^2}\right\}$ and

Sigmoidal Kernel: $K(x,x_i)=\frac{1}{1+e^{-\frac{x.x_i+b}{\sigma^2}}}$

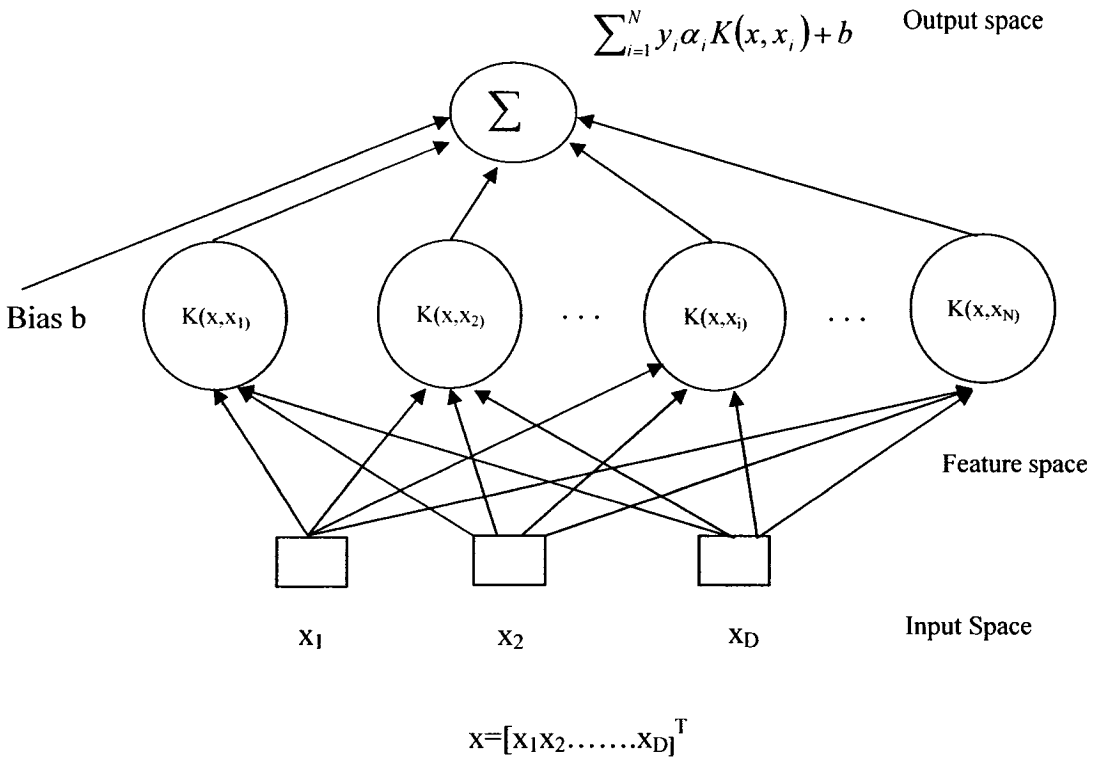

Figure 32: The two-layer architecture of SVM.

The adjustment of the penalty parameter for error term *C* and the kernel parameters are also important to improve the generalization performance. A careful selection of a training subset and a validation set with a small number of classes is required to avoid the training of SVM with all classes and evaluate its performance on the validation set due to its high computational cost when the number of classes is higher. In the proposed approach II, the optimum parameters are selected to tune the SVM. The approach proposed in [20] is applied here to reduce the cost of selection procedure as well as to adjust the parameters of SVM. According to [20], after assigning the class label to the training data, we divide 70% of training data of each class for training and the rest for validation. Here, the Fisher's least square linear classifier is used with a low computation

cost for each class. The performance of this linear classifier is evaluated on the validation set and the confusion matrix, CM is measured as follows

$$CM = \begin{pmatrix} m_{11} & m_{12} & \cdots\cdots & m_{1n} \\ m_{21} & m_{22} & \cdots\cdots & m_{2n} \\ . & . & & . \\ & & \cdots\cdots & \\ . & . & & . \\ m_{n1} & m_{n2} & \cdots\cdots & m_{nn} \end{pmatrix} \tag{5.53}$$

Here, each row i corresponds to the class w_i and each column j represents the number of classes classified to w_j. The number of misclassified iris pattern is estimated for each class as follows

$$err_i = \sum_{j=1, j\neq i}^{n} m_{ij} \tag{5.54}$$

and then we sort number of misclassified pattern, $err_i, i = 1,2,.....n$ calculated from (5.54) in the decreasing order and the subscripts $i_1, i_2, ...i_I$ are assigned to the top I choices assuming that $I << N$. Now we determine the number of classes whose patterns can be classified to the class set $\{w_{i_1}, w_{i_2}, ...w_{i_I}\}$ based on the following confusion matrix

$$V = \bigcup_{k=1}^{I} \{w_j \mid m_{i_k j} \neq 0\} \tag{5.55}$$

Now from the class set V, we select the training and the cross validation set to tune C and kernel parameters for SVM. After a careful selection of C, and kernel parameters, the whole training set with all classes are trained.

5.6.1 Asymmetrical Support Vector Machines

The main drawback of the traditional SVM is that it does not differentiate between False Accept and False Reject which plays a very important role to meet different

security requirements. Another issue is to control the unbalanced data of a class with respect to other classes. Therefore, the traditional SVM is modified to an asymmetrical SVM ([19], [30]) to satisfy several security demands for the specific applications and to handle the unbalanced data in the proposed approach II, as follows:

1. In order to change the traditional SVM to asymmetrical SVM, a constant g is used which is called asymmetrical parameter, and it is used to adjust the decision hyperplane. Thus (5.30) becomes

$$x.w+b+g=0 \tag{5.56}$$

2. Therefore, the decision function of (5.52) changes to

$$f(x)=\sum_{i=1}^{N} y_i \alpha_i K(x,x_i)+b+g \tag{5.57}$$

When g>0, it indicates that the classification hyperplane is closer to positive samples. By changing the value of g, False Accept can be reduced and the statistically under-presented data of a class with respect to other classes can be controlled with the variation of the value of penalty parameter, C. The training and testing procedures with SVM for approaches I and II are depicted in appendix A.

Chapter 6

Experimental Results & Discussions

6.1. Introduction

We have used the CASIA (Chinese Academy of Sciences-Institute of Automation) iris image database and each iris class is composed of 7 samples taken in two sessions, three in the first session and four in the second [109]. Sessions were taken with an interval of one month which is a real world application level simulation. Images are 320x280 pixels gray scale taken by a digital optical sensor designed by National Laboratory of Pattern Recognition (NLPR). There are 108 classes of irises in a total of 756 iris images. The experimentation is conducted in two stages: performance evaluation of the proposed approaches I & II, and comparative analysis of our proposed methods with the existing schemes of iris recognition. In the first stage of the experimentation, we emphasize on performance evaluation of the proposed approaches based on classification and matching accuracy. We evaluate our proposed methods by comparing its recognition accuracy with other classical classification methods and matching strategies. We demonstrate the performance of PCA with Bhattacharyya Distance (BD) to reduce the dimensionality of the features. We also show the performance of the proposed genetic process for selecting the optimum features as well as to increase the overall system accuracy. The verification

performance of the proposed approaches is shown using a Receiver Operator Characteristics (ROC) curve. We exhibit the effect of False Accept Rate (FAR) and False Reject Rate (FRR) to meet different security requirements by changing the value of asymmetrical parameter of SVM. We also measure the performance of iris recognition systems using Equal Error Rates (EER). During the second stage, we carry out a series of experimentation to provide a comparative analysis of our method with the existing methods in respects of recognition accuracy and computational complexity. We show the average time consumption of the different parts of the proposed iris recognition system.

6.2. Performance Evaluation of the Proposed Approaches I & II

In this thesis, we examine the performance of the proposed approaches I & II on CASIA iris database. However, we focus on approach II and show the comparison between the proposed approaches.

In approach I, we use the whole iris information for recognition and traditional SVM is used for classification. Figure 33 reveals the classification accuracy of traditional SVM over FFBP, FFLM, and k-NN and the matching accuracy are depicted in Figure 34 with different feature dimensions. From Figures 33 & 34, we find that the performance of SVM is better than other classifiers used in this thesis for comparison. The number of nodes in hidden layers for FFBP and FFLM are kept at 110 and 140 respectively as the highest accuracy is obtained for these numbers of hidden nodes. From the experimentation it is found that both FFBP and FFLM provide minimum classification error when the iteration epoch is 150 and 120 respectively.

In approach II, we evaluate the success rate of the proposed method on the CASIA dataset by detecting the pupil boundary and the zigzag collarette area using chain code.

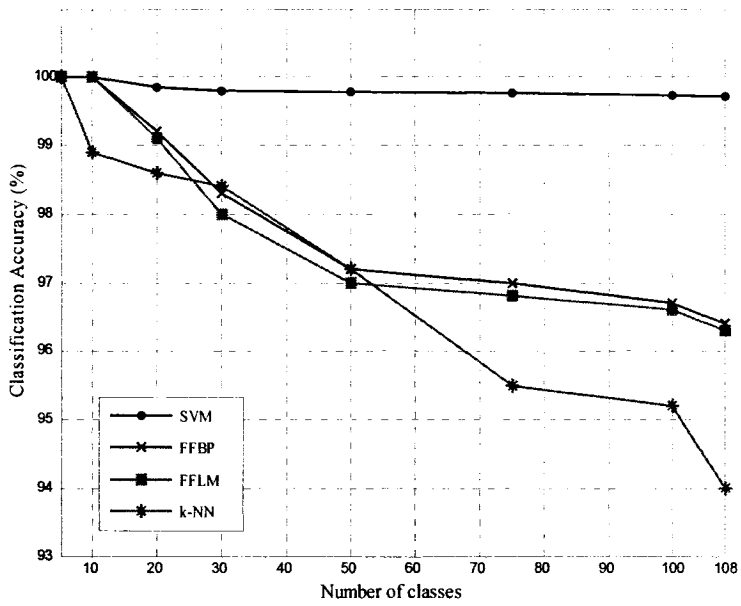

Figure 33: Comparison of classification accuracy among traditional SVM, FFBP, FFLM and k-NN for 600-bit feature sequence in Approach I.

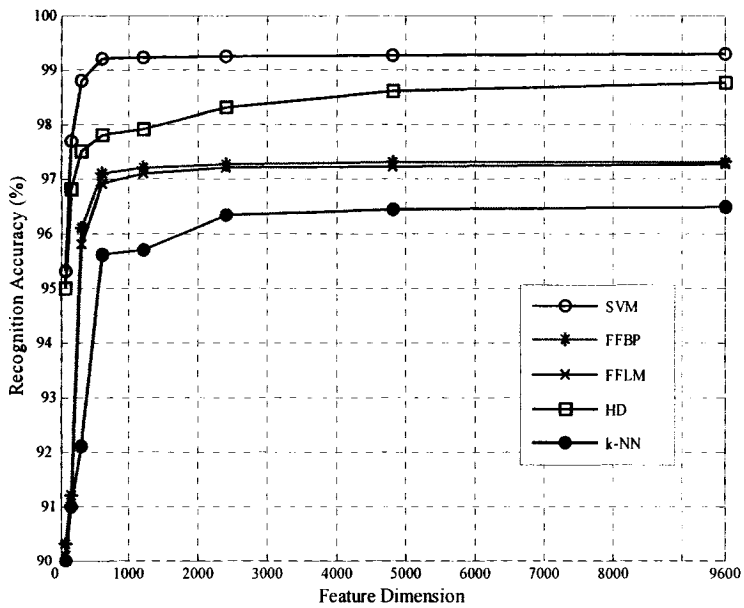

Figure 34: Comparison of recognition accuracy of traditional SVM with FFBP, FFLM, k-NN and HD for different feature dimension in Approach I.

The obtained success rate is 99.73%, where the proposed algorithm is failed to identify the pupil boundary in two cases only as our iris detection method erroneously segments the iris boundary. From the experimental results, it is observed that the reasonable recognition accuracy is achieved when the zigzag collarette area is isolated by increasing the previously detected radius value of the pupil by chain code up to 22 pixels. Tuning the SVM parameters is an important step to improve the classification performance. In order to reduce the computational cost and speed up the classification, a Fisher's least square linear classifier is used as a low cost pre-classifier so that reasonable cumulative recognition accuracy can be achieved to include true class label to a small number of selected candidates. Here, ten candidates are chosen and the cumulative recognition accuracy at rank 10 is 99.84%. In this thesis, the selected cardinal number of set found from the experimentation by using the algorithm proposed in [20] for adjusting SVM parameters is 24. As a result the sizes of training and validation sets for selecting the optimal value of C and σ^2 are 118 (=24*7*70%) and 50 (=24*7*30%) respectively. The parameter σ^2 is set at 0.6 and C at 100 when the highest accuracy on validation set has been achieved with the RBF kernels. Table 1 shows the performance of different kernel functions along with linear kernel for selected number of classes to choose the optimal values of SVM parameters. Since the highest classification accuracy is obtained by RBF kernel, this kernel is used in our system for iris patterns classification. In order to evaluate the matching accuracy, zigzag collarette area is used for recognition purpose. For each pattern, three irises are used build the iris templates for training and the remaining four irises for testing. In order to show the effectiveness of SVM as a classifier, extracted features are fed again as input to FFBP, FFLM, and k-NN for

classification and accuracy of classification for various numbers of classes among FFBP, FFLM, SVM, and k-NN (k=2) are shown in Figure 35 for the 600 bit feature sequence. The number of nodes in hidden layer for FFBP and FFLM are kept at 220 and 160 respectively as the highest accuracy is obtained for these numbers of hidden nodes. From the experimentation, it is found that both FFBP and FFLM provide minimum classification error when the iteration epoch is 140 and 110 respectively. Later the Principal Component Analysis (PCA) [22] is used to reduce the dimension of the extracted feature vectors and the iris pattern of only 5 features is used to measure the classification performance of SVM with the Mahalanobis distance classifier (MDC) [22] along with the other classic methods as shown in Figure 36. Figure 36 shows the poor classification accuracy since only 5 features are used for classification. Furthermore, based on 5 features, it is not trustworthy to make a decision that the performance of Mahalanobis distance as a classifier is not good enough as compared to SVM in the area of iris recognition. However, from Figure 36 it is found that for 5 features all other classification schemes perform almost equally with SVM and also we can say that MDC may work well if the number of samples is increased.

Table 1: Efficiency of various kernel functions.

Kernel Type	Classification Accuracy (%)
Linear	98.7
Polynomial	98.1
RBF	99.3
Sigmoid	98.2

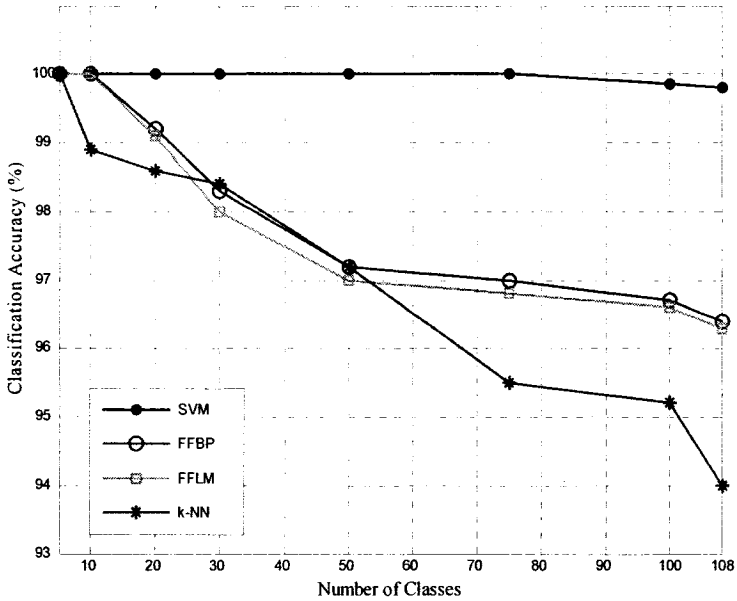

Figure 35: Comparison of classification accuracy among SVM, FFBP, FFLM and k-NN for 600-bit feature sequence in Approach II.

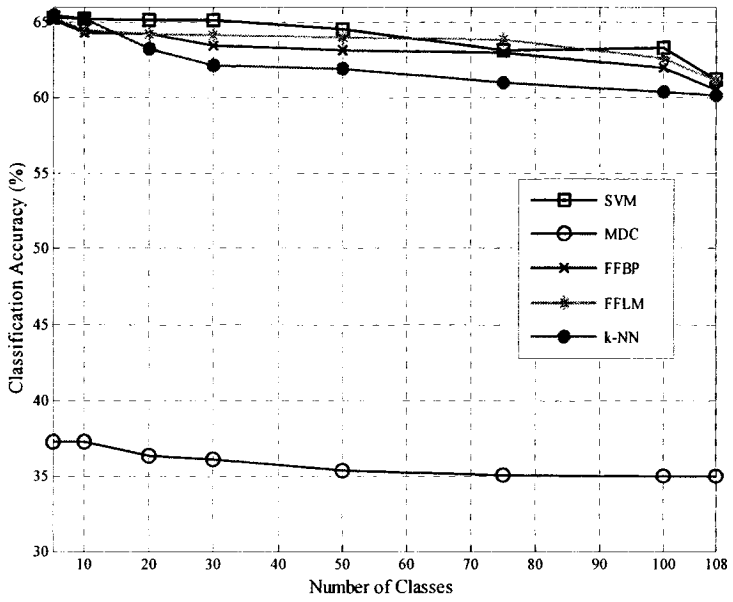

Figure 36: Comparison of classification accuracy of SVM with FFBP, FFLM, k-NN and MDC for 5-bit feature sequence in Approach II.

Dimension reduction is required due to the smaller sample sizes per class which are not suitable for Mahalanobis distance. From Figure 35, it is noted that the performance of SVM as an iris classifier is far better than the other classical methods though the classification accuracy is decreased as number of classes are increased. From Figure 36, we observe that SVM still performs reasonably well even though the sample size is limited. Figure 37 shows the comparison of the feature dimension versus recognition accuracy among Hamming Distance (HD), FFBP, FFLM, k-NN and SVM. In this case only the RBF kernel is considered due its reasonable classification accuracy for SVM as mentioned earlier. From Figure 37, we can see that with increasing dimensionality of the feature sequence, the recognition rate also increases rapidly for all similarity measures. However, when the dimensionality of the feature sequence is up to 600 or higher, the recognition rate starts to saturate at an encouraging rate of about 99.56% for approach II.

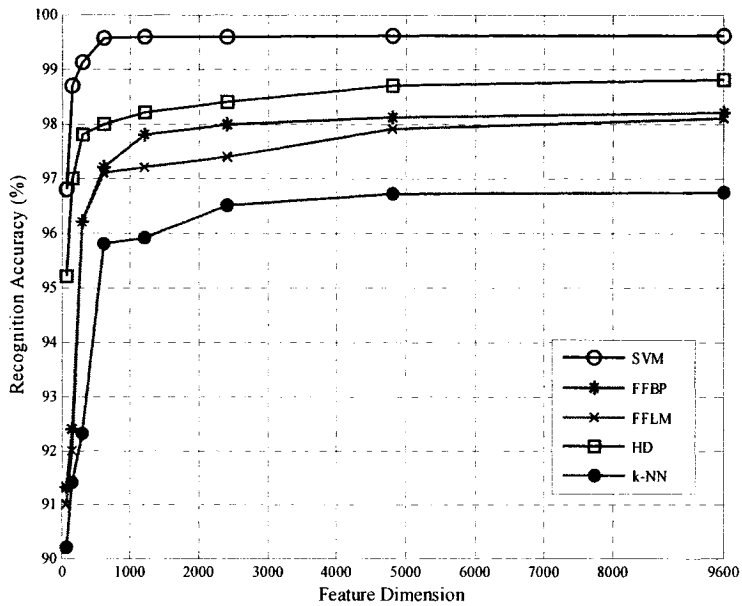

Figure 37: Comparison of recognition accuracy of SVM with FFBP, FFLM, k-NN and HD for different feature dimension in Approach II.

In this thesis, we use the BD measure with PCA for feature reduction. Figure 38 plots the number of features (*nf*) versus BD and it is noticeable from this figure that increasing *nf* does not show any sign of saturation and therefore, it is necessary to keep on increasing the new features or we can simply find that this proposed feature reduction technique has no significant benefit since the number of features per sample is much higher than that of the number of samples for each iris pattern. This proposed feature reduction scheme may work better if the number of samples per class is increased. Since the proposed feature reduction technique with BD and PCA do not perform well in our case, we decide to use MOGA to reduce the dimensionality. For selecting the optimum features to increase the accuracy of the matching process, MOGA involves running the genetic process for several generations as shown in Figure 39.

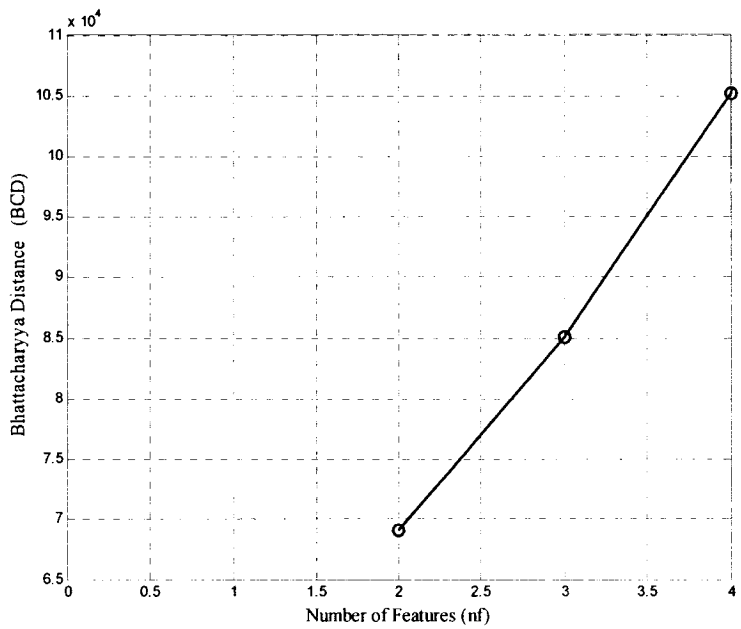

(a)

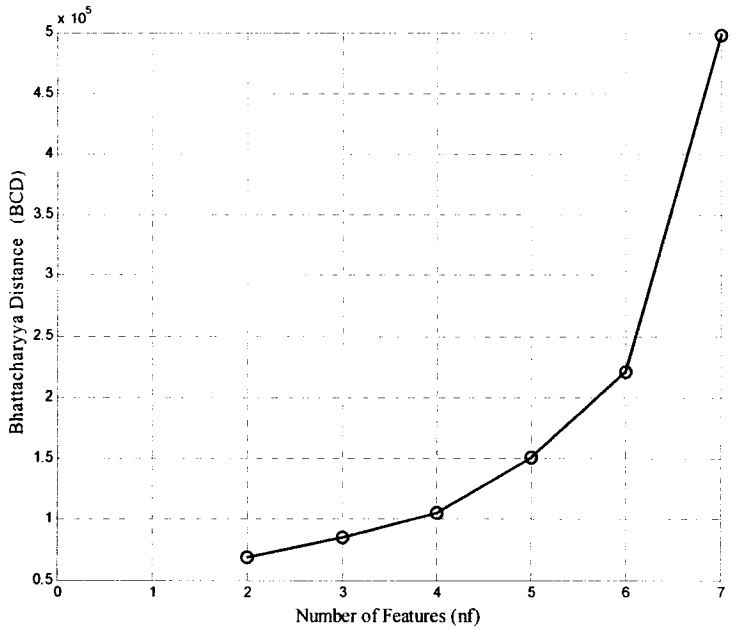

(b)

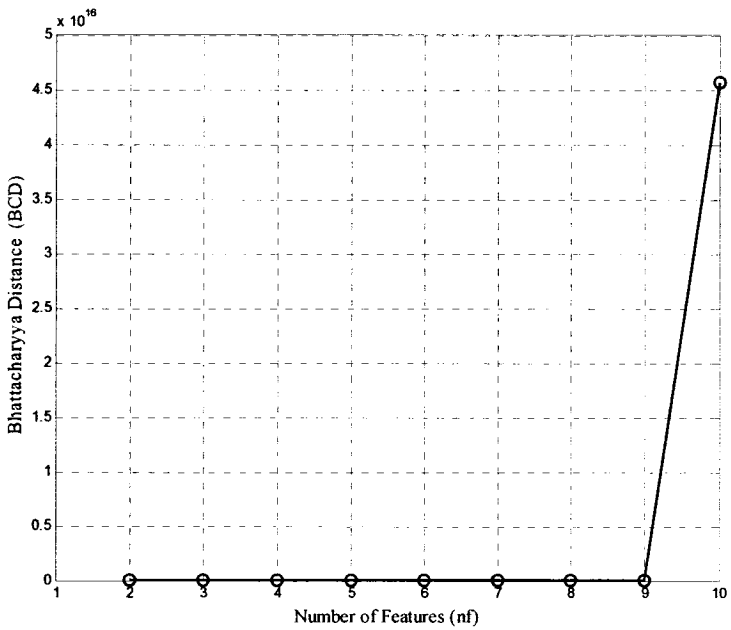

(c)

Figure 38: (a), (b), and (c) demonstrate that *nf* does not show any sign of saturation and it requires more samples per iris pattern class to obtain a saturated situation after a certain number of features reduction.

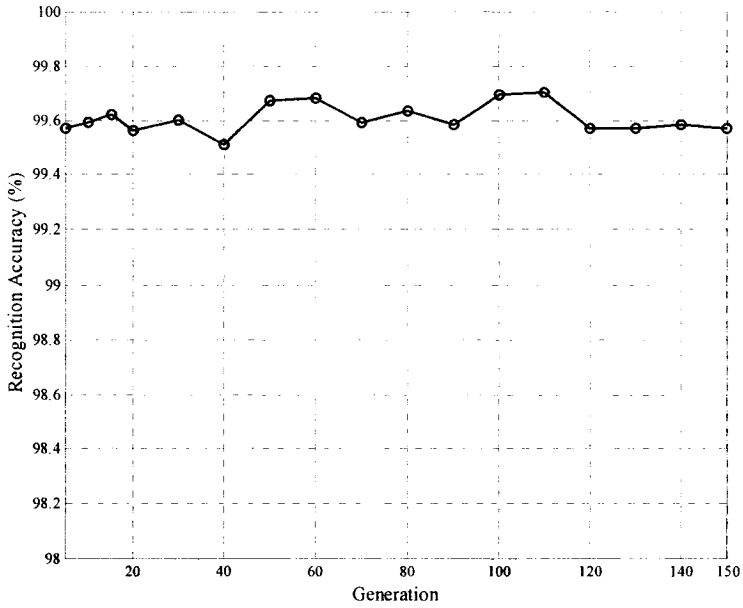

Figure 39: Variation of recognition rates with generation for approach II.

From this figure, it is noted that the highest matching accuracy of 99.71 % is achieved at the generation 110. The evolution of the MOGA can be observed in Figure 40.

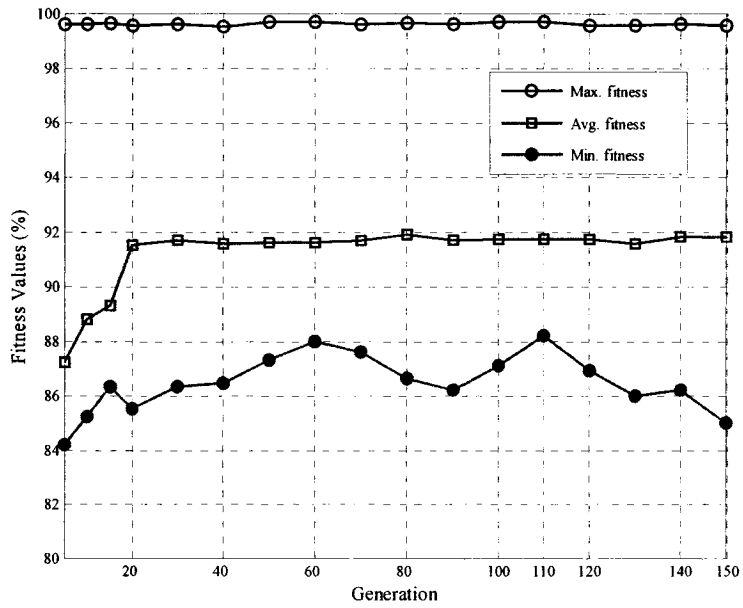

Figure 40: Variation of fitness values with generation for approach II.

It is observed from Figure 40 that the MOGA represents a good convergence since average fitness of the population approaches with that of the maximum individual along the generations. We conduct several experimentations and the arguments of the MOGA are set as follows when the reasonable accuracy is obtained:

- Population size: 108 (the scale of iris samples)
- Length of the chromosome code: 600 (selected dimensionality of feature sequence)
- Crossover probability: 0.7
- Mutation probability: 0.005
- Number of generation: 110

The recognition accuracy is compared between the proposed method using the zigzag collarette area and the approach I [72] where the whole iris information between pupil and sclera boundary are considered for recognition. However, for comparative analysis, we apply the tuned and asymmetrical SVM on approach I which utilizes the features of whole iris region. Figure 41 shows the efficiency of the approach II with and without MOGA in comparison with the approach I and it is noticeable that the proposed approach II performs better with an accuracy of 99.71 % where we consider the zigzag collarette region and therefore, it is found that the performance of approach II is increased when we use MOGA for feature selection. The proposed approach II leads to a reasonable recognition accuracy in the case where eyelashes and eyelids occlude irises badly so that the pupils are partly invisible. The adjustment of asymmetrical parameter g can be made to satisfy several security issues in iris recognition applications and handle the unbalanced data of a specific class with respect to other classes. The performance of a verification system is evaluated using ROC curve, see Figure 42, which demonstrates

how the Genuine Acceptance Rate (GAR) changes with a variation in FAR for our proposed approaches I and II.

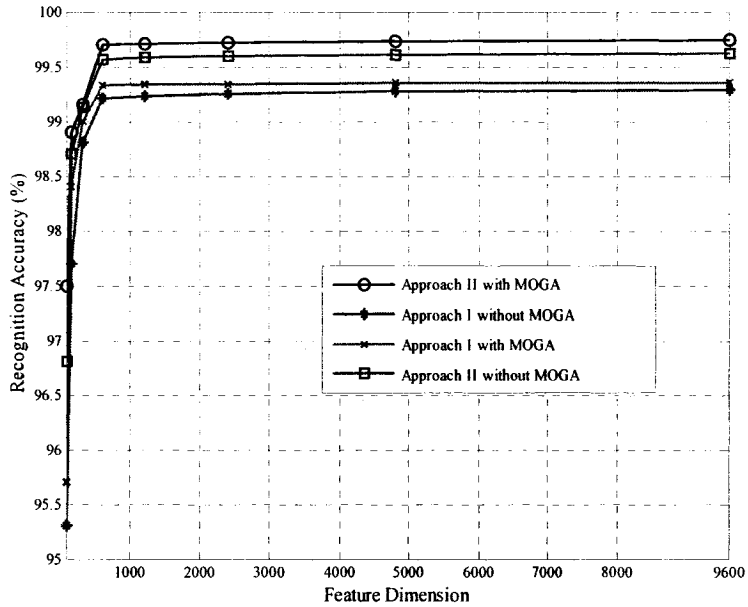

Figure 41: Comparison of recognition accuracy between approaches I and II.

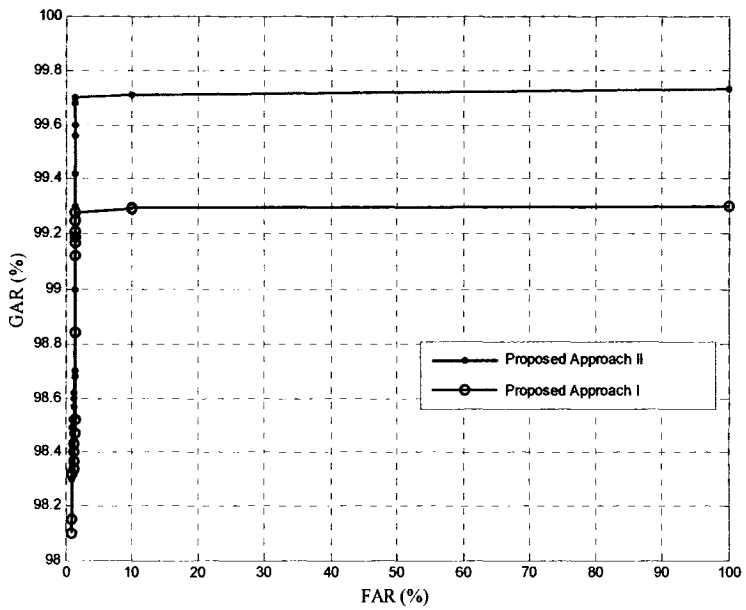

Figure 42: ROC curve shows the comparison between GAR and FAR for proposed approaches I & II.

From the experimentation, we find that the proposed approach II reduces EER from 0.38% of approach I which is based on whole complete iris information to 0.15%, which represents a good improvement of our proposed approach II. Figure 43 reveals that the proper selection of the asymmetrical parameter g leads to low recognition error both in the cases of proposed approaches I & II.

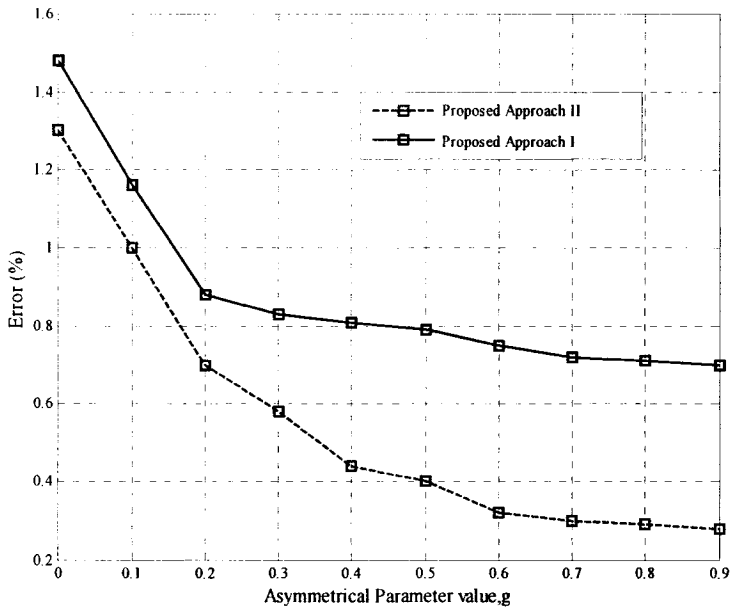

Figure 43: Comparison of recognition error between proposed approaches I &II with different values of asymmetrical parameter, g.

6.3. Comparison with Existing Methods

The methods proposed in ([5], [15], [16], [17]), ([96], [50], [51], [82], [69]) and ([53], [55], [56]) are considered as the promising solutions for iris recognition among the existing approaches. Furthermore, these methods are based on phase, texture analysis, and zero-crossing representation of iris. Therefore, we decide to compare our algorithm with these methods. Table 2 reveals the comparison of the correct recognition rates (CRR) between several methods. From this table, we see that methods reported in [16]

and [56] have better performance than our proposed approach II, followed by the methods of ([5], [50], [51], and [55]). Table 2 also demonstrates a comparison of the EER between different methods and from this table we see that our proposed approach II has less EER than the methods reported in ([96], [5], [55], and [50]) and higher EER than the methods of ([16], [56]). As no EER is reported in [51], we ignore the EER from our consideration. In our proposed approaches I & II, we use 538 reduced number of features for recognition purpose which is smaller than the number of features used in [16] and [56] where number of components are 2048 and 660 respectively. However, only 200 reduced features are used in [55] which are much smaller than our proposed approach II. One problem of the method in [55] seems to be that the spatial filters are used which may fail to capture the fine spatial changes of the iris. We overcome this possible drawback by using the phase based approach using log-Gabor filters and then we use MOGA to select the most discriminating feature sequence. In [33], zigzag collarette area is used with only eyelash detection technique for iris recognition. However, in our proposed scheme, we successfully isolate the zigzag collarette region along with eyelashes, eyelids and noise detection method which helps to increase the recognition accuracy and consequently overcome the problem when the pupil is occluded badly by eyelids and eyelashes. We conduct the above experimentation on a 3.00 GHz Pentium IV PC with 512M RAM and we implemented our code in Matlab 7.1. The overview of the subsystems and MatLab functions are given in appendix B. Table 3 shows that our proposed approach II significantly reduces the time complexity than the approach I. The main reason is that in the approach II, we employ a faster pupil detection technique using chain code than our

approach I where Hough transform and Canny edge detection are used which are more time consuming.

Table 2: Comparison of recognition rates and equal error rates.

Methods	Correct recognition Rate (%)	Equal Error Rate (%)
Daugman [16]	**100**	**0.08**
Wildes et al. [96]	**-**	**1.76**
Boles et al. [5]	**92.64**	**8.13**
Ma et al. [55]	**99.60**	**0.29**
Ma et al. [56]	**100**	**0.07**
Liu et al. [50]	**97.75**	**1.79**
Liu et al. [51]	**89.64**	**-**
Proposed approach I	**99.28**	**0.38**
Proposed approach II	**99.71**	**0.15**

Table 3: Comparison of average time consumption of different parts of iris recognition system.

Methods	Iris Segmentation (ms)	Normalization (ms)	Feature Extraction (ms)	Recognition (ms)	Total (ms)
Proposed Approach I	**34580.0**	**23.7**	**11.80**	**150.2**	**34755.70**
Proposed Approach II	**13240.5**	**19.1**	**10.27**	**140.0**	**13409.87**

We can observe from this table that both of our proposed methods consume significant time for segmentation since the Hough transform is used in both approaches. We can improve time complexity if exclude the Hough transform part for iris detection. However, in that case the accuracy of the segmentation may decrease since the whole eye region is

involved for pupillary detection instead of a predetermined iris area. In [50], a modified Hough transform with Canny edge detection was employed for segmentation to reduce the edge points which overcomes the segmentation problem of the approach I [72]. However, the method reported in [50] seems to have a problem of large time consumption which we may overcome by using the proposed chain code to isolate the pupil. In Table 4, where the results of first five rows are taken from [56], we see that our current approach consumes less time than the other methods for feature extraction. The reason is that our method is based on 1D signal analysis and the method of [16] involves 2D mathematical calculation. However, our approach takes much time for recognition as SVM is used for matching process. From this table, we notice that the over all time consumption is less than the other existing methods which is really encouraging. Our current approach requires extra cost as in [55] for feature reduction. In [69], a basic genetic algorithm was used to find a distribution of points over the iris region which leads the system to reasonable accuracy of 99.70 % which is almost same in comparison with the matching rate of our proposed approach II. However, in this thesis, we propose the MOGA where the main concerns are to minimize the recognition error based on SVM performance on testing set and reduce the number of features. In [82], a traditional SVM is used for pattern matching which seems to fail to separate the FAR and the FRR with a matching accuracy of 98.24%. The usage of asymmetrical SVM in proposed approach II differentiates the FAR and the FRR to meet the several security requirements depending on the various application areas with a reasonable recognition rate of 99.71%. However, a faster feature reduction approach was used in [82] based on direct discriminant analysis than the approach II proposed in this thesis with MOGA.

Table 4: Comparison of the computational complexity.

Methods	Feature Extraction (ms)	Matching (ms)	Feature Extraction +Matching (ms)	Others
Daugman [16]	**682.5**	**4.3**	**686.8**	**-**
Wildes et al. [96]	**210.0**	**401.0**	**611.0**	**Registration**
Boles et al. [5]	**170.3**	**11.0**	**181.3**	**-**
Ma et al. [55]	**260.2**	**8.7**	**268.9**	**Feature reduction**
Ma et al. [56]	**244.2**	**6.5**	**250.7**	**-**
Proposed approach I	**11. 80**	**150.2**	**162.0**	**-**
Proposed approach II	**10.27**	**140.0**	**150.27**	**Feature reduction**

6.4. Discussions

Based on the above experimental results we can depict the following points:

- The proposed method can be considered as a phase based analysis method from the viewpoint of feature representation strategy as the phase information are characterized by our representation scheme.
- Though the zigzag collarette area is insensitive to the pupil dilation and usually not affected by eyelids and eyelashes, there might be few cases where this region is partially occluded since it is closed to pupil. Our proposed method of detecting the zigzag collarette area along with eyelids, eyelashes (both in the cases of separable and multiple eyelashes) and noise removal techniques successfully overcome this problem and this also helps to increase the over all matching accuracy.
- We find from experimental results that the selection of SVM parameters

contributes in improving the classification accuracy while the number of classes is higher. The tuned SVM with an additional asymmetrical parameter separates FAR and FRR according to different security demands and controls the unbalanced data with respect to other classes.

- It is noted that the feature selection method by MOGA increases the recognition accuracy and contributes in reducing the feature dimension.
- Although the proposed feature selection strategy with BD and PCA does not perform well for our scheme, this feature selection strategy may perform better in the case where the number of samples per iris pattern class is increased.
- The experimental results exhibit that the proposed algorithm of approach II performs reasonably well if we consider the speed and accuracy. The adopted pupil detection method by chain code contributes to a drastic speed-up in the whole process.
- Although one might think that the proposed method using zigzag collarette has lesser information available as compared to the other methods using the whole iris information, the proposed method can be used effectively for personal identification since the zigzag collarette area contains enough discriminating features.

Chapter 7

Conclusions

7.1. Summary of Thesis Work

In this thesis, we present iris recognition approaches using SVM as iris pattern classifiers. In order to verify the claimed performance, proposed approaches are tested using a database of grayscale iris images.

In the proposed approach I, an automatic segmentation scheme based on Canny edge detection and circular Hough transform is used to localize the iris and pupil regions from the eye image and the linear Hough transform is applied to isolate the occluded eyelids. A thresholding method is utilized to separate the eyelashes which occlude the iris region. Next, the segmented iris region is transformed into normalized form in order to avoid the dimensional inconsistencies in subsequent processing. Daugman rubber sheet model is employed to normalize the iris region into a rectangular block with constant polar dimension. Finally, the 1D log-Gabor filters are convolved with the normalized iris pattern to extract the iris features and a bit-wise iris pattern is produced by the phase quantization of the output. Finally, the conventional SVM is deployed to classify the generated iris patterns. In the proposed approach II, an iris recognition method is presented using an efficient iris segmentation approach based on chain code and zigzag

collarette area with the incorporation of eyelashes and eyelids detection techniques. First, we localize the iris region using the circular Hough transform based on the prior knowledge of iris. The chain code is applied to isolate the pupil from the localized iris region and the zigzag collarette area is detected through the previously obtained center value and radius of pupil. We utilize the similar approach for eyelids and eyelashes detection used in approach I. The isolated collarette region is unwrapped into a fixed dimension using Daugman rubber sheet model where the collarette area is modeled as a flexible rubber sheet. We use 1D log-Gabor filters to extract the discriminating features from the unwrapped collarette region and MOGA is applied for feature subset selection based on the matching accuracy of SVM. We also propose another feature selection strategy with BD and PCA. In order to increase the feasibility of SVM in biometrics applications, it is modified as an asymmetrical SVM to meet several security demands and deal with the unbalanced data of a specific class with respect to other classes. In order to improve the generalization performance of SVM, the optimum values of SVM parameters are selected.

7.2. Findings of Thesis Work

Based on the analysis of proposed iris recognition methods, we find a number of interesting conclusions. Segmentation can be treated as one of the crucial stages for iris recognition since the incorrect segmentation results the poor recognition accuracy. In this thesis, we find that the performance of segmentation depends on the quality of iris images. The chain code applied in the approach II separates the pupil from an iris image and accelerates the segmentation process. Generally, the zigzag collarette region is not occluded by the eyelids and eyelashes, however, there are few instances where the

eyelashes and eyelids affect the collarette region. However, the proposed method for localizing the collarette region with eyelashes and eyelids detection techniques successfully eliminates the irrelevant iris regions. The proposed method using zigzag collarette has lesser information available as compared to the other methods which use the whole iris information. However, the proposed method can be used effectively for personal identification since the zigzag collarette area contains enough distinctive features.

Another interesting finding is that 1D log-Gabor filters can be used for accurate recognition since the use of multi scale representation is possible for the encoding process. In approaches I & II, the proposed method of feature extraction consumes less time since it is based on the 1-D signal analysis rather than the involvement of 2-D mathematical operation. We also observe that the optimum center wavelength is dependent on the imaging conditions. The scheme for feature selection using BD and PCA reveals poor results since the number of samples per iris class is smaller compared to the extracted feature dimension. The feature selection scheme based on BD and PCA may perform reasonably well if the number of samples per class is increased. From the experimental analysis, it is found that MOGA increases the recognition accuracy and furthermore, contributes in reducing the feature dimension. The experimental analysis reveals that the tuning of SVM parameters improves the classification accuracy. We also find that the tuned SVM with an additional asymmetrical parameter isolates FAR and FRR according to different security demands, and controls the unbalanced data of a class with respect to other classes. The proposed iris recognition method with the exploitation of features of zigzag collarette area and asymmetrical SVM as classifiers can be applied

in wide range of security related application areas. Experimental results exhibit the encouraging performance of the proposed approach II for both in the cases of accuracy and speed. The method proposed in approach I acquire the matching accuracy of 99.28% with EER of 0.38% while the proposed approach II reaches the accuracy of 99.71% having an EER of 0.15%. In particular, a comparative study of existing methods for iris recognition has been conducted. The performance evaluation and comparisons with other methods indicate that the proposed schemes are viable and very efficient for iris recognition.

7.3. Suggestions for Future Development

In this thesis, the proposed approaches perform reasonably well. However, there are number of issues, which should be addressed and resolved. In order to increase the accuracy of the system, a more accurate and elaborate eyelids and eyelashes detection scheme can be employed. Since the quality of the images affect the overall matching accuracy, an iris image quality assessment scheme can be deployed. We see that the most computation intensive part involves the segmentation with Hough transform technique. Since we implement the system in Matlab, which is an interpreted language, a development in speed can be achieved if the most time consuming parts are implemented in C or C++. In future, the SVM boosting strategy can be employed to reduce the computational time for the overall iris recognition system. In order to make the proposed approach applicable in real-time situation, reducing the time consumption may be considered as an important factor. Many efficient systems for iris recognition are available nowadays. However, the properties of iris texture and the underlying processes of generating it have not been explored. Therefore, an additional room for the extension

of the successful iris recognition system is to give an insight into these aspects. Although the experimental results exhibit that the proposed approaches work well, there are still some anomalies that should be considered. The iris liveness detection is a major issue in this respect, otherwise a high resolution photograph can be presented in an iris recognition camera which may result an unauthorized match. Fake iris detection is another important factor which should be handled carefully. Contact lenses are vastly used nowadays which can change the color of an individual's iris. This may create a problem to any iris recognition system, since a fake iris pattern is printed on the surface of the lens, and may falsely reject an enrolled user, or falsely accept them, if the fake iris pattern has been enrolled in the database. We also find another problem, although quite minor, the border of any contact lens is slightly visible in an eye image, and this circular border may be regarded as the iris boundary by the automatic segmentation algorithm during the time of iris localization. Furthermore, the spectacles may introduce too much specular reflection which results in failure of automatic segmentation and/or recognition.

References

[1] K. Bae, S. Noh, and J. Kim, "Iris feature extraction using independent component analysis," *Proc. of 4th Internat. Conf. on Audio and Video-Based Biometric Person Authentication*, pp. 838–844, 2003.

[2] D. Ballard, "Generalized Hough transform to detect arbitrary patterns," *IEEE Trans. on Pattern Anal. Machine Intell.*, vol. 13, pp. 111–122, 1981.

[3] S. Bandyopadhyay, S. K. Pal, and B. Aruna, "Multuobjectives GAs, quantitative indices, and pattern classification," *IEEE Trans. on Systems, Man, and Cybernatics part B,* vol. 34, pp. 2088-2099, 2004.

[4] C. M. Bishop, *Neural networks for pattern recognition,* Oxford University Press, New York, 1995.

[5] W. Boles, and B. Boashash, "A human identification technique using images of the iris and wavelet transform," *IEEE Trans. on Signal Processing*, vol. 46, pp. 1185–1188, 1998.

[6] R. Bolle, J. H. Connell, S. Pankanti, N. K. Ratha, and Andrew W., *Guide to biometrics,* New York, Springer, 2003.

[7] B. Bonney, R. Ives, D. Etter, and Y. Du, "Iris pattern extraction using bit planes and standard deviation," *Asilomar Conf. on Signals, Systems, and Comp.*, vol.1, pp. 582-586, USA, 2004.

[8] C.C Chang, and C.J. Lin, *LIBSVM: a library for support vector machines*, 2001. Software available at http://www.csie.ntu.edu.tw/~cjlin/libsvm.

[9] Y. Chen, S. C. Dass, and A.K. Jain, "Localized iris image quality using 2-D wavelets," *Internat. Conf. on Biometric Authentication*, Springer Lecture Note Series in Computer Science, vol. 3882, pp. 373-381, 2006.

[10] C.S. Chin, A.T.B. Jin, and D.N.C. Ling, "High security iris verification system based on random secret integration," *Elsevier J. on Comp. Vision and Image Understanding*, vol. 02, pp. 169-177, 2006.

[11] S. C. Chong, A. B. J. Teoh, and D. C. L. Ngo, "Iris authentication using privatized advanced correlation filter," *Internat. Conf. on Biometric Authentication,* Springer Lecture Note Series in Computer Science, vol. 3882, pp. 382-388, 2006.

[12] J. Cui, Y. Wang, J. Huang, T. Tan, and Z. Sun, "An iris image synthesis method based on PCA and super-resolution," *Internat. Conf. on Pattern Recog.*, vol. 04, pp. 471-474, Cambridge, UK, 2004.

[13] J. Cui, L. Ma, Y. Wang, T. Tan, and Z. Sun, "An Appearance-based method for iris detection", *Asian Conf. on Comp. Vision*, vol. 2, pp. 1091-1096, Korea, 2004.

[14] C. H. Daouk, L.A. El-Esber, F.D. Kammoun, and M.A.Al Alaoui, "Iris recognition," *IEEE Internat. Sympos. on Signal Processing and Info. Tech.*, pp.558-562, Morocco, 2002.

[15] J. Daugman, "High confidence visual recognition of persons by a test of statistical independence," *IEEE Trans. on Pattern Anal. Machine Intell.*, vol. 15, pp. 1148–1161, 1993.

[16] J. Daugman, "Statistical richness of visual phase information: update on recognizing persons by iris patterns," *Internat. J. on Comp. Vision*, vol. 45, pp. 25–38, 2001.

[17] J. Daugman, "Demodulation by complex-valued wavelets for stochastic pattern recognition," *Internat. J. on Wavelets, Multi-Res. and Info. Processing*, vol. 1, no. 1, pp. 1–17, 2003.

[18] J. Daugman, *Biometric personal identification system based on iris analysis*, U.S. Patent No. 5291560, 1994.

[19] P. Ding, Z. Chen, Y. Liu, and B. Xu, "Asymmetrical support vector machines and application in speech processing, *IEEE Internat. Conf. on Acousts., Speech, and Signal Process.*, vol. 1, pp. 73-76, 2002.

[20] J. Dong, A. Krzyzak, and C. Y. Suen, "An improved handwritten chinese character recognition system using support vector machines," *Pattern Recog. Lett.*, vol. 26, pp. 1849-1856, 2005.

[21] Y. Du, R. Ives, D. Etter, and T. Welch, "A new approach to iris pattern recognition," *Proc. Of SPIE,* vol. 5612, pp. 104-116, 2004.

[22] R.O. Duda, P.E. Hart, and D.G. Stork, *Pattern Recognition*, 2nd. ed., John Wiley, NY, 2001.

[23] D. Field, "Relations between the statistics of natural images and the response properties of cortical cells," *J. on the Optical Society of America*, 1987.

[24] L. Flom and A. Safir, "Iris Recognition Systems," U.S. Patent No. 4641394, 1987.

[25] H. Freeman, "Computer processing of line drawing images", *ACM Computing Surveys*, vol. 6, pp. 57-97, 1974.

[26] J. Fu, H.J. Caulfield, S. Yoo., and V. Atluri, "Use of artificial color filtering to improve iris recognition and searching," *Pattern Recog. Lett.*, vol. 26, pp. 2224-2251, 2005.

[27] K. Fukunaga, *Introduction to statistical pattern recognition*, Second ed., Academic Press, New York, 1990.

[28] J. Gan, and Y. Liang, "Applications of wavelet packets decomposition in iris recognition," *Internat. Conf. on Biometric Authentication*, Springer Lecture Note Series in Computer Science, vol. 3882, pp. 441-449, 2006.

[29] D.E. Goldberg, *Genetic algorithms in search, optimization and machine learning*, Addison-Wesley Reading, MA, 1989.

[30] H. Gu, Z. Gao, and F. Wu, "Selection of optimal features for iris recognition," *Internat. Sympos. on Neural Networks*, Springer Lecture Note Series in Computer Science, vol. 3497, pp. 81-86, 2005.

[31] M. T. Hagan, and M. B. Menhaj, "Training feedforward networks with the Marquardt algorithm," *IEEE Trans. on Neural Networks,* vol. 5, No. 6, 1994.

[32] J. Havlicek, D. Harding, and A. Bovik, "The multi-component AM-FM image representation," *IEEE Trans. on Image Processing*, vol. 5, pp. 1094–1100, 1996.

[33] X. He, and P. Shi, "An Efficient iris segmentation method for recognition", *Internat. Conf. on Adv. Pattern. Recog*, Springer Lecture Note Series, vol. 3687, pp. 120-126, 2005.

[34] X. He, and P. Shi, "A novel iris segmentation method for hand-held Capture device," *Internat. Conf. on Biometric Authentication*, Springer Lecture Note Series in Computer Science, vol. 3882, pp. 479-485, 2006.

[35] F.V.D. Heijden, R.P.W. Duin, D.D. Ridder, and D.M.J. Tax, *Classification, parameter estimation and state estimation: An engineering approach using Matlab*, John Wiley, UK, 2004.

[36] Y.P. Huang, S.W. Luo, and E.Y. Chen, "An efficient iris recognition system," *IEEE Internat. Conf. on Machine Learning and Cybernetics*, pp. 450-454, Beijing, China, 2002.

[37] J. Huang, L. Ma, T. Tan, and Y. Wang, "Learning based resolution enhancement of iris images," *British Machine Vision Conference,* Norwich, UK, 2003.

[38] C. Huo, and P. Bhattacharya, "Content-based indexing of volumetric images using principal component analysis," *Internat. J. on Pattern Recognition and AI,* vol. 15, pp. 1299-1309, 2001.

[39] A.K. Jain, A. Ross, and S. Prabhakar, "An introduction to biometric recognition," *IEEE Trans. on Circuits and Systems for Video Technology*, vol. 14, no.1, 2004.

[40] A.K. Jain, R. Bolle, and S. Pankanti, *Biometrics: personal identification in a networked society*, Kluwer, Norwell, MA, 1999.

[41] D. S. Jeong, H. Park, K. R. Park, and J. Kim, "Iris recognition in mobile phone based on adaptive Gabor filter," *Internat. Conf. on Biometric Authentication*, Springer Lecture Note Series in Computer Science, vol. 3882, pp. 457-463, 2006.

[42] T. Kailath, "The divergence and Bhattacharyya distance measures in signal selection", *IEEE Trans. on Comm. Tech.*, vol. 15, no. 1, pp. 52-60.

[43] J. Kim, S. Cho, and J. Choi, "Iris recognition using wavelets," *J. on VLSI Signal Processing,* vol. 38, pp. 147–156, 2004.

[44] E. Krichen, M.A. Mellakh, S. Garcia-Salicetti, and B. Dorizzi, "Iris identification using wavelet packets," *Internat Conf. on Pattern Recog.,* vol. 04, pp. 335 – 338, 2004.

[45] W. Kong, and D. Zhang, "Accurate iris segmentation based on novel reflection and eyelash detection model," *Internat. Sympos. on Intelligent Multimedia, Video and Speech Process*, Hong Kong, 2001.

[46] B. Kumar, C. Xie, and J. Thornton, "Iris recognition and verification using correlation filters," *Internat. Conf. Audio- and Video-based Biometric Person Authentication*, pp. 697–705, 2003.

[47] S.Y. Kung, M.W. Mak, and S.H. Lin, *Biometric authentication: a machine learning approach,* 1st Ed., Prentice Hall information and system science series, USA, 2005.

[48] E. C. Lee, K. R. Park, and J. Kim, "Fake iris detection using purkinje image," *Internat. Conf. on Biometric Authentication*, Springer Lecture Note Series in Computer Science, vol. 3882, pp. 397-403, 2006.

[49] S. Lim, K. Lee, O. Byeon, and T. Kim, "Efficient iris recognition through improvement of feature vector and classifier," *Electronic and Telecomm. Research Inst. J.*, vol. 23, pp. 1–70, 2001.

[50] X. Liu, K.W. Bowyer, and P.J. Flynn, "Experiments with an improved iris segmentation algorithm," *IEEE Workshop Automatic Identification Advanced Technologies*, pp. 118-123, 2005.

[51] X. Liu, K.W. Bowyer, and P.J. Flynn, "Experimental evaluation of iris recognition", *IEEE Conf. on Comp. Vision and Pattern Recog.*, vol. 3, pp. 158-165, 2005.

[52] L. Ma, Y. Wang, and T. Tan, "Iris recognition based on multichannel Gabor filtering," *Asian Conf. on Comp. Vision*, vol. I, pp. 279–283, 2002.

[53] L. Ma, Y. Wang, and T. Tan, "Iris recognition using circular symmetric filters," *Internat. Conf. on Pattern Recog.*, vol. II, pp. 414–417, 2002.

[54] L. Ma, "Personal identification based on iris recognition," *Ph.D dissertation*, Inst. of Automation, Chinese Academy of Sciences, Beijing, 2003.

[55] L. Ma, T. Tan, Y. Wang, and D. Zhang, "Personal identification based on iris texture analysis", *IEEE Trans. on Pattern Anal. Machine Intell.*, vol. 25, pp. 1519-1533, 2003.

[56] L. Ma, T. Tan, Y. Wang, and D. Zhang, "Efficient iris recognition by characterizing key local variations", *IEEE Trans. on Image Processing*, vol. 13, pp. 739-750, 2004.

[57] S. Makthal, "Analysis and synthesis of iris images," *Master's dissertation*, Dept. of Electrical Engineering, West Virginia University, 2005.

[58] S. Mallat and W. Hwang, "Singularity detection and processing with wavelets," *IEEE on Trans. Inform. Theory*, vol. 38, pp. 617–643, 1992.

[59] T. Mansfield, G. Kelly, D. Chandler, and J. Kane, "Biometric product testing", *Final Rept.*, Nat. Physical Lab., U.K., 2001.

[60] D. Martin-Roche, D. Sanchez-Avila, and C.R. Sanchez-Reillo, "Iris recognition for biometric identification using dyadic wavelet transform zero-crossing," *IEEE Internat. Carnahan Conf. on Security Tech.*, pp. 272-275, UK, 2001.

[61] L. Masek, "Recognition of Human Iris Patterns for Biometrics Identification," *B.Eng. thesis*, University of Western Australia, 2003.

[62] K. Miyazawa, K. Ito, T. Aoki, K. Kobayashi, and H. Nakajima, "A phase-based iris recognition algorithm," *Internat. Conf. on Biometric Authentication*, Springer Lecture Note Series in Computer Science vol. 3882, pp. 356-365, 2006.

[63] T. Moriyama, T. Kanade, J. Xiao, and J. F. Cohn, "Meticulously detailed eye region model and its application to analysis of facial images," *IEEE Trans. on Pattern Anal. Machine Intell.*, vol 28, pp. 738–752, 2006.

[64] K.W. Nam, K. L. Yoon, J. S. Bark, and W.S. Yang, "A feature extraction method for binary iris code construction," *Internat Conf. on Info. Tech. for Application,* pp. 284-287, China, 2004.

[65] L.S. Oliveira, R.F. Sabourin, C.Y. Bortolozzi, and C.Y. Suen, "Feature selection using multiobjectives genetic algorithms for handwritten digit recognition," *Internat. Conf. on Pattern Recog.*, vol. 1, pp. 568–571, 2002.

[66] C. Park, J. Lee, M. Smith, and K. Park, "Iris-based personal authentication using a normalized directional energy feature," *Internat. Conf. on Audio- and Video-Based Biometric Person Authentication*, pp. 224–232, 2003.

[67] K.R. Park, and J. Kim, "A real-time focusing algorithm for iris recognition camera," *IEEE Trans. on Systems, Man, and Cybernetics C*, vol. 35, no. 3, pp. 441-444, 2005.

[68] C. Park, J. Lee, S. Oh, Y. Song, D. Choi, and K. Park, "Iris feature extraction and matching based on multiscale and directional image representation," *Internat. Conf. on Scale Space Methods in Comp. Vision,* Springer Lecture Notes in Computer Science, vol. 2695, pp.576-583, UK, 2003.

[69] M. B. Pereira, and A. C. P. Veiga, "Application of genetic algorithms to improve the reliability of an Iris Recognition System", *IEEE Workshop on Machine Learning for Signal Process.*, pp. 159-164, 2005.

[70] S. Prabhakar, S. Pankanti, and A.K. Jain, "Biometric recognition: security and privacy concerns," *IEEE Computer Society*, IEEE Security & Privacy, pp.33-42, 2003.

[71] X. Qiu, Z. Sun, and T. Tan, "Global texture analysis of iris images for ethnic classification," *Internat. Conf. on Biometric Authentication*, Springer Lecture Note Series in Computer Science, vol. 3882, pp. 411-418, 2006.

[72] K. Roy and P. Bhattacharya, "Iris recognition with support vector machine," *Internat. Conf. on Biometric Authentication*, Springer Lecture Note Series in Computer Science, vol. 3882, pp. 486-492, 2006.

[73] K. Roy, and P. Bhattacharya, "Iris recognition system using backpropagation artificial neural network for person identification," *Internat. Conf. on Comp. Science and its Applications,* pp. 1-5, USA, 2005.

[74] K. Roy and P. Bhattacharya, "An iris recognition method based on zigzag collarette area and asymmetrical support vector machines", *accepted in IEEE Conf. on Systems, Man, and Cybernetics*, Taiwan, 2006.

[75] K. Roy, and P. Bhattacharya, "An iris recognition method based on zigzag collarette area and support vector machines", *Internat. Biometrics Conf.,* Montreal, Canada, 2006.

[76] C. Sanchez-Avila and R. Sanchez-Reillo, "Iris-based biometric recognition using dyadic wavelet transform," *IEEE Aerosp. Electron. Syst. Mag.*, vol. 17, pp. 3–6, 2002.

[77] R. Sanchez-Reillo and C. Sanchez-Avila, "Iris recognition with low template size," *Internat. Conf. on Audio and Video-Based Biometric Person Authentication*, pp. 324–329, 2001.

[78] N. A. Schmid, M. V. Ketkar, H. Singh, and B. Cukic, "Performance Analysis of Iris-Based Identification System at the Matching Score Level," a*ccepted for publication in IEEE Trans. Trans. Info. Forensics and Security*, 2006.

[79] D. Schonberg and D. Kirovski, "Eyecerts," a*ccepted for publication in IEEE Trans. Info. Forensics and Security*, 2006.

[80] J. Shen, W. Shen, and D. Shen, "On geometric and orthogonal moments," *Internat. J. Pattern Recog. Artific. Intell.*, vol. 14, pp. 875–894, 2000.

[81] O. Sirvan, B. Karlik, and A. Ugur, "An efficient iris recognition for security purposes," *ICGST internat. Conf. on Graphics, Vision and Image Processing*, Egypt, 2005.

[82] B. Son, H. Won, G. Kee, and Y. Lee, "Discriminant iris feature and support vector machines for iris recognition" *IEEE Internat. Conf. on Image Process.* vol. 2, pp. 865-868, 2004.

[83] Z. Sun, T. Tan, and X. Qiu, "Graph matching iris image blocks with local binary pattern," *Internat. Conf. on Biometric Authentication,* Springer Lecture Note Series in Computer Science, vol. 3882, pp. 366-372, 2006.

[84] Z. Sun, Y. Wang, T. Tan, and J. Cui, "Improving iris recognition accuracy via cascaded classifiers", *IEEE Trans. on Systems, Man and Cybernetics C*, vol. 35, pp. 435 – 441, 2005.

[85] C. Sun, C. Zhou, Y. Liang, and X. Liu, "Study and improvement or iris location algorithm," *Internat. Conf. on Biometric Authentication*, Springer Lecture Note Series in Computer Science, vol. 3882, pp. 436-442, 2006.

[86] H. Sung, J. Lim, J. Park, and Y. Lee, "Iris recognition using collarette boundary localization," *Internat. Conf. on pattern Recog.*, vol. 04, pp. 857-860, Cambridge, UK, 2004.

[87] H. Tan, and Y. Zhang, "Detecting eye blink states by tracking iris and eyelids," *Pattern Recog. Lett.*, vol. 27, pp. 667-675, 2006.

[88] K.C Tan, E.F Khor, and T.H. Lee, *Multiobjective evolutionary algorithms and applications,* Springer-Verlag, London, UK, 2005.

[89] T. Tangsukson and J. Havlicek, "AM-FM image segmentation," *IEEE Internat. Conf. on Image Processing*, pp. 104–107, 2000.

[90] P. Thoonsaengngam, K. Horapong, S. Thainimit, and V. Areekul, "Efficient iris recognition using adaptive quotient thresholding," *Internat. Conf. on Biometric Authentication*, Springer Lecture Note Series in Computer Science, vol. 3882, pp. 397-403, 2006.

[91] Q. Tieng and W. Boles, "Recognition of 2D object contours using the wavelet transform zero-crossing representation," *IEEE Trans. on Pattern Anal. Machine Intell.*, vol. 19, pp. 910–916, 1997.

[92] C. Tisse, L. Martin, L. Torres, and M. Robert, "Person identification technique using human iris recognition," *Vision Interface Conf.*, 2002, pp. 294–299.

[93] V. N. Vapnik, *Statistical learning theory,* J. Wiley, New York, 1998.

[94] M. Vatsa, R. Singh, and A. Noore, "Reducing the false rejection rate of iris recognition using textural and topological features," *Internat. J. on Signal Process.*, vol. 02, pp.66-72, 2005.

[95] Z. Wei, T. Tan, Z. Sun, and J. Cui, "Robust and fast assessment of iris image quality," *Internat. Conf. on Biometric Authentication*, Springer Lecture Note Series in Computer Science, vol. 3882, pp. 464-471, 2006.

[96] R. Wildes, J. Asmuth, G. Green, S. Hsu, R. Kolczynski, J. Matey, and S. McBride, "A machine-vision system for iris recognition," *Machine Vision Applications*, vol. 9, pp. 1–8, 1996.

[97] R.Wildes, J. Asmuth, S. Hsu, R. Kolczynski, J. Matey, and S. Mcbride, "Automated, noninvasive iris recognition system and method," U.S. Patent No. 5572596, 1996.

[98] R. Wildes, "Iris recognition: an emerging biometric technology," *Proc. of IEEE*, vol. 85, pp. 1348–1363, 1997.

[99] S. Yoon, S. Choi, S. Cha, Y. Lee, and C. C. Tappert, "On the Individuality of the Iris Biometric," *ICGST Internat. J. on Graphics, Vision and Image Process,* vol. 5, issue 05, 2005.

[100] L. Yu, K. Wang, and D. Zhang, "A novel method for coarse iris classification", *Internat. Conf. on Biometric Authentication*, Springer Lecture Note Series in Computer Science, vol. 3882, pp. 404-410, 2006.

[101] Z. Zheng, J. Yang, and L. Yang, "A robust method for eye features extraction on color image," *Pattern Recog. Lett.*, vol. 26, pp.2252–2261, 2005.

[102] Y. Zhu, T. Tan, and Y. Wang, "Biometric personal identification based on iris patterns," *Internat. Conf. on Pattern Recog.*, vol. II, pp. 805–808, 2000.

[103] J. Zuo, and N.A. Schmid, "A model based, anatomy based method for synthesizing iris images," *Internat. Conf. on Biometric Authentication*, Springer Lecture Note Series in Computer Science, vol. 3882, pp. 428-435, 2006.

[104] http://iris.nist.gov/ICE/.

[105] Personal webpage of John Daugman, University of Cambridge, UK, Materials available at http://www.cl.cam.ac.uk/~jgd1000/.

[106] Computer vision source codes of P. D. Kovesi, School of Computer Science & Software Engineering, The University of Western Australia. available at: <http://www.csse.uwa.edu.au/~pk/research/matlabfns/>.

[107] A pattern recognition toolbox is available at http://www.prtools.org/.

[108] Support vector machines resources are available at http://www.isis.ecs.soton.ac.uk/isystems/kernel/.

[109] CASIA iris image database is available at http://www.nlpr.ia.ac.cn/English/irds/irisdatabase.htm.

Appendix A

Training and Testing Procedures of the Proposed Approach I & Approach II

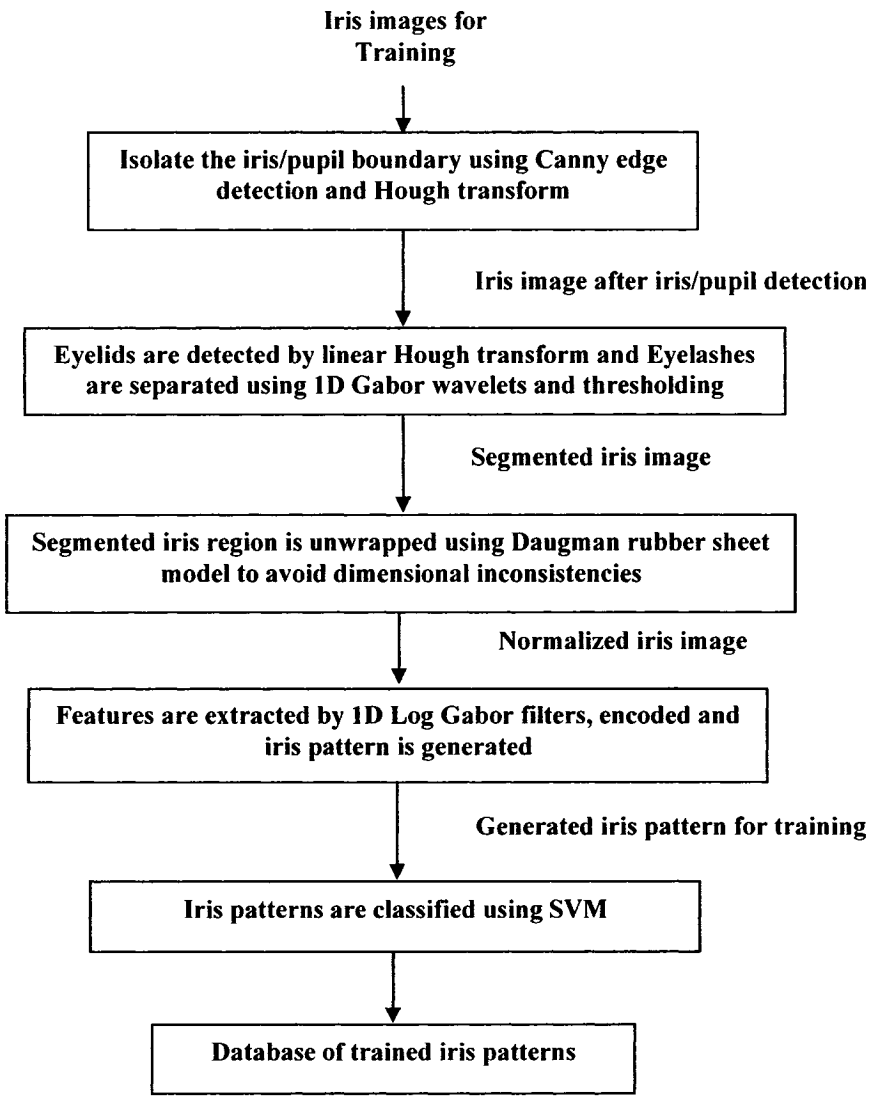

Figure 44: Training procedure of the proposed approach I.

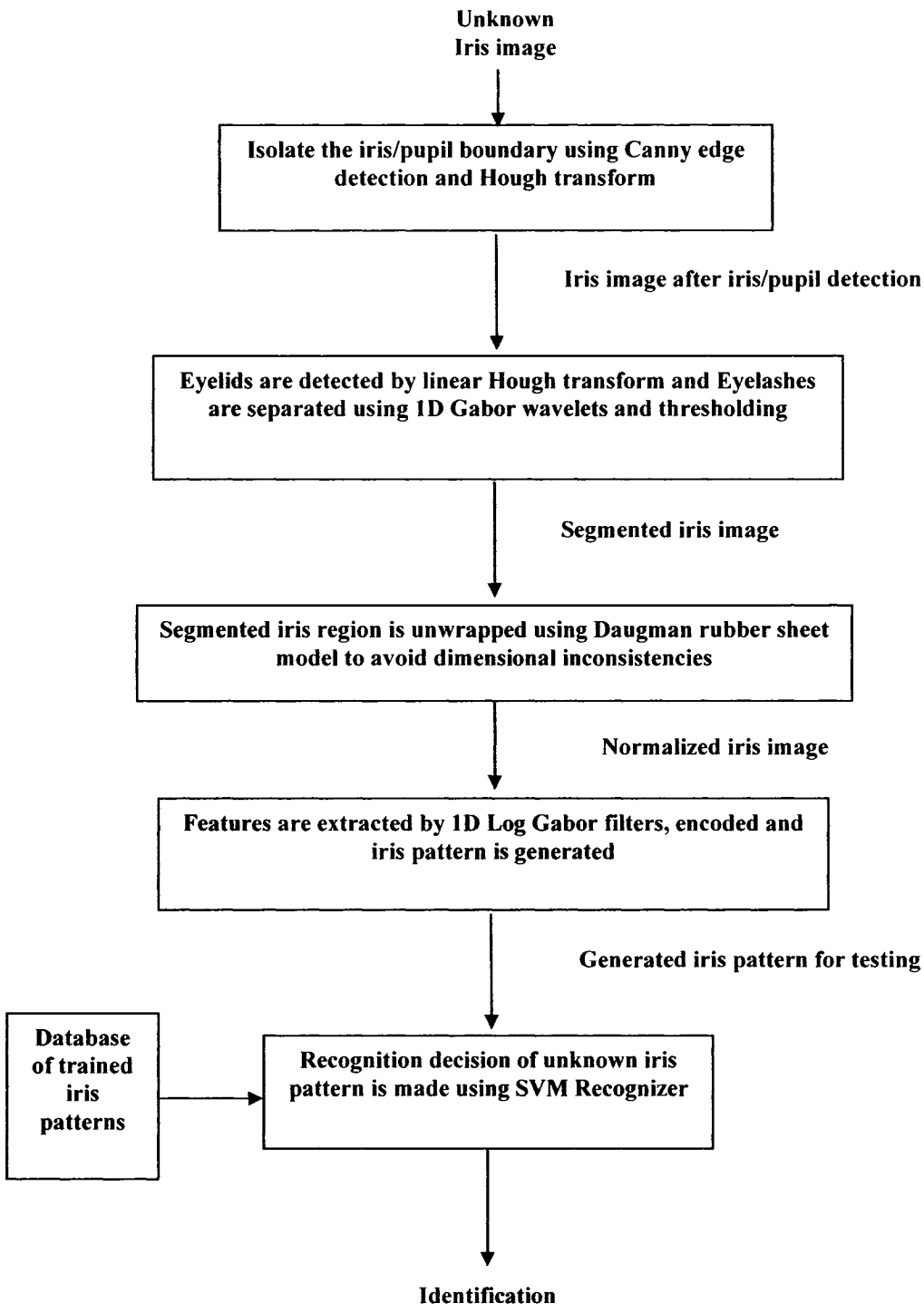

Figure 45: Testing procedure of the proposed approach I.

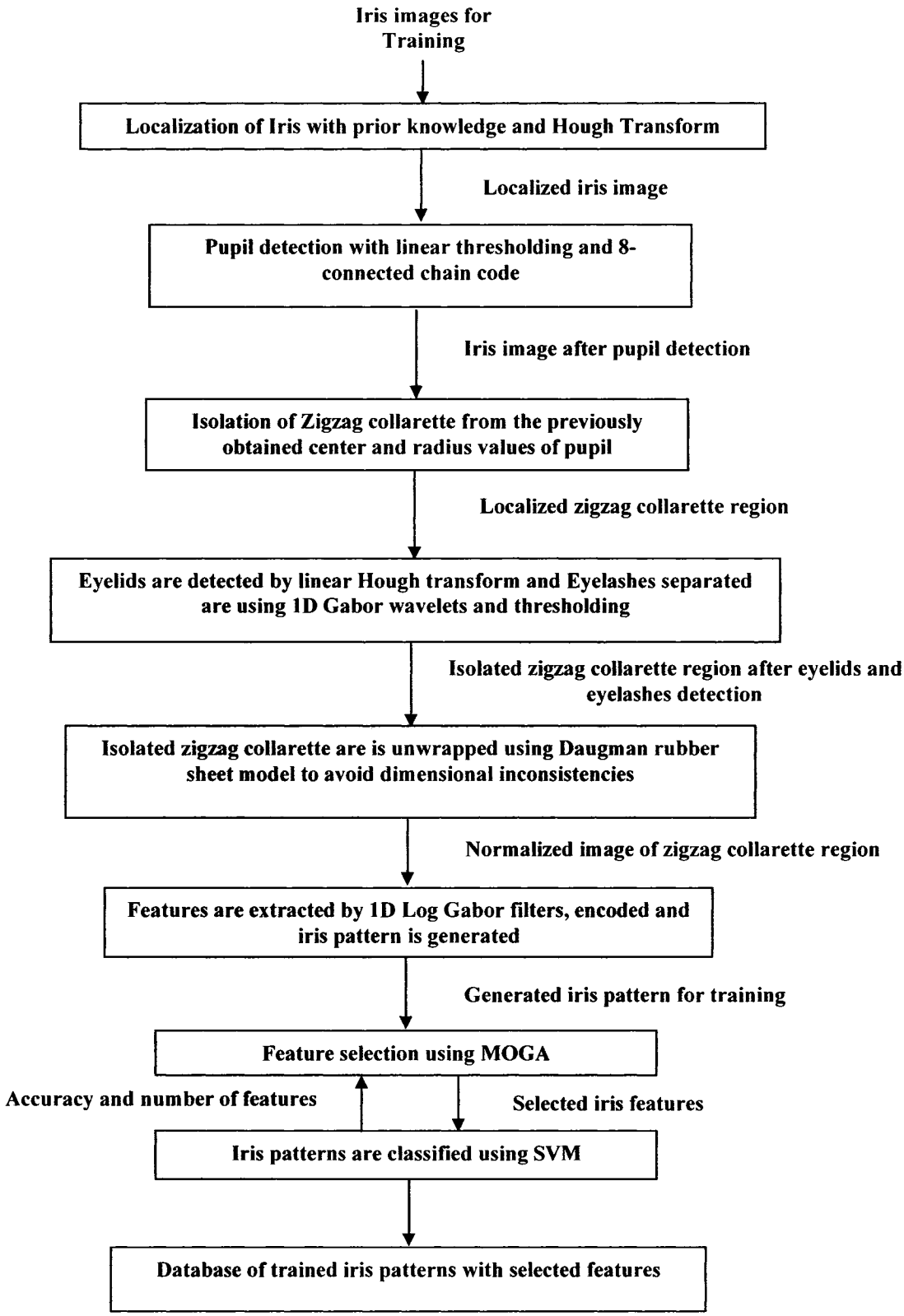

Figure 46: Training procedure of the proposed approach II.

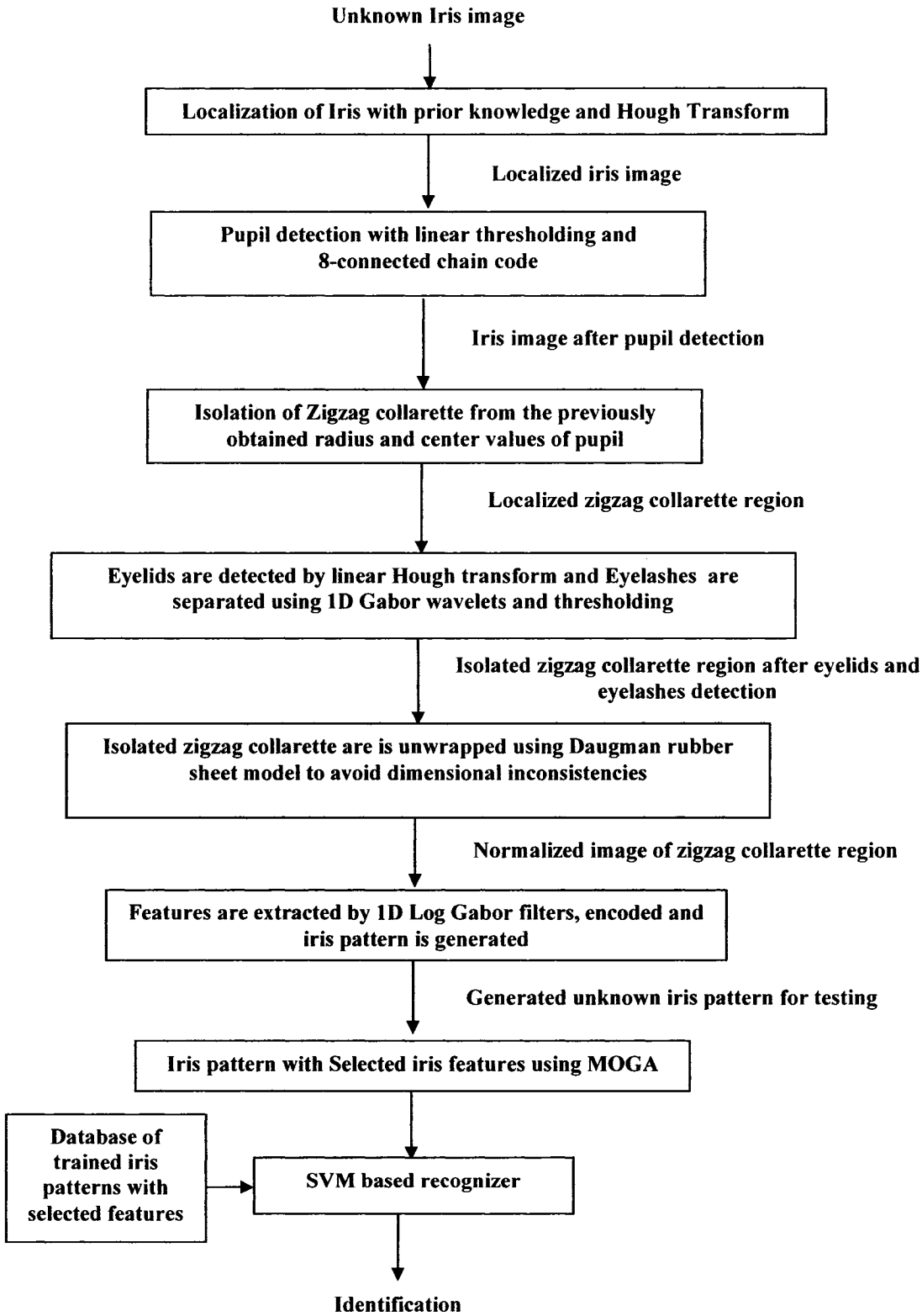

Figure 47: Testing procedure of the proposed approach II.

Appendix B

Functional Overview of Approach I & Approach II

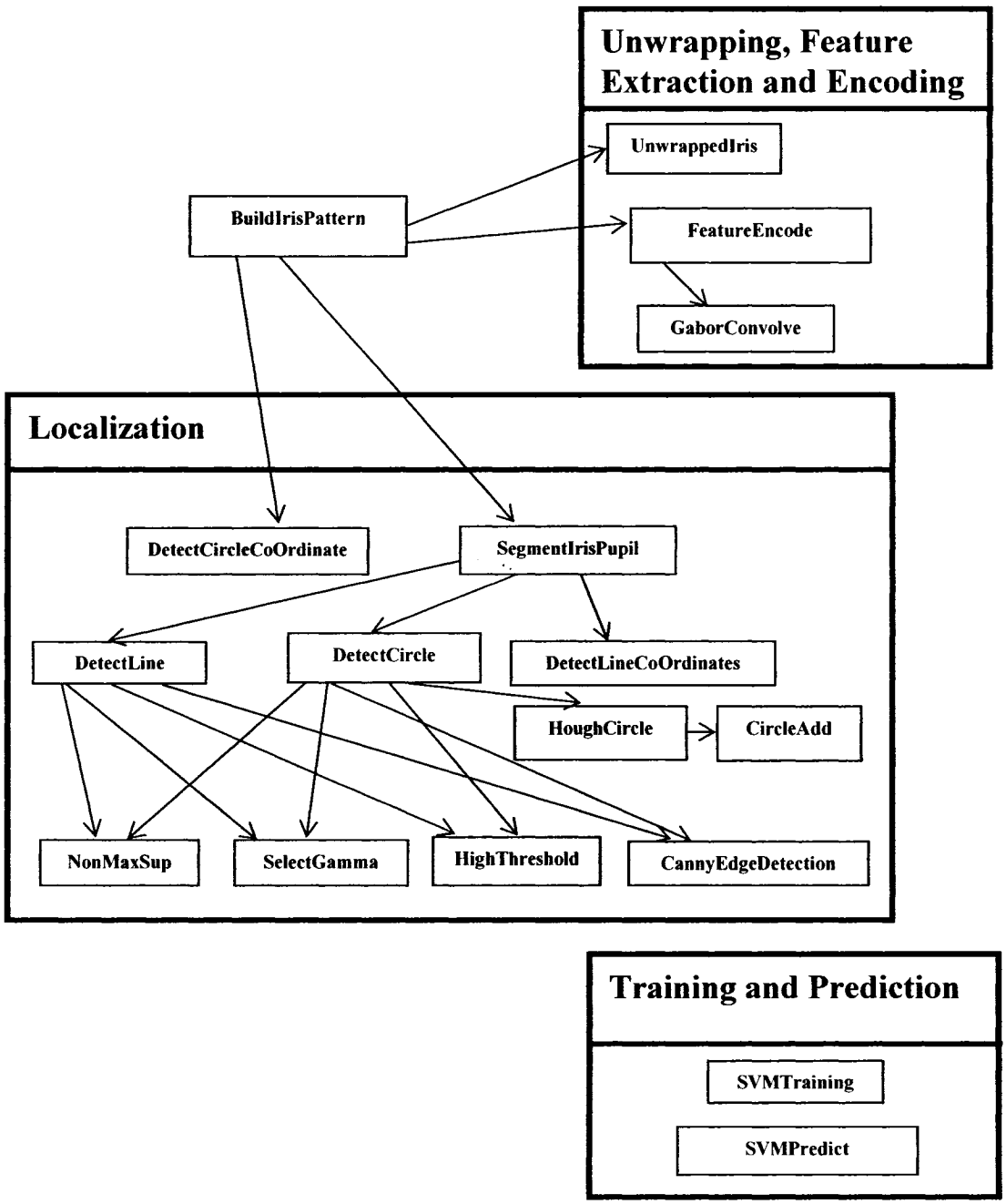

Figure 48: Overview of subsystems and MatLab functions for Approach I.

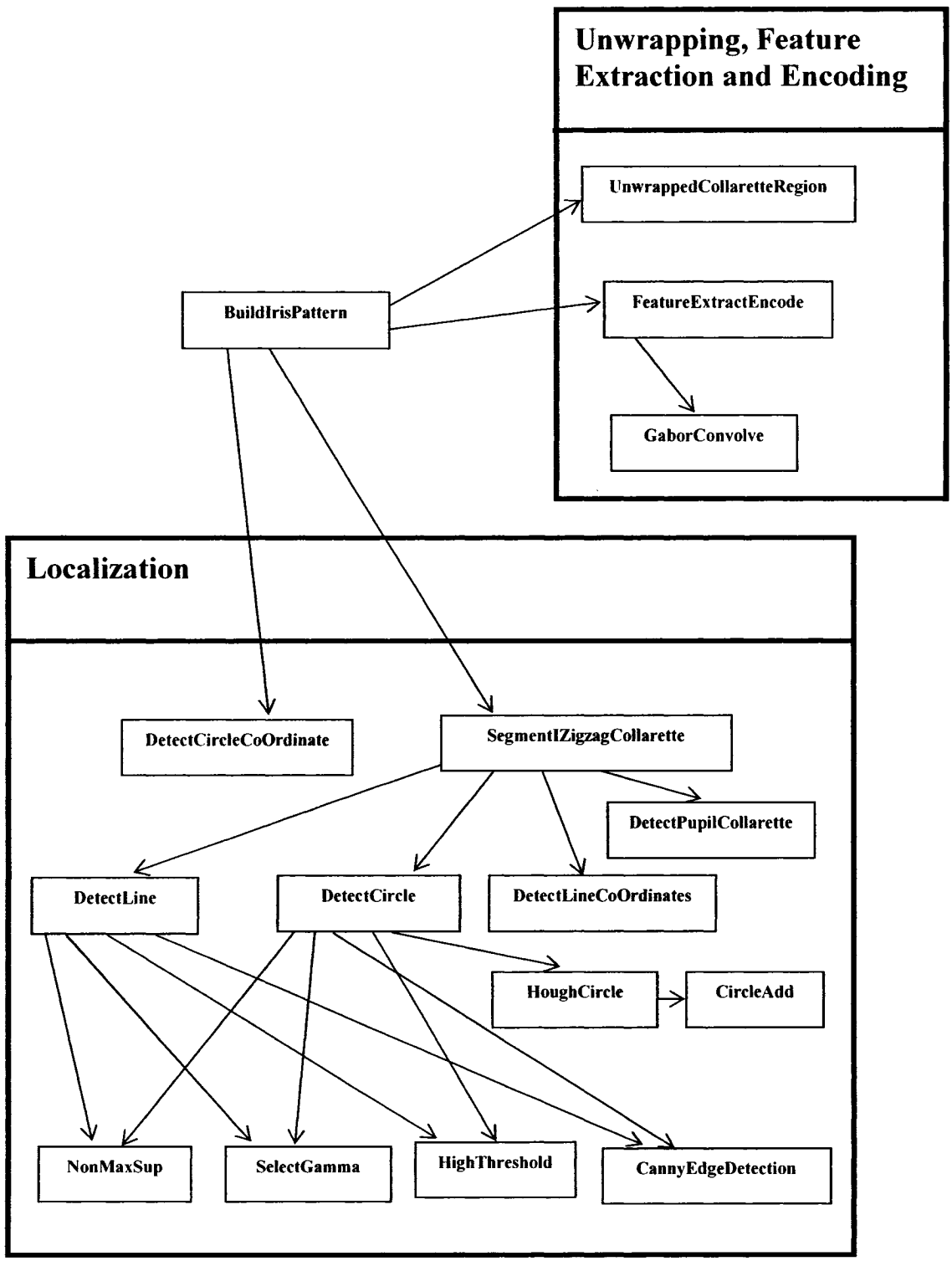
Unwrapping, Feature Extraction and Encoding
UnwrappedCollaretteRegion
BuildIrisPattern
FeatureExtractEncode
GaborConvolve
Localization
DetectCircleCoOrdinate
SegmentIZigzagCollarette
DetectPupilCollarette
DetectLine
DetectCircle
DetectLineCoOrdinates
HoughCircle
CircleAdd
NonMaxSup
SelectGamma
HighThreshold
CannyEdgeDetection

(a)

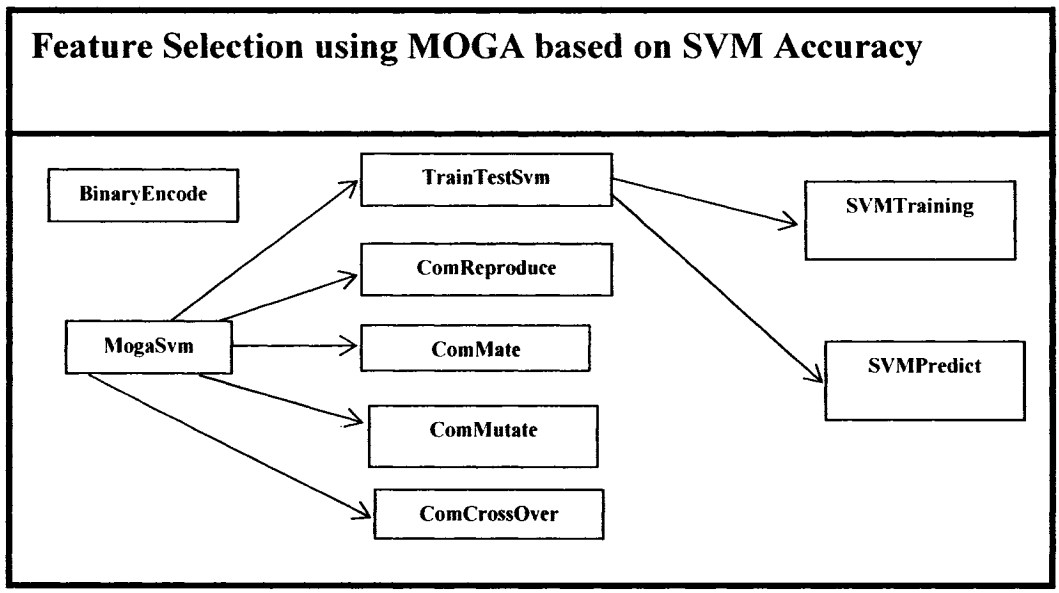

(b)

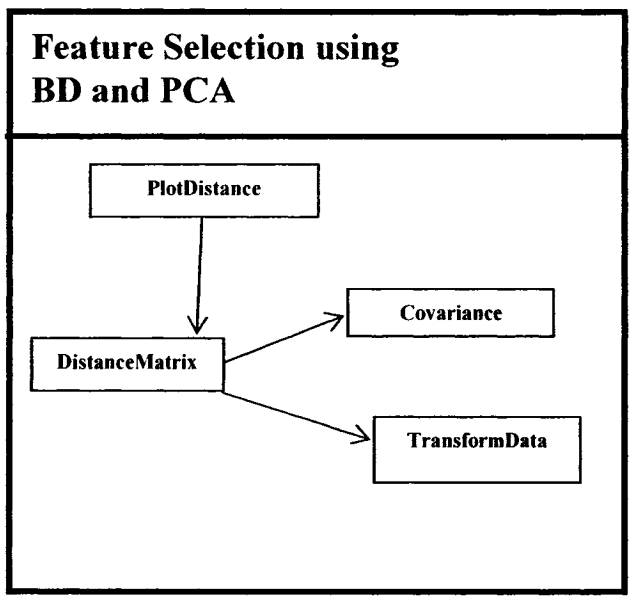

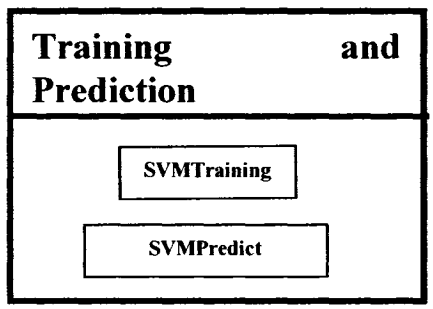

(c)

(d)

Figure 49: Overview of subsystems and MatLab functions of Approach II for (a) localization, unwrapping, and feature extraction and encoding (b) feature selection using MOGA, (c) feature selection with BD and PCA, and (d) training and prediction.

Appendix C

List of Abbreviated Terms

SVM: Support Vector Machines.

SV: Support Vectors.

HD: Hamming Distance.

BD: Bhattacharyya Distance.

BCD: Bhattacharyya Cumulative Distance.

MD: Mahalanobis Distance.

MDC: Mahalanobis Distance Classifier.

ANN: Artificial Neural Network.

FFBP: Feed-Forward Neural Network using Backpropagation.

FFLM: Feed-Forward Neural Network using Levenberg-Marquardt rule.

k-NN: k-Nearest Neighbor.

GA: Genetic Algorithms.

MOGA: Multi Objectives Genetic Algorithms.

PCA: Principal Component Analysis.

FA: False Accept

FAR: False Accept Rate.

FR: False Reject.

FRR: False Reject Rate.

ER: Equal Error.

ERR: Equal Error Rate.

GAR: Genuine Acceptance Rate.

CRR: Correct Recognition Rates.

ROC: Receiver Operator Characteristics.

WPD: Wavelet Packets Decomposition.

SVD: Single Value Decomposition.

ICA: Independent Component Analysis.

WED: Weighted Euclidean Distance.

LVQ: Learning Neural Network.

LDA: Linear Discriminant Analysis.

DLDA: Direct Linear Discriminant Analysis.

LFC: Local Feature Based Classifiers.

DFB: Directional Filter Bank.

DFT: Discrete Fourier Transform.

CASIA: Chinese Academy of Sciences-Institute of Automation.

NLPR: National Laboratory for Pattern Recognition.